Rune Harald Hestmo

Laboratory Studies of Paper Calendering using a Pendulum Device

Dr. Ingeniøravhandling 2001: 108

Norges teknisk-naturvitenskapelige universitet

Acknowledgements

This dr.ing thesis is the result of my study at the Faculty of Mechanical Engineering, Dept. of Applied Mechanics, Thermodynamics and Fluid Dynamics, at the Norwegian University of Science and Technology.

My greatest and deepest thanks goes to my supervisor, Magne Lamvik, who has been an excellent supervisor and a really support during my work.

Erling Mikkelsen has made the experimental work possible with excellent work at the laboratory, helping out problems and giving fruitfull discussions.

Elisabeth Hovda has been my "mate of study" and travelling companion during interesting "expeditions" across the world through these years. I wish to send her a warm compliments.

The studies have been made possible by grant from The Research Council of Norway and Norske Skog ASA, and by support from the Norwegian Pulp and Paper Research Institute (PFI). On this occasion it is appropriate to emphasize the initial discussion of the research program for the calendering process, namely with Per Erik Lindem, Senior Scientist and Per Johan Houen, Head of Research, Paper, (PFI), who generously gave "nearly free hands to extend the knowledge of the calendering process". Later on, Per Erik Lindem left PFI, and thereafter Hans-Erik Høydahl, Head of Research and Development, Norske Skog, and Per Johan Houen constituted the discussion group, giving important advice and stating relevant industrial considerations.

Finally a thank to my colleagues, friends, and family. Especially Gunnar Prytz, Hege Widerøe, Rune Holmen and Tore Myhrvold.

Contents

1 Introduction **1**

2 The pendulum device as a calender simulator **6**

2.1 Model experiments of calendering with a pendulum device. Paper I 6

2.2 Supplements to Paper I 26

2.2.1 Experiments with moistening the paper specimen 26

2.2.2 Compressive work on the paper by impact in z-direction 27

2.2.3 Dwell time 35

2.2.4 Paper properties 41

2.2.5 Calendering equations 48

3 The deformation of paper and its fibres by calendering **50**

3.1 Calendering of wood containing paper: A laboratory study of temperature, moisture and pressure effects on fibre wall damage. Paper II 50

3.2 Supplements to Paper II 61

3.2.1 Relative crack distribution using two calendering techniques . . 62

3.2.2 Calender blackening 64

3.2.3 Fibre cracks versus dwell time 64

4 Thermal conductivity of newsprint under compression **67**

4.1 Determination of thermal conductivity of newsprint under compression. Paper III 67

5 Heat transfer during calendering **78**

5.1 Heat transfer during calendering of paper. Paper IV 78

6 Concluding remarks **97**

List of papers

The thesis is mainly based on the following orginal papers, which are referred to in the text by Roman letters (and are incorporated in the text).

I Lamvik, M., Hestmo, Rune H. and Mikkelsen, E.(2000)"Model experiments of calendering with a pendulum device". Nordic Pulp & Paper Research Journal No. 2, Vol. 15, p. 133-141.

II Hestmo, Rune H., Gregersen, Øyvind W. and Lamvik, M.(2001)"Calendering of wood containing paper: A laboratory study of temperature, moisture and pressure effects on fibre wall damage". Nordic Pulp & Paper Research Journal No. 4, Vol. 16.

III Hestmo, Rune H. and Lamvik, M.(2001)"Determination of thermal conductivity of newsprint under compression", presented at the 26th International Thermal Conductivity Conference, 6-8 August 2001, Cambridge, Massachusetts USA.

IV Hestmo, Rune H. and Lamvik, M.(2002)"Heat Transfer by Calendering of Paper", accepted for publishing in Journal of Pulp and Paper Science, in April issue, 2002.

Nomenclature

a [-] Volumetric fraction
B [-] Empirical parameter
Bi Biots tall
c_1, c_2 [-] Empirical parameters
C_0, C_0' [-] Empirical parameters
C $[J\ (kg\ ^oC)^{-1}]$ Specific heat capacity
d [-] Material constant
D [m] Diameter
e [-] Restitution coefficient
E $[Nms^{-1}]$ Kinetic energy
$f_a[-]$ Contact area fraction
$f_c[-]$ Coverage fraction
$f_v[-]$ Volum fraction
F, F_{max} [N] Force
Fo Fourier number
G [Pa] Modulus of elasticity
G^* [-] Equivalent modulus of elasticity
h $[W(m^2\ ^oC)^{-1}]$ Heat transfer coefficient
i [Pa s] Specific impulse
I [Ns] Impulse
j $[Wm^{-2}]$ Heat flux
k $[W(m^oC)^{-1}]$ Thermal conductivity
K, K_0 [-] Stiffness
l_c [m] Nip width
L, L_m $[Nm^{-1}]$ Line load
m, m' [-] Empirical parameters
M [kg] Mass
n [-] Number of impact
P, P_{max} [Pa] Pressure
q $[Jm^{-2}]$ Heat transfer
Q $[W]$ Heat flow
r_1, r_2 [m] Radius of rollers
R^* [-] Equivalent radius
s, s_0 [m] Thickness dimension
t [s] Time
T $[^oC]$ Temperature

u, v $[ms^{-1}]$ Linear velocity
V [volt] Voltage reading
w_f [mm] Fibre width
W [Nm] Work
z [m] Length dimension

α [-] Energy conversion ratio
$\beta_f [gm^{-2}]$ Basis weight
γ [-] Material constant
ϵ [-] Strain
ε [-] Emissivity
ζ, ζ_0 [-] Converted energy
ρ $[kgm^{-3}]$ Density
σ [Pa] Stress
σ_b $[Wm^{-2}\ K^{-4}]$ Stefan-Boltzmann constant
υ, υ_f $[m^3kg^{-1}]$ Specific volume
ϕ_n [-] Empirical parameter
χ_n [-] Empirical parameter
φ [-] Porosity
η [-] Relative dwell time
θ, θ_{int} [−] Relative temperature
ϑ, ϑ_s [m] Displacement
κ $[m^2s^{-1}]$ Thermal diffusivity
Λ [s] Nominal period
ν_1, ν_2 [-] Poisson‘s number
ξ [-] Empirical parameter
ψ [-] Material constant

Chapter 1

Introduction

The word *calender* is according to Webster's Dictionary (1978) related to the Greek *kylindros*, and to the Latin *cylindrus* and denotes

"a machine consisting of two or more cylinders revolving so nearly in contact with each other that cloth or paper passing between them is smoothed and given a glossy finish by their pressure".

When the paper passes through the contact zone, the nip, it is exposed to a pressure that increases from zero, goes through a maximum and then decreases to zero. The pressure can be expressed by a more or less symmetrical mathematical function over time. This is the essential impact on the paper by calendering. Its purpose is to improve the surface properties of the paper, to make it fit for printing. In addition to the pressure, the hardness of the rollers, the dwell time of the paper under pressure, as well as the temperature of the rollers and the moisture content of the paper are decisive parameters for achieving the goal.

Industrial calenders can be classified in several ways. According to their position in the production line, they may be on-line, where the rollers are running with the same speed as the paper machine, a machine calender. When the calendering process require a different speed of the rollers, the calender is placed off-line, as, for example, a supercalender. The calenders can also be classified from the design of the rollers, hard nip calenders, with pairs of steel rollers, and soft nip calenders with one steel roller together with a steel roller covered by a relatively soft material, as a polymer. Fig. 1.1 illustrates an industrial single soft nip calender. Fig. 1.2 illustrates a socalled supercalender with a stack of several nips in series, and where both sides of the paper in turn are smoothened.

The geometry of a soft nip and a hard nip is different in shape and size, and the distribution of the pressure acting on the paper is also different. A soft nip gives a more evenly calendered paper compared to a hard nip, giving the paper a smoother surface, and a higher tensile strength than paper calendered in a hard nip under similar running conditions. In the last decades, the trend has been to implement on-line soft

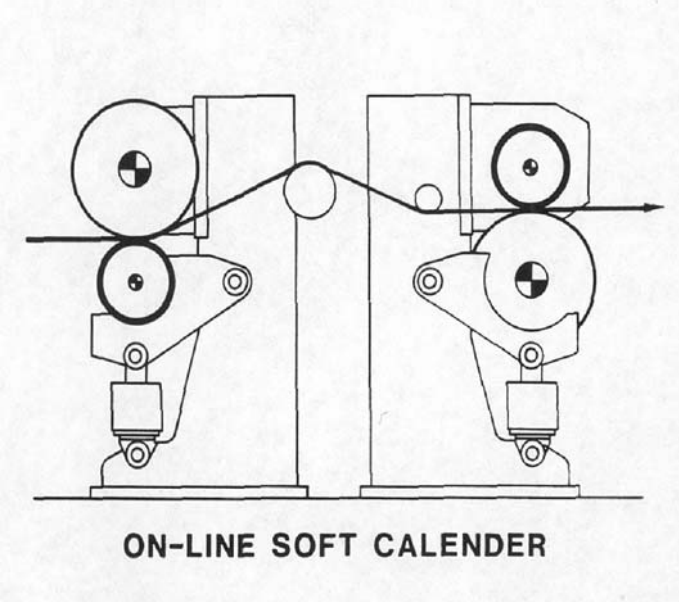

Figure 1.1: Soft nip calender. Nip formed by a steel roller and an elastomer covered roller.

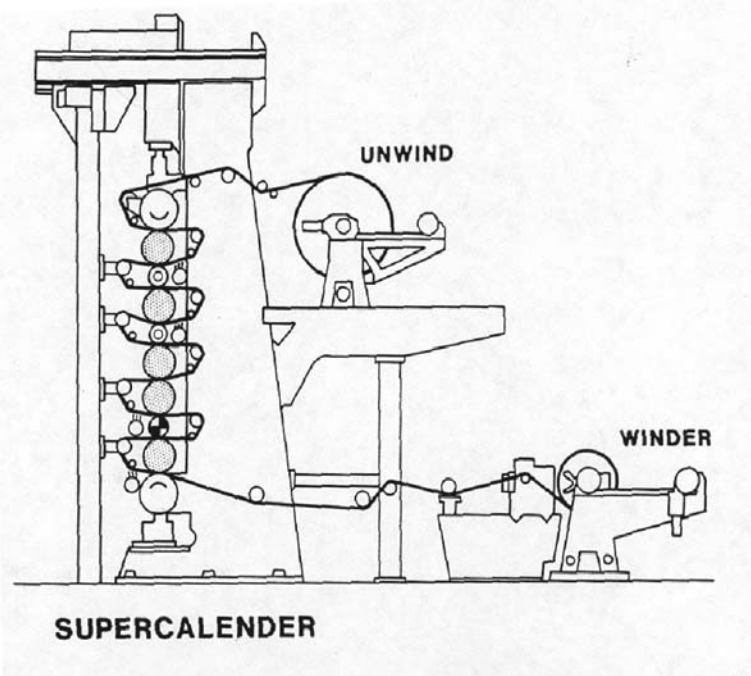

Figure 1.2: Supercalender with a stack of alternating hard and soft rolls.

calendering in the production line of paper, especially for newsprint. This means rollers running with high-speed, and the paper will have a very short dwell time in the nip, involving two types of engineering challenges. Firstly, there are formidable tasks in the design, in the production and in the operation of the rollers. Secondly, the selection of the data for the running conditions of the rollers has to be made in view of the required final properties of the paper. The limitation of the line load can be compensated by the appropriate choice of temperature of the roller and the moisture content of the paper to soften the paper fibres.

A comprehensive literature refers, mostly experimental, investigations of the paper calendering process. The experiments have been made under a systematic variation of the pertinent parameters: nip pressure, dwell time of the paper under pressure, temperature of the rollers and the paper, and moisture content of the paper, all for given paper qualities. Furthermore, the experiments fell in three groups, 1) the running of full-scale industrial calenders, giving the most realistic results, 2) the running of small-scaled roller calenders in a laboratory, where a wider variation of the parameters can be performed, and being much cheaper than full-scale experiments, and finally 3) by experimental simulation of the calender process, where the way the pressure upon the paper is accomplished in many different ways, for example by the hammer-anvil arrangement.

The last-mentioned group inheres the most versatile techniques for studies of the different phenomena taking place in the calender process. The present investigation belongs to this group. Instead of a falling hammer and a resting anvil, two pivoting pendulums are used, allowing to swing in the way that their hammers perform an impact, with the paper specimen between. The pendulums are designed to give an impulse to the specimen that is comparable with the impulse given in high-speed roller calenders, where a paper speed of about $1500m(min)^{-1}$ is realistic. The dwell time of the paper in the nip is then of the order of magnitude 1 ms. The operation of the pendulum equipment can be described by elementary laws of mechanics, and the parameters can be measured properly. That is for example the case in the determination of the impulse, i.e. impact force versus time. The impulse on the paper is hardly to achieve by rotating rollers. It can, however, be given as a nominal specific mean value over the nip, in $Pa \cdot s$, that can be used as a the reference for comparing the feature of the calendering processes by the rollers and the pendulums. Several phenomena in the paper taking place during calendering, can better be studied using the hammer-anvil type, among which the pendulum device reveals some advantages.

The present thesis refers experimental and theoretical studies of the calendering process making use of the pendulum device as a means to simulate the roller calendering. The main task has been to clarify characteristic feature of the device in its capacity to simulate the calendering process with rollers. Measurements are made to

enlighten the dependency of the paper characteristics gloss, smoothness and density by the running conditions as nip load, dwell time, roller temperature and moisture content of the paper. Furthermore, the deformation of the fibres and the thermal conduction in the paper during the compression are studied. Finally, an experimental and analytical study of the heat transfer between the hammer and the paper specimen is made. The results are compared with results from roller calenders in the extent they are available in the literature. The subjects are organized in the following chapters:

- the pendulum device as a calender simulator
- the deformation of paper and its fibres by calendering
- the thermal conductivity of newsprint under compression
- the heat transfer from roller/pendulum surface to the paper

Chapter 2 introduces the pendulum device that has been used in the experimental studies of the calendering process of paper. The device simulates fairly well the process taking place in roller calendering concerning the surface properties of the paper. Therefore it has also been applied in several connected studies, specially in the study of the heat transfer between the pendulum hammer, or roller, and the paper, that is dealt with in a chapter below.

The device is described in Paper I. Its capabilities for simulating the roller calender are shown by some introductory experimental results. Paper gloss and smoothness as well as density are determined in dependency of nip pressure and temperature of the pendulum hammer, keeping temperature and moisture content of the specimen constant according to the room climate.

Additional experiments with the pendulum device are also reported in this chapter. Measurements are made of paper surface properties in dependency of moisture content of the paper. Several ways of adding moisture to the paper specimen have been applied.

By passing the nip the paper undergoes a compression, and a permanent reduction of its thickness, the z-direction, is recognized. It follows by a density increase and deformation of fibre cross section, and the fibre wall may eventually crack, with a reduction of the strength of the paper as a consequence. The thickness reduction has been studied by some preliminary experiments, and the crack of the fibres have been studied in specimens calendered by the pendulums as well as by rollers. The differences that can be noticed of the cracks, are discussed under the hypothesis of differences in the stress-strain conditions of the respective devices. The investigations are reported in **Chapter 3**.

Thermal conductivity of paper under compression is investigated and reported in **Chapter 4**. The results reveal a higher value of the thermal conductivity when the

paper is under pressure in the nip than after it is released and expanded from the pressure. While in the nip a better contact between neighboring fibres in the thickness direction is assumed.

In modern calenders the paper can be run at high speed, up to $30ms^{-1}$. This means that the paper has a dwell time in the nip of order of magnitude 1 ms, and the heat transfer features a pulse heating. It is therefore of interest to look at the heat transfer between the pendulum/roller and the paper surface, as well as the thermal conduction within the paper during the dwell time. The heat transfer from pendulum hammer to the paper surface is analyzed in **Chapter 5**. A formal heat transfer coefficient is derived in dependency of the nip pressure. Experimental and numerical results are in fair qualitative agreement. The ideal conditions for the socalled temperature gradient calendering seems to exist at high speed calenders, i.e. only the fibres in the surface of the paper are heated while the fibres of the layers beyond are substantially unaffected by the hot hammer/roller.

Chapter 2

The pendulum device as a calender simulator

2.1 Model experiments of calendering with a pendulum device. Paper I

(*M.* Lamvik, R. H. Hestmo and E. Mikkelsen(2000).
"Model experiments of calendering with a pendulum device"
*N*ordic Pulp and Paper Research Journal, No. 2, Vol. 15 p. 133-144)

SUMMARY: The calendering process of paper is discussed, and an experimental setup is described for simulating the industrial process. The experiments involved the use of pendulums, where weights were made to collide to give an impact on the paper specimen, to simulate the line load acting on the paper between the rollers of industrial calenders. The mechanics of the pendulums was analyzed, and the unit for specific impulse, (Nsm^{-2}), was used for comparison of the measuring results with the results from roller calendering. Measurements were made on specimens of newspaper, magazine paper (SC-paper) and some specimens made specially for the experiments. The results from measurements of gloss, smoothness, and thickness reduction were compared with data in the literature from roller calendering. They correspond reasonably well, and it is assumed that the pendulum technique is suited for the experimental simulation of industrial calendering.

Introduction

Calendering is one of the final processes in the paper-making production line. In an industrial plant it takes place by conveying the paper through the contact line, the nip, between two rotating parallel cylindrical rollers. Due to the line load in the nip, in Nm^{-1}, the paper undergoes a deformation that smoothes the surfaces of the paper. The deformation depends on the mechanical strength of paper, i.e. its modulus of elasticity that depends on temperature and moisture content, as indicated by Salmén and Back (1980). The ideal procedure is to add heat and moisture to the surface region of the paper, in order to localize a plastic deformation at the surface, while the fibres of the inner layers of the sheet avoid the thermal treatment and thereby keep their mechanical strength. This procedure, called the temperature gradient calendering, has received high attention in the last few decades. A concise description of the calendering process is given by Gratton (1997).

The main purpose of calendering the paper is to make its surface suitable for printing, and the process has to be evaluated from relevant surface qualities of the paper. The surface can be characterized by properties such as the gloss, the evenness, as data for Parker Print Surf, PPS, and the density of the paper, properties that are determined by use of standard instruments. Research on calendering is aiming at increased knowledge about the optimal operation parameters for running calenders, in view of the requirement of the printing process.

Investigations have been done on full-scale calenders, involving, however, high cost and time consumption. Thus, smaller sized calenders have been built for laboratory use, that can operate with parameters in accordance with the industrial calenders. The empirical method is often used in such investigations, i. e. altering the operation conditions until the results are acceptable, even though it may be hard to explain in detail the physical reasons for the result.

Mardon (1964) give a comprehensive analysis of the properties of paper from industrial calenders together with a discussion of the influence of the pertinent parameter of the process.

The majority of the relevant literature refers laboratory investigations relating the calendering process, that clarifies the significance of the different parameters. The investigations seems to fall in two groups, one where the line load and its distribution over the nip has been studied, the other dealing with the impact on the topical properties of the paper.

Keller (1992) measured the load distribution by rotating rollers with, as well as without, paper passing the nip. By rotating rollers, the load acting upon the paper in the nip, has to be recognized as a function of time. The load versus time, will have a sequence with an increase from zero to a maximum followed by a decrease back to zero.

In the first part of the sequence, the paper and the rollers undergo a compression, and in the final part an expansion, by which the structure of the paper may not be fully restored, i.e. it had attained a permanent plastic deformation. Keller's measurements indicate that the load distribution is asymmetric when calendering with paper, while it is nearly symmetric without paper. A shape factor for the load distribution function over the nip can be defined as the ratio of the integrated mean load to the maximum load (Luong and Lindem (1997)). Keller's results give a shape factor of 0.49 and 0.64 for calendering with and without paper in the nip, respectively. van Haag (1997) simulated numerically the load distribution in the nip for stationary as well as for rotary rollers, assuming the mechanical properties of the paper. The results for rotating rollers show that the load goes to a higher maximum and then falls off steeper, i.e. the width of the nip is reduced, compared with the results from stationary rollers. The shape factor for the load distribution can be evaluated to 0.46 and 0.52 for stationary respectively rotary rollers. From these investigations a shape factor of the load distribution by rotating rollers seems to be about 0.5. Luong and Lindem (1995), measured the load distribution from stationary rollers to have a shape factor of 0.63.

The literature on the physical change of the paper during the calendering process is quite extensive. The experimental investigations make use of equipments that intend to simulate the industrial calender process, either as small scaled roller calenders or as a sort of a hammer and anvil, between which the paper specimen can be compressed. While the roller calenders render the industrial process to a large extent, the results from the investigation with hammer/anvil equipment seems to be lacking an adequate comparison with the roller calendering.

De Montmorency (1967) studied the calendering of newsprint using a laboratory calender, while Chapman and Peel (1969) studied the deformation of newsprint using the hammer/anvil equipment. It can be shown that Chapman's results gave a substantial higher density increase of the specimen, compared with Montmorency's result, by approximately the same calendering impulse and temperature, a discrepancy that may be due to different kinetic at the rollers and the hammer/anvils.

Colley and Peel (1972) studied the creep and the recovery of the specimens by pulsed loads, in dependence of temperature and moisture content. Compression load and dwell time were varied within ranges, however, that are large compared to the conditions for high speed calenders. Zotterman and Wahren (1978) designed an hammer/anvil-apparatus to give short pulses, fit for simulating the line load of roller calenders running up to the highest speed. A similar apparatus was modified by Back and Olsson (1983) for investigating the calendering process of bleached kraft board. They measured the load on the anvil versus time. The curves for the load distribution show some asymmetric, as the rise time of the load is shorter than the fall time, a circumstance that can be referred to differences in the kinetic of the fall and rise of the load. Any perma-

nent deformation of the paper specimen would else be expected to shorten the fall time compared to the rise time. The dwell time for the paper under load could be varied down to about 4 ms. The investigation clarifies the influence of relevant parameters as temperature of the hammer, the impulse and the moisture content of the paper upon paper qualities as gloss, smoothness and density. An investigation with a roller calender under the same conditions would be worthy.

In the following an apparatus for laboratory use is described in which the mechanical impact on the paper is achieved by two hammers. They are activated by the movement of two pendulums making a hammer/hammer type of calender. The dynamics of the pendulums is described by which the inherent phenomena are studied with reference to roller calendering. Measurements are made on specimens of newsprint and magazine paper. Results for gloss, smoothness and density are presented and compared with data from relevant roller calendering.

Mathematical descriptions

When two bodies impact, mechanical laws give three relations that deserve attention, (Den Hartog (1948)):

1. the force between the bodies during the time of contact, i.e. the impulse equal the integral of the force versus time
2. the momentum of the pendulums before and after impact, and
3. the conversion of kinetic energy during impact

For the present case the bodies are represented by the hammers of two pendulums that can oscillate in the same plane and can be brought to impact.

Impulse

The mutual normal forces acting on the hammers, will be equal at any moment during the impact. The force will increase from zero at a given time t_1 to a maximum, and then fall back to zero at a time t_2. This is illustrated, from measurements, in Fig. 2.1, where the force is drawn versus time. The impulse during the impact can be evaluated as

$$I = \int_{t_1}^{t_2} F dt \quad (Ns) \tag{2.1}$$

The force versus time, as illustrated in the Fig. 2.1, is nearly symmetric, indicating that the bodies are nearly elastic. When plastic deformation occurs, for example when we put a piece of paper on the impact area, the material on the hammers may not be able to respond elastically when the force diminishes. The force distribution may then be asymmetric.

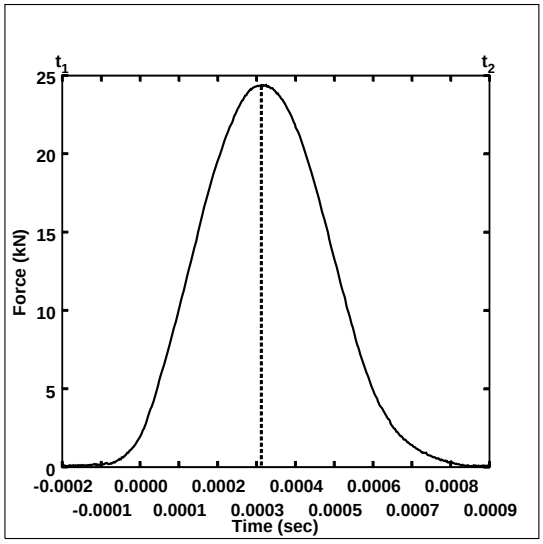

Figure 2.1: Force versus time during impact, as registered on an oscilloscope.

Momentum

The impulse of the respective hammers at impact changes the momentum of the pendulums. The sum of the momentum before and after impact, is equal. This can be expressed by

$$M_1 u_1 = M_1 v_1 + M_2 v_2 \quad (Ns) \tag{2.2}$$

where M_1 and M_2 are the masses of the respective pendulums P1 and P2, u and v are the respective velocities of the hammers before and after impact, assuming that velocity of P2 before the impact $u_2 = 0$.

It is advantageous to introduce a restitution coefficient, e, a kinematic quantity, as a ratio between the relative velocities of the pendulums before and after, as

$$e = \frac{v_2 - v_1}{u_1} \tag{2.3}$$

From the foregoing equations we get the velocity of pendulums after impact, relative to the velocity of P1 before impact:

$$\frac{v_1}{u_1} = (1 - e\frac{M_2}{M_1})\frac{M_1}{M_1 + M_2} \tag{2.4}$$

resp.

$$\frac{v_2}{u_1} = (1 + e)\frac{M_1}{M_1 + M_2} \tag{2.5}$$

Energy

The energy entering the system by operating the pendulums, is the kinetic energy of P1 just before the impact takes place, expressed by

$$E_1 = \frac{1}{2} M_1 {u_1}^2 \quad (Nms^{-1}) \tag{2.6}$$

After impact, the kinetic energy of the pendulums is

$$E_2 = \frac{1}{2} M_1 {v_1}^2 + \frac{1}{2} M_2 {v_2}^2 \tag{2.7}$$

and converted kinetic energy during the impact is

$$\Delta E = E_1 - E_2 \tag{2.8}$$

ΔE comprises the kinetic energy dissipated in the pendulums as vibration, heat and permanent deformation of the inherent materials, among which is the paper specimen.

By combining the foregoing expressions of the momentum and the energy, the converted kinetic energy can be expressed by

$$\Delta E = \frac{1}{2}(1 - e^2) {u_1}^2 \frac{M_1 M_2}{M_1 + M_2} \tag{2.9}$$

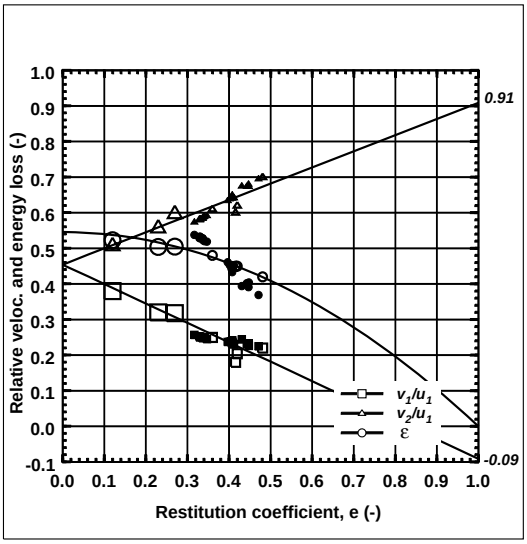

Figure 2.2: Diagram for operational feature of the pendulums, e restitution coefficient of impulse, v_1 and v_2 relative of hammer H_1 resp. hammer H_2 after impact, ζ relative converted kinetic energy of pendulum 1 by the impact. Large symbols $-H_2$ of steel, small symbols, H_2 with layer of elastomer. Open symbols, impact without paper, filled symbols, impact on newsprint.

or relative to the initial energy, 2.6,

$$\zeta = \frac{\Delta E}{\frac{1}{2}M_1 {u_1}^2} = \frac{1 - e^2}{1 + \frac{M_1}{M_2}} \tag{2.10}$$

This expression relates the energy transfer to the impulse by the coefficients ζ and e. It demonstrates, as expected, that the conversion of kinetic energy by the impact decreases, for example, with increasing restitution coefficient, as the plasticity of the hammers decreases. Equations [2.4,2.5,2.10] are illustrated by solid lines in Fig. 2.2.

Roller and pendulum criterion.

For roller calenders, the mechanical impulse imposed on the paper can be expressed by the integral of the line load over time, as

$$I_r = \int L dt = L_m \Delta t_n \quad (Nsm^{-1}) \tag{2.11}$$

or as a specific impulse per unit area, defined as

$$i_r = L_m u^{-1} \quad (Nsm^{-2}) \tag{2.12}$$

where L_m is the mean line load, Nm^{-1}, acting during the nominal dwell time, Δt_n of the paper in the nip, u is the velocity of the paper. With a nip width l_c, the dwell time is $\Delta t_n = l_c u^{-1}(s)$. The specific impulse i_r is illustrated in Fig. 2.3, as solid lines as functions of the paper velocity u.

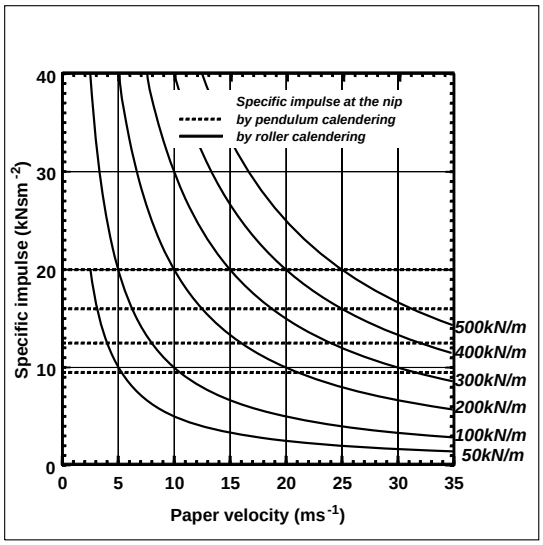

Figure 2.3: Specific impulse by pendulum calender and by roller calender versus paper velocity and the line force.

A similar analysis of the operation of the pendulums gives an impulse

$$I_p = \int F dt \quad (Ns) \tag{2.13}$$

and a specific impulse

$$i_p = 4I_p(\pi D^2)^{-1} \quad (Nsm^{-2}) \tag{2.14}$$

where D is the diameter of the contact area, and that of the test specimen of the paper. In the experiments, the integral of the impulse I_p is achieved from the oscilloscope, as an integral of the function of force versus time.

Experimental

Equipment and testing procedure

Fig. 2.4 shows the principle of the apparatus. Its main parts are two pendulums, P1 and P2, made of steel, with individual pivots mounted on a frame, allowing them to oscillate in the same vertical plane. The weights at the lower end of the arms are facing each other as hammers with a circular area, the impact area, diameter 50 mm. By operation, P1, the active pendulum, is swung out and held at a given position, while P2, the passive pendulum, is resting at its lower position. When P1 is released, it swings back and its hammer collides with the impact area of P2, on which the paper specimen is fixed. The hammers are machined to fine grade and polished. The hammer of P2, can alternatively be given a layer of a relatively soft material, an elastomer, to simulate the soft roller on the roller calenders. At the present, the elastomer is 24

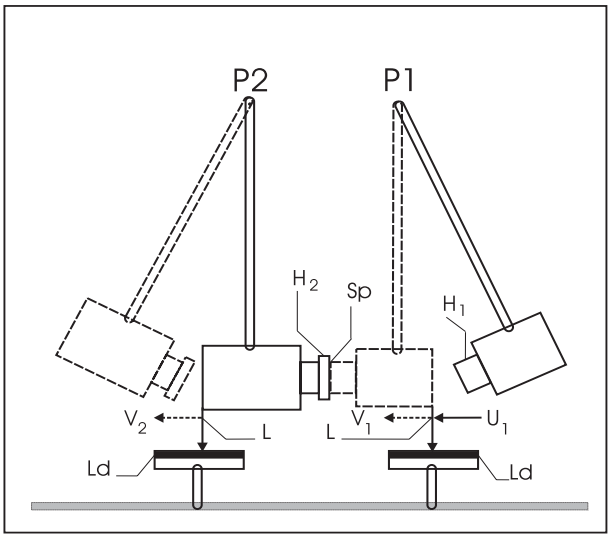

Figure 2.4: Principle sketch of the apparatus. P1, P2, pendulums, L laser, Ld linear detector, H_1 heated hammer with layer of elastomer, S_p paper specimen.

mm thick, having a modulus of elasticity, measured to $4380 MNm^{-2}$, in an INSTRON 1126, at a compression rate of $0.5mm(min)^{-1}$. When the pendulums are hanging free, the impact surface of the respective hammers are parallel and are just touching each other. The final adjustment of this position was done by means of screws at the pivot bearing. The parallelism of the surfaces was finally checked using a film that changed colour proportionate to the impact force, (from Fuji). The length of the arm of the pendulums, from the pivot axis to the centerline of the hammer, was 784 mm, and the total mass of P1 and P2 was 24.433 kg and 29.333 kg, respectively. The centers of impact is within 0.5% to the centerline of the hammers, determined from measurement of the period of the free oscillation of the pendulums.

The paper specimens were newsprint, based on TMP from Norway spruce, and uncalendered SC-paper(magazine paper). The newsprint samples on average had an initial thickness of 105 micron, and grammage $45gm^{-2}$. The SC-paper samples had an average grammage of $62gm^{-2}$. It was made of pulp(65%) from Norway spruce(90% TMP and 10% sulphate pulp) and kaolin(35%). For each experimental condition 3 measurements were made from which a mean value was evaluated for reporting. The paper test specimens were cut as circular pieces, diameter 50mm, with two "arms" protruding diametrically (resembling the Greek capital letter ϕ), by which the specimen could be fixed by paper tape at the impact area of hammer P2. In this way it was assumed that the specimen could expand radially during impact. Further, the time of contact was 0.3 - 0.6 ms, i.e. too short for the specimen to get any significant heating from P1. The temperature of the specimen was thereby assumed to be at room temperature for succeeding impacts. The apparatus was kept in a room with a temperature at $22^oC \pm 1^oC$ and the relative humidity was 45-50%, for most of the experiments. The moisture content of the paper specimen was measured, by spot check, to $8 \pm 1\%$.

In the experiments, P1 was swung out to alternative positions 1 - 4, giving velocities at impacts equal 1.10, 1.46, 1.83, resp. 2.19 ms^{-1}.

The impact force between the hammers, was measured by piezo-electric load cells, that were mounted in the respective weights, PCB Type 206A, having a rise time $10\mu s$. The signals from the cells were registered on an oscilloscope and stored in a computer for further analysis. The hammers were provided with an electric heating element that could give the hammers an automatically controlled temperature, less than 250^oC. By the present measurements, the temperature of P2 was kept at room temperature. The temperatures were measured by thermocouples. On the weights, a small laser was mounted, where a beam of light could sweep a linear detector beneath. The signal from the detector was registered on an oscilloscope that could give the sweep time for a given distance on the detector. From these registrations could the velocity of the hammers before and after the impact be determined.

The experiments were started by making measurements without paper specimen. The signals from the piezoelectric cells gave the force-time curve, from which the load-time integral, i.e. the impulse, the maximum load, the maximum as well as the mean time span of the curves, were read. To simulate multi-nip calendering, the test paper was kept on the hammer P2, while the operation of the pendulums was repeated at the given number of impacts.

The specific impulse from P1 at the impact was measured to be 9.5, 12.5, 16.0, and 20.0 $kNsm^{-2}$, from the respective starting positions. In addition, some experiments were done with other values of the impulse.

The following characteristics of the paper specimens could be determined: geometrical deformation in three coordinates, surface smoothness, by Parker Print Surf, PPS, and surface gloss, Hunter gloss 75^o.

The thickness of the specimen, recognized as the z-coordinate, ZD, was measured before and after impact by use of a standard micrometer. From the ratio of these measures, the relative change of the density of the paper upon impact could be determined. In addition to the strain in the z coordinate, some indicative measurements were made, on magazine paper, of the deformation of the surface in the machine direction, MD, as x-coordinate, and in the cross direction, CD, as y-coordinate. For the measurements two small holes 20 mm apart, were stuck into the specimen in the MD, and in the CD. The distance between the holes was measured under microscope, before and after the calendering, from which the relative displacement of the respective holes could be evaluated.

Results

In the following, experimental results are given to demonstrate some characteristic features of the pendulum apparatus.

Pendulum criterions

Experimental results from the operation of the pendulums gave, for the respective starting position of P1, values for the specific impulse indicated as dotted lines in Fig. 2.3. The operational domain of the pendulum apparatus covers, to a large extent, the operational domain of industrial calenders, especially high speed calenders. For example, the line for the impulse of the pendulum, $i_p = 16(kNsm^{-2})$, correlates the condition of rollers running at a speed $25ms^{-1}$, having a nominal line pressure of $400kNm^{-1}$. Fig. 2.3 features the basis from which the pendulum apparatus has to be recognized for the simulation of an industrial roller calender.

The value of the integrated impulse of the respective pendulums, differed within

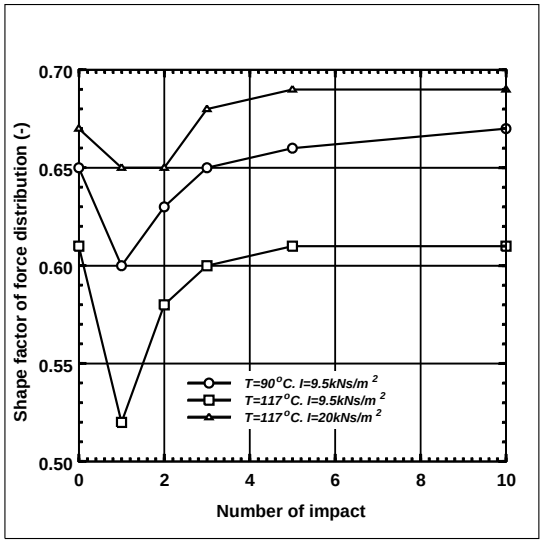

Figure 2.5: Shape factor of force distribution by impact, versus number of impacts. Number zero is for impact without paper.

1.5%, their mean value was evaluated for further calculations. The shape factor of the load distribution curve was found to be higher than 0.5, as given in the literature for rotating rollers. This is illustrated in Fig. 2.5, from measurements on newsprint. The shape factor depends on the impulse and on the mechanical properties of the hammer inclusive the paper specimen. It increases with increasing impulse and decreases with increasing temperature. The factor's decrease, as seen in the curves, when the temperature increases from 90 to 117^oC, may indicate transition of a glassification temperature of the paper. The shape factor seems to be a useful parameter in this context.

Energy conversion

In Fig. 2.2 some values are plotted of the relative velocities after impact and the relative converted kinetic energy ζ of the pendulums, large marks from measurements without paper specimen, small marks from the measurements with newsprint. The restitution coefficient of the impact is low, indicating that a large part of the kinetic energy is converted to internal energy of the pendulums. The coefficient is depending on the mechanical property of the hammers and the specimen. Measurements with the P2 steel hammer, gave a coefficient $e < 0.2$, with the elastomer layer on P2 the coefficient was increased, indicating a decrease of vibration of the pendulums after impact. The discrepancy between the plots from the measurements on newsprint and the theoretical curves, calls for further studies of the velocities of the pendulums after impact.

Deformation of paper specimen

Fig. 2.6 shows results of the permanent compression of newsprint after first impact, as the relative density versus temperature, for two levels of specific impulse. The density increases with increasing impulse and, to a lesser extent, with increasing temperature of the hot hammer. The figure gives also, for comparison, some derived results for newsprint from soft roller calendering under similar conditions, that indicate the same trends, van Haag (1997), Keller (1992) and from steel roller calendering, Browne et al. (1993).

The permanent compression of the paper depends in complex relations on the exerted load, the dwell time under load, and on thermal and mechanical properties of the rollers/hammers and of the paper specimen between. In the literature attempts have been made to derive the functional relation between them, (Nutting (1921), Buchdahl and Nielsen (1951)). Nutting proposed the expression for the permanent deformation, $\epsilon_p = \psi\sigma^\gamma t^d$, as a function of a characteristic stress σ, the maximum stress, resp. dwell time t, where ψ, γ and d are material constants. For rollers resp. pendulums is the relation between load resp. impact force and dwell time mechanically coupled as the integrated impulse. By the rollers, the nip width, and thereby the dwell time of the paper, increases with the line load, whereas the dwell time for the present physical pendulums decreases with increasing impulse, which, besides, differs from the behav-

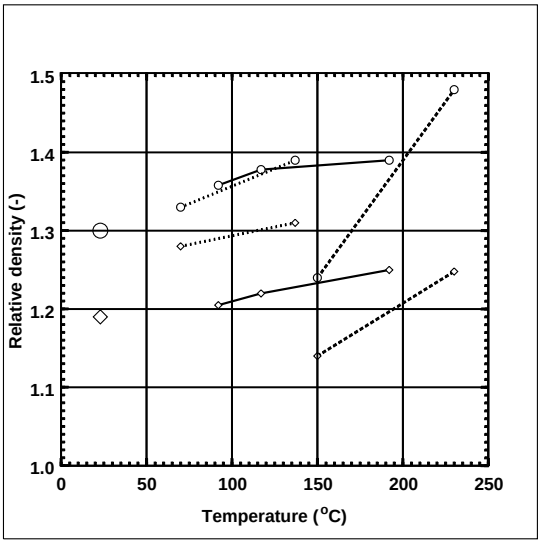

Figure 2.6: Relative density of newsprint versus temperature of hot hammer by pendulum calendering. ◇ impulse $9.5kNsm^{-2}$, ∘ impulse $20kNsm^{-2}$, — our measurements, and ⎯ ⎯ Keller (1992) resp. .... van Haag (1997) from soft roller calendering. ♢, ◯, Browne et al. (1993) from steel rollers.

iour of ideal pendulums with elastic spherical bodies, having a dwell time by impact that increases slightly with increasing impact, (Hertz (1881)). The proper basis for a comparison of the permanent compression of paper by the respective techniques, rollers/pendulums, seems, from the discussion above, to be the specific impulse, as the integrated load versus dwell time, a conclusion that is supported by the findings of Keller (1992). Alternatively, a combination of the maximum line load and the shape factor of the load distribution in the nip, might also form a useful variable.

van Haag determined, by numerical simulation, the nip width at varying nip load in soft calendering of newsprint, (van Haag (1997)). The data from his results are insufficient for the estimation of the specific impulse, however, they indicate that the width/dwell time depends on the maximum line load raised to a power of approximately 0.26. Wickström et al. (1997a) studied the calendering of coated paper in an extended soft nip. Their findings gave values for the Nutting equation $\gamma = 0.618$ and $d = 0.143$. In this case the dwell time is partly a free variable by operating the extended nip, and is of marginal interest in the discussion above.

From our measurement on magazine paper, with steel/steel hammers, the density was found to depend on the maximum impact pressure raised to - 0.13, and on the specific impulse raised to - 0.15. For soft/steel hammers the exponent was - 0.15, in both cases slightly depending on the temperature and on the number of impacts. For newsprint on soft/steel hammer, the exponent for the specific impulse was found to be -0,22, also depending on the impact number and on the temperature of the hot (steel) hammer. The dwell time decreased by increasing number of impacts tending to the value for the case without paper specimen, it increased by increasing temperature of the hot pendulum. The results indicate that the specific impulse has a stronger influence upon the dwell time of newsprint than on magazine paper, reflecting the different constituent of these paper qualities. The relative weak dependency of the temperature indicates that heat is transferred, during dwell time, to the fibres of a very thin layer of the paper surface, and that this layer attain the temperature of the hot hammer. The fibres inside that layer are more or less unaffected by the temperature increase of the surface.

The deformation in MD- resp. CD-coordinates of the specimen, is illustrated in Fig. 2.7, where the relative expansion is plotted against the number of impact. The strain seems to be equal in the two directions after the first impact. For successive impacts, however, the deformation in MD quickly approached a nearly constant value, while in CD it proceeded to a substantially higher value. Under the assumption that the fibres are more orientated in the MD, the results is reasonable. The fibres strengthen the paper in MD, it can therefore withstand a certain radial pressure. In CD, the binding between the fibres is probably weaker, and the deformation will be larger.The results gave a strain of order 1%, that is an order of magnitude smaller than the strain in the

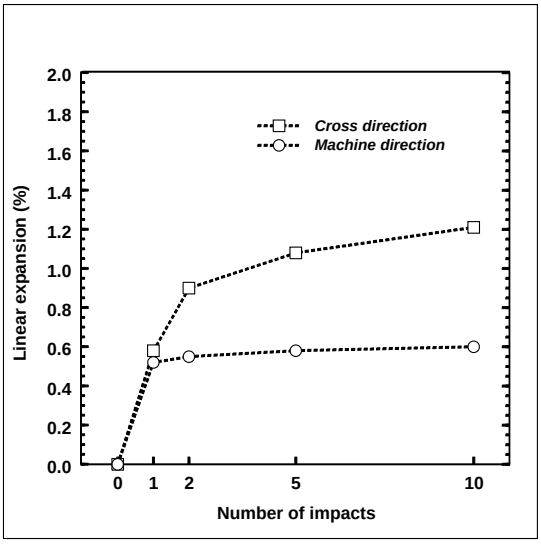

Figure 2.7: Linear expansion in MD and CD of the surface of SC paper after given number of impacts, at room temperature, moisture content $6 \pm 1\%$, temperature 126^oC, specific impulse $12.5kNsm^{-2}$.

z-direction. The permanent deformation versus the number of impact, is qualitatively confirmed by results from roller calendering, (Baumgarten (1975)).

The force that is exerted on the paper by the pendulums, has in principle, axial symmetry. Any asymmetry in the results of the radial deformation reflects therefore the anisotropy of the paper. Roller calenders may not be appropriate for a study of this effect, where the load on the paper introduces a linear symmetry. However, Gratton's results, (Gratton (1997)), from roller calendering of newsprint, show qualitatively a similar relation between the deformation in MD and CD. Rodal (1993) made a numerical analysis of the deformation of paper in the roller nip under static load. His results show the plastic deformation in CD to be roughly one third of the deformation in ZD, substantially larger than by pendulum impact.

Gloss

Fig. 2.8 shows a plot of the gloss in MD and CD in relation to the deformations of the surface. In MD, the gloss seems to gain by the increasing number of impacts, without any further deformation of the surface as seen in Fig. 2.7. In CD, the contrary seems to be the case, the gloss is relatively stable despite that the paper continues to deform.

In this investigation it is of interest to find relevant results in the literature from roller calendering, that could be compared with our results from the pendulum calendering, namely from roller calendering in single nip under given line pressure and

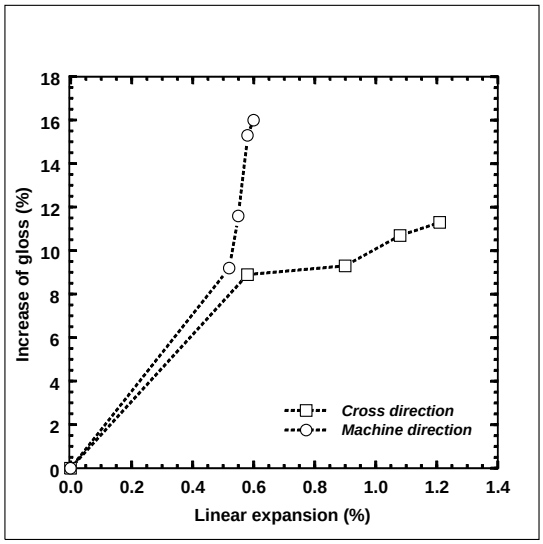

Figure 2.8: Increase of gloss versus linear expansion by pendulum impacts. Conditions as in Fig. 2.7.

roller speed. Only two papers seems to satisfy this, dealing with roller calendering of newsprint.

Fig. 2.9 illustrates the results from our measurements on newsprint, where the gloss, after one impact, is plotted as a function of the temperature of the pendulum, P1, at three specific impulses. The open plots show the front side of the specimen, facing the steel hammer, the filled plots the back side. The figure also shows the results of Kurtz and Hess (1991), for the calendering of newspaper in a single nip in a laboratory calender. The conditions used in their measurements were nearly the same as ours, ($i_p = 9.5 kNsm^{-2}$), namely specific impulse $i_r = L_r/u = 8.6 kNsm^{-2}$, (Nip line force $L_r = 150 kNm^{-1}$, speed $u_r = 17.5 ms^{-1}$, temperature of the paper 20^oC, and moisture content 8%). Our plots report the mean values of the gloss in MD and in CD, while Kurtz and Hess do not indicate the orientation of the gloss measurements, giving data that are slightly higher than ours. As mentioned earlier, the shape factor of the load distribution upon the paper seems to be lower with rollers than with the pendulums. This means that the dwell time is relatively longer by roller, indicating that the gloss is improved by increasing dwell time. This may be a reason for the difference between the plots from Kurtz and from our measurements. They show a similar functional dependency of the temperature. Fig. 2.9 shows also two plots from Keller and Waech (1992), describing roller calendering in two nips, first by a hot steel roller, and then by a soft roller, both at specific impulse $20.6 kNsm^{-2}$. The result at 60^oC is relatively high, probably due to higher gloss of the uncalendered paper, 7.3%, compared to our 4.2%. At 230^oC, the temperature is a dominant factor for the gloss, the plot fits reasonably

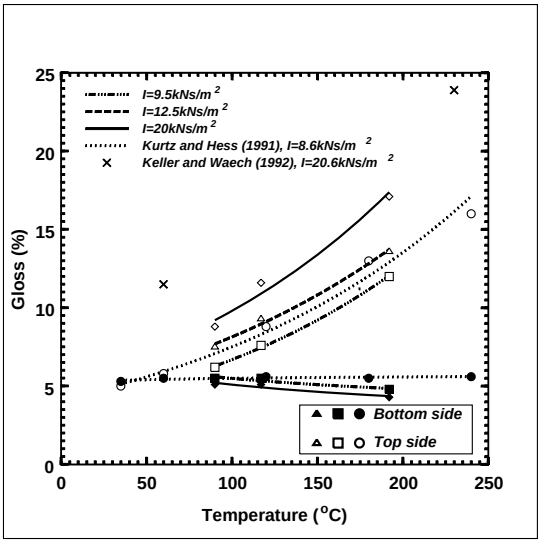

Figure 2.9: Gloss for newsprint versus temperature of hot hammer after one impact.

well to our plots for 192^oC. As indicated by the foregoing plots, the soft roller adds very little to the gloss. It can therefore be concluded that the results from Keller and Waech agree fairly well with ours, and that the pendulum device simulate fairly well the operation of roller calenders.

Fig. 2.10 shows the gloss versus density of the newsprint, with the temperature as

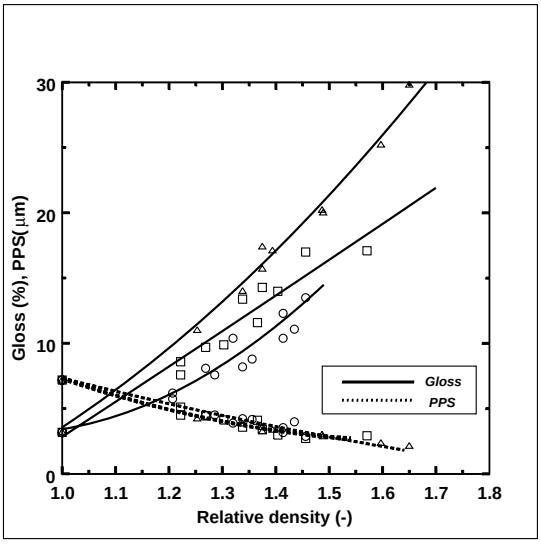

Figure 2.10: Gloss respective PPS by pendulum calendering of newsprint versus relative density of paper. — gloss, __ PPS. ∘ 90^oC, □ 117^oC, △ 192^oC.

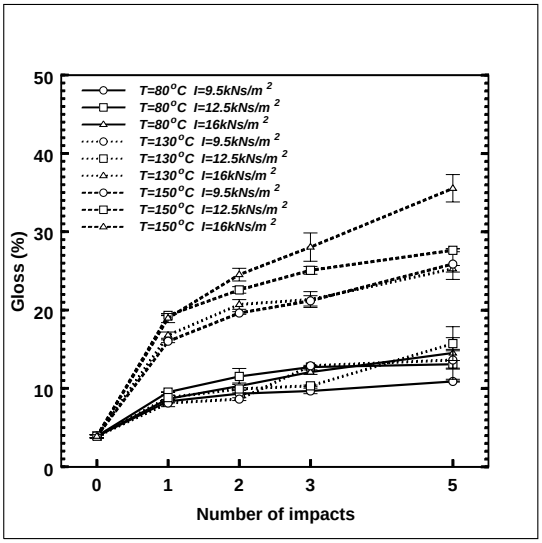

Figure 2.11: Gloss versus number of impact of SC-paper.

parameter. The curves are fitted to the plots as second order polynom.

Fig. 2.11 gives results of the gloss from measurements on magazine paper depending on the number of impacts. They show the strong dependency of the temperature, and also a nonlinear character upon the number of impacts.

Smoothness

Fig. 2.10 shows the results of measurements of PPS on newsprint versus relative density. They indicate a very close relationship between smoothness of the surface and the density of the bulk, and seems to be one of the closest relationship that the calendering process can give.

Fig. 2.12 illustrates PPS by two specific impulse levels, 9.5 and $20kNsm^{-2}$, for different temperatures. In addition, results from the literature on roller calendering are shown, Keller and Waech (1992), and Tuomisto (1992). The data are derived for corresponding specific impulses and temperatures. Keller (1992) calendered in a single nip of steel rollers. He points out that the smoothness seems to be strongly impulse related, as also indicated by our data. It can be noticed that the data from pendulum calendering are slightly lower than those from the roller calender, a circumstance that may be referred to the higher shape factor of the pendulum calender. The two other references are dealing with calendering in two nips. First, a hot roller of steel, and then a soft roller, both with specific impulses corresponding to ours. These plots indicate that the soft roller improves the PPS substantially.

Results from the measurements on SC-paper, are given in Fig. 2.13, showing data

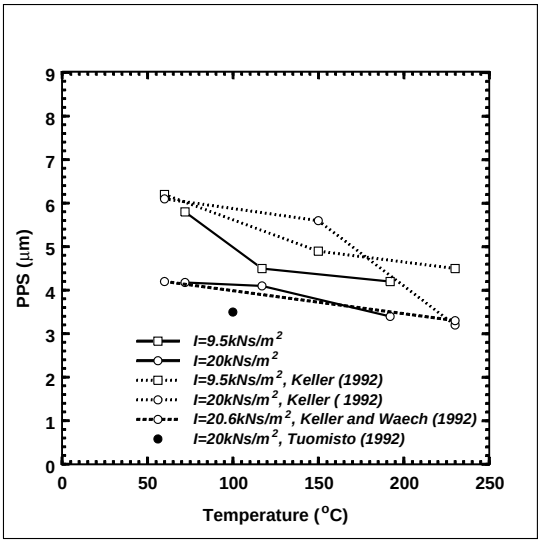

Figure 2.12: PPS data for newsprint versus temperature at two levels of specific impulse. Keller : single nip by steel rollers, Keller and Waech, Tuomisto : two nips, a single hot steel roller, followed by a soft nip.

of PPS in dependency of the number of impacts, temperature of the hammer and the specific impulse.

A relevant question is, to which extent the product of the number of nips and the specific impulse is relevant for achieving a given surface property of paper. Our mea-

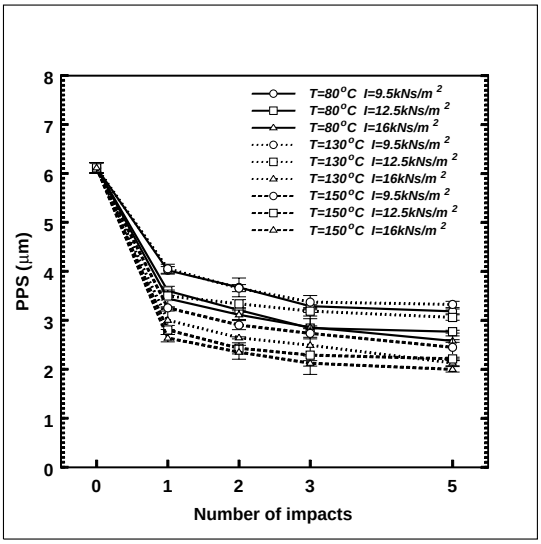

Figure 2.13: PPS data for SC paper versus number of impacts.

surements, Fig. 2.11 and Fig. 2.13, indicate a decreasing sensitivity of the gloss, resp. PPS upon increasing number of impacts/nips. The first impact at high temperature is most effective. For successive impacts, it can be shown that for example, a doubling of the specific impact and a halving the number of impacts, increased the gloss about 20% at a given temperature of the paper. PPS-data showed even less improvement.

Energy absorption

The energy brought into the impact is the kinetic energy of P1. About half of it is converted into other forms, of which a very small amount may enter the paper specimen as compression work. It can tentatively be expressed as a ratio between the measured kinetic energy that is converted, with paper, ζ, and without paper ζ_0. The energy conversion ratio for the paper is then

$$\alpha = \frac{\zeta}{\zeta_0} \tag{2.15}$$

A value of $\alpha \geq 1$ indicates an increase of converted kinetic energy, an amount that may be assumed to represent the work that is absorbed by deforming of the paper specimen.

Fig. 2.14 shows some results of α at three hammer temperatures, from measurements on newsprint, plotted against the number of impacts. At 90^oC, the energy absorbed by the paper was substantial, of the order of 10% of the converted energy,

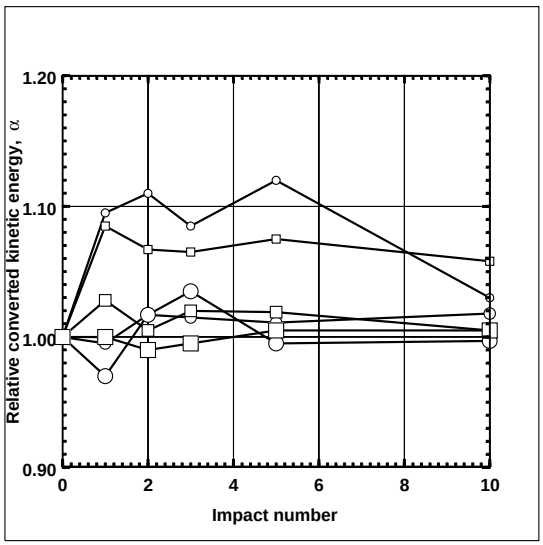

Figure 2.14: Relative converted kinetic energy α, versus number of impacts. $9.5kNsm^{-2}$: □ 90^oC, □ 117^oC, □ 192^oC. $20kNsm^{-2}$: ○ 90^oC, ◯ 117^oC, ◯ 192^oC.

while for higher temperatures, 117^oC, and 192^oC, it was smaller. The low energy absorption may be due to the temperatures being above the glass transition temperature for the paper, Back and Olsson (1983). The plots in Fig. 2.14 indicate further that, by increasing number of impacts, the mechanical work on the paper diminishes while the surface gloss is increasing, as seen from Fig. 2.11. More measurements should be made on different paper qualities to deepen this discussion.

Conclusions

The experimental apparatus described, represents a supplement to the existent equipments for studying the calender process. The apparatus is relatively cheap, easy to operate, and its operation is based on the fundamental laws of mechanics. It features elementary quantities for the measurements, that, in principle, can be developed to high precision.

The results from the present, preliminary measurements, gave a reasonable basis to recognize the apparatus for simulating the industrial roller calenders. It seems also to be a convenient tool by studying details of the paper physics related to the calendering process.

2.2 Supplements to Paper I

This paragraph includes a further discussion of the capacity of the pendulum device, and the results of experiments in addition to those reported in Paper I. The discussion of the differences and similarities of the calendering feature of the rollers resp. the pendulums are brought further. Additional experiments are made with variation of among other the moisture content of the paper specimen, concerning:

- the compression of the paper in z-direction by the impact
- dwell time
- paper properties
- calender equation

2.2.1 Experiments with moistening the paper specimen

The surface properties of the paper achieved by calendering has so far been discussed in dependency of impulse force, temperature and the number of impacts. In this paragraph the influence of moisture content in the paper is discussed. Experiments were made with different mean bulk moisture content as well as with moisture gradient throughout the specimen. However, to establish a controlled moisture gradient is experimentally much harder than to introduce a similar temperature gradient throughout the paper specimen. The investigation should therefore be looked upon as an attempt to get some qualitative indications of the influence of the moisture content.

The improvement of the surface properties gloss and smoothness by calendering, is achieved at the cost of loss of fibre strength and of paper thickness reduction. This loss can be reduced if plastic deformations is created at or near the surface of the paper, which is promoted by increased temperature and moisture content of the fibres of the surface layer, Back and Salmén (1980). The temperature gradient calendering is therefore improved further by adding moisture to the paper as its enters the nip. In this way the fibre material can reach the glass transition state, and a reduced nip pressure can be applied. Lyne (1977) demonstrated the effect of moistening. Dunfiled et al. (1986) showed that spraying water on the paper is less effective on improving the surface properties than blowing steam. Water may have a cooling effect of the paper as well as the roller, depending on the psychrometric effect.

For the present experiments the pendulum apparatus was placed inside a closed room, a greenhouse, where the relative humidity of the air could be kept at constant levels within 45 - 85%, at the room temperature 22^oC.

Two methods were used in giving the paper specimen its moisture content:

- a mean moisture content was achieved by storing the specimen in the greenhouse for at least 24 hour to attain the equilibrium moisture content, and

- at a given time before impact the surface of the specimen was moistened by a spray of air-water mixture. An amount of approximately one $gram(m)^{-2}$ was thereby added to the surface. The delay time between spraying and the first impact, alternatively prior the each successive impact was one second. This method was an attempt to establish a moisture gradient in the paper.

At given temperature on the hammer and moisture content, five levels of impulse were applied. The paper specimens were evaluated for gloss and thickness. Gloss was determined as 75^o Tappi norm in MD as well as CD. Initial and final density of the specimen was calculated from thickness as grammage/thickness, (kgm^{-3}).

2.2.2 Compressive work on the paper by impact in z-direction

SUMMARY: The experiments were made with the intention to record the deformation of the paper specimen during the impact. Several measuring techniques were discussed, counting on resources as well as expected time consumption for the experiment. It ended up with the application of a linear variable differential transformer LVDT for recording the deformation. The experiments were made on specimen of uncalendered SC-paper and on specimen having undergone one or two impacts beforehand. Results are given as thickness of the specimen versus time during the impact. From the recorded data the mechanical work absorbed in the specimen is evaluated, and compared with data from literature. The uncertainties of the results are discussed.

Introduction

The calendering process has mainly two purposes, one is to increase the bulk density, in order to control the mechanical properties of the paper, the other is to improve the qualities of the paper surface for printing. The density increase of the paper by compression has been subjected to numerous investigations. Experimentally they have been directed toward describing the thickness reduction in its dependency of the related parameters, pressure and its dwell time as well as the temperature and moisture content of the paper. The experiments have been carried out by typically two methods, by using a laboratory roller calender, or by using hammer-anvil type of equipment, where static as well as dynamic techniques could be used. The results from the experiments were, generally, given as thickness reduction at the end of the compression, while the thickness decrease during the compression has been less described.

Brecht and Schadler (1961) compressed paper specimen between two parallel plates and studied the mechanical as well as printing properties of the paper by measuring the strain under dwell times 2 ms, 0.1 s, resp 2.5 s.

De Montmorency (1967), studied the thickness reduction and surface properties of newsprint using a laboratory roller calender. Osaki and Yoshihiko (1978), compressed handsheet paper using static as well as dynamic technique and studied a modulus of elasticity in the z-direction, the results of which indicates that the modulus is strongly depending on the compressive pressure, i.e. of the density of the paper.

Burton and Sprague (1987), determined the density profile in the z-direction during the compression of handsheet paper, in which reference position targets were imbedded. Rodal (1989) used data from de Montmorency's paper to evaluate the elasticity properties in z-direction of newsprint.

The work that is imposed on the paper during the compression has been investigated in a lesser extent. The basis for evaluating the work is the product of compression force and the reduction of the thickness of the paper. It can be expressed by $Nm(m)^{-2}$ or Jm^{-2}. As far as we have recognized two papers are dealing with this, namely papers by Howe and Lambert (1961), resp. by Colley and Peel (1972). Howe and Lambert found that about 30 % of the total energy input to the machine calender was consumed by the compression work of the paper. Colley and Peel pressed groundwood paper by 35 MPa and found a value for the compression work to be typically $400Jm^{-2}$.

The intention of the present study is to investigate the rate of compression of the paper during the impact of the pendulums. The lateral compression of the paper during the impact is studied and the compression work imposed on the paper is evaluated.

Theoretical considerations

The impulse force by the impact of the pendulum hammers introduces a wave of distortion in the contact zone. The wave propagates axially through the different bodies making the hammer, i.e the paper specimen, eventually the polymer layer and finally through the steel body, with a velocity depending on the mechanical properties of the respective materials. The wave will be reflected at the boundaries between the bodies, according to their natural frequencies. The natural frequency is evaluated as

$$2\pi/\Lambda = 1/Z\sqrt{G/\rho} \quad (s^{-1}) \tag{2.16}$$

where Z is the axial dimension of the body, G is modulus of elasticity and ρ is density of the material, and with Λ as the nominal period for the wave. In the present case Λ can be evaluated to $1\mu s$, 0.06 ms and 0.23 ms for the paper specimen, the polymer cover resp. for the steel body. The impact force featuring an impulse with a period of about 2 ms, thus it is orders of magnitude higher than the values of the respective

constituents. From this it can be assumed that the stress-strain relation in the paper specimen follows the impulse force during the impact duration, and we assume, as a first approximation, that the deformation of the paper is proportionate to the force.

During the impact the impulse force will be balanced by the stress created in the assembly. The differential equation of the work balance during the impact is

$$dW = -Fdz = -\sigma d\epsilon_a \quad (Nm) \tag{2.17}$$

where F is impulse force, z is axial coordinate for the impulse, σ is compressive stress in the paper, and ϵ_a is the apparent strain in the paper and the support, and with minus sign indicating the work to be positive by compression. This work is converted into elastic and plastic deformation of the paper as well as of the hammer, in which also vibrations are created.

The sequence of decreasing force, an eventual increase of the thickness will take place, the paper is pushing back and the force is doing negative work. The nominal work done on the paper is the difference between the work W_c, from the compressive resp. W_e, from the expansive sequence of the thickness. When the paper behaves complete elastic, the net work is zero. Normally the paper is given permanent deformation during the compression, and the net work will have a finite value, that is to be correlated to the permanent deformation of the paper. This net work can be evaluated as

$$W = W_c - W_e = \int_0^{t_m} F(t)z(t)dt \; - \; \int_{t_m}^{t_e} F(t)z(t)dt \tag{2.18}$$

where the force resp. the thickness of the paper are function of time t. t_m indicates the time when the force is at a maximum, and t_e the end of the dwell time. The force versus time and the paper thickness versus time are to be determined by measurements.

Experimental

Apparatus and instrumentation

A sketch of the pendulum apparatus is described in chapter 2 and shown in Fig. 2.4

For the measurement of the paper compression in the nip a linear variable differential transformer (LVDT) was chosen. Fig. 2.15 shows a sketch of the arrangement of the LVDT. It is mounted on the hammer P2 with its sensing rod touching a bracket on P1. The LVDT output varied linearly with displacement, and the slope of the calibration was stable with repeated calibrations. The linearity is $\pm 0.25\%$ of full range output, and the sensivity is $0.165 mV/\mu m$. The sensivity of the sensor was increased by adding a spring load force, in addition to the existing spring load. The LVDT output was registered, filtered, and amplified with a Shaevitz LVDT compatible signal conditioner, type ATA-2001 LVDT amplifier. The gauge head was fixed at the lower end of

pendulum P2. At the lower end of P1, a solid face, made of aluminum, was fixed, and when impact area of P1 and P2 are touching each other, a signal from the LVDT was generated as the tip of the gauge was moving.

The LVDT was calibrated using a standard thickness gauge, a spring loaded AC operated gauge, type GCA-121-050 Shaevitz, designed for $\pm 1.27mm$ range measurement.

A Nakamitzu micrometer and LVDT sensor were compared by measuring the thickness of aluminum foil with a thickness of $30\mu m$. The foil readings agreed with the LVDT sensor within 1%.

The tip of the gauge head is following the displacement as long there is contact between the two pendulums. Hence, $z(t)$ for times larger than dwell time is not registered.

Experimental procedure and measurements

Standard SC-paper samples were examined in this study, and had been taken from machine reels before supercalendering and cut into circular sheets with a diameter of 50mm.

All measurements were made under isotherm conditions. The paper was conditioned in a room maintained at $50 \pm 5\%$ relative humidity and 23 ± 1^oC. The initial moisture content of the paper specimens were measured, by spot check, to $8 \pm 1\%$.

In addition to the experimental runs with impact on paper specimen, some runs were made without paper to trace some intrinsic deformation of the hammer system. The output from the oscilloscope of these measurements was given as compression $z_{ref}(t)$ versus t, the dwell time of impact. Similar function for runs with paper specimen was $z_s(t)$. The thickness of the specimens before and 1 min after impact were z_0 resp. z_r, measured by the micrometer. The results of the thickness measurements are given as mean from five measurements.

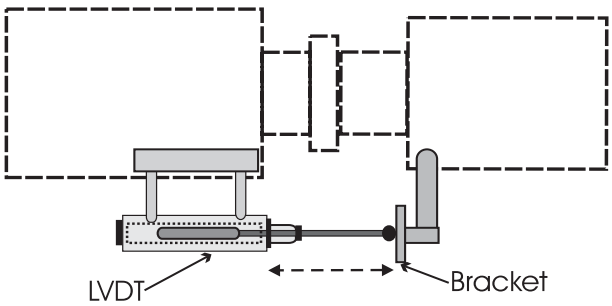

Figure 2.15: Principle sketch of the arrangement of the LVDT.

Results and discussions

Fig. 2.16 and Fig. 2.17 show the compression curves of the results of SC-paper specimen taken after successive impacts of the pendulum apparatus. The bell shaped curve is the pressure versus time for the impacts. The pressure curve has a maximum pressure of 25 and 16MPa, and the dwell time is approximately 0.5 and 1ms, respectively for hard nip and soft nip. The compression curve of the system with paper is denoted as dotted lines, where the upper and middle curve represents the first and second impact respectively. The lower dotted curve is the compression curve by means of blank runs without paper. The calculated apparent dynamical compression curve of a single specimen corrected for press deformation is shown as solid lines. The specimen taken before the impact has a large peak compression as the paper progresses through the successive impacts, there is a decrease of the peak compression and a small increase of the peak pressure reached in the testing. The increased peak pressure is due to a more compressed paper giving a higher restitution coefficient of the paper(smaller plasticity of the paper).

Tab. 2.1 show the manner in which the paper thickness changes as the specimen progresses through the number of impacts. Minus sign indicates a thickness reduction. The "initial" thickness is the measured thickness of uncalendered specimen. "Max. compression" thickness denotes the peak compression of the specimen during the impact, and "recovered" thickness is the measured thickness after the impact. An average recovery of the paper history was found to be approximately 30%.

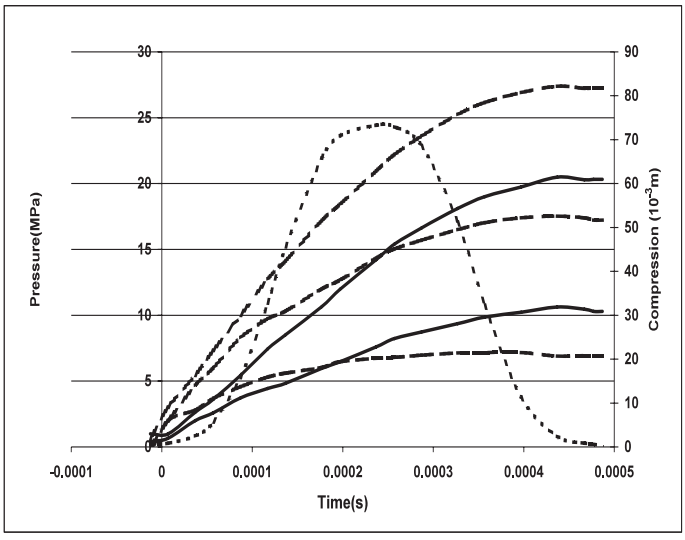

Figure 2.16: Dynamic compression curve versus dwell time for SC-paper calendered in a hard nip with a maximum pressure of 25MPa. For explanation, see text.

The results of soft nip calendering gave a higher recovered thickness and a lower peak compression after one and two impacts compared to hard nip as shown in Fig. 2.17 (see also Tab. 2.1.). The kinetic impulse at impact was the same for hard and soft

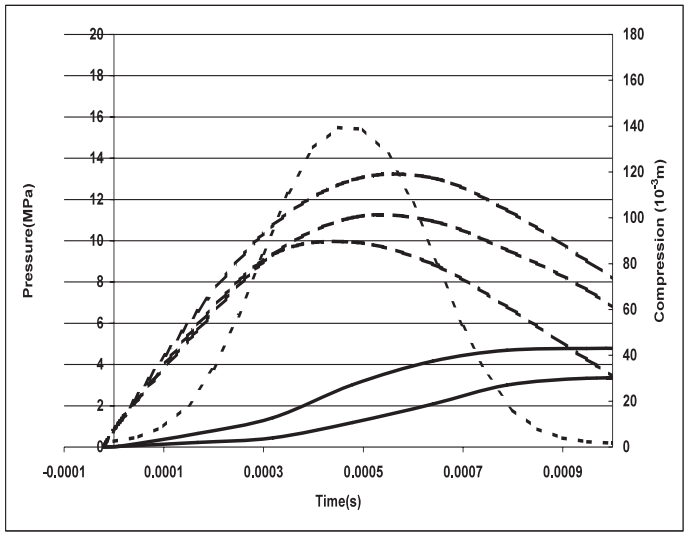

Figure 2.17: Dynamic compression curve versus dwell time for SC-paper calendered in a soft nip with a maximum pressure of 16MPa. For explanation, see text.

nip, but hard nip (machine calenders) generally produces bulkier papers than soft nip calenders, and the different actions of the two concepts may be explained as follows. Paper has a non-uniform thickness, the result of both basis weight and bulk variations on a microscale. The reduction in a thickness brought about by hard nip calendering is limited by the need to avoid the formation of glossy plateaux, which give the effect of fibres, particularly at high spots, to the almost rigid hammer surfaces. The soft nip, with a much softer cover, does not impose such great extremes of normal stress on high spots, so that these local (plastic) conformations will be less extensive.

Table 2.1: Paper history through the number of impacts for SC-paper calendered with hard- and soft nip at respective pressures of 25 and 16MPa.

Number of impact		Thickness (μm)	
		Hard nip	Soft nip
	Initial	90	90
1	max.compression	-60	-40
	recovery	60	73
2	max.compression	-30	-31
	recovery	47	58

Work of compression

This quantity for hard nip and soft nip calendering of SC-paper is estimated from the appropriate areas of the estimated curves of work shown in Fig. 2.18 and 2.19, denoted as dotted lines. As can be seen, the maximum compression work is approximately 2.3 J and 0.8 J for respectively hard- and soft nip in the first impact. Approximately 1.2 and 0.4 J after second impact. Due to the compression area, work per area is then estimated to be approximately $500 Jm^{-2}$. The energy brought into the impact by the pendulum apparatus is the kinetic energy of P1. It is estimated that about half of it is converted into other forms, of which a very small amount enter the paper specimen as compression work. It is shown that the energy absorbed by the paper is substantial, of the order of 10% of the converted energy. However, our results seems to correspond well to values found by Colley and Peel (1972).

The permanent deformation and dynamic compression of the paper is strongest in the first cycle of loading-unloading series, and thereby a decreasing work, and this indicates that the remaining compression of the paper from subsequent cycles, is approaching elastic in nature. In other words, the properties of the paper sheet is reaching a maximum value for permanent set and elastic modulus, with a corresponding minimum in relative compression.

Uncertainty analysis

The bias errors of the instruments were determinated by calibration tests conducted before and after the experiments combined by the root-sum square method, estimates of errors that influence the measurement of the respective variables. The deviation

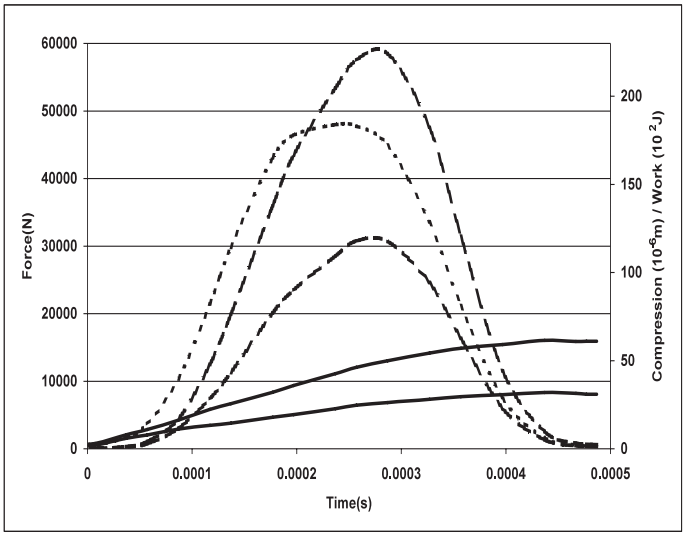

Figure 2.18: The product of paper deformation and load, work, as a function of the dwell time for hard nip.

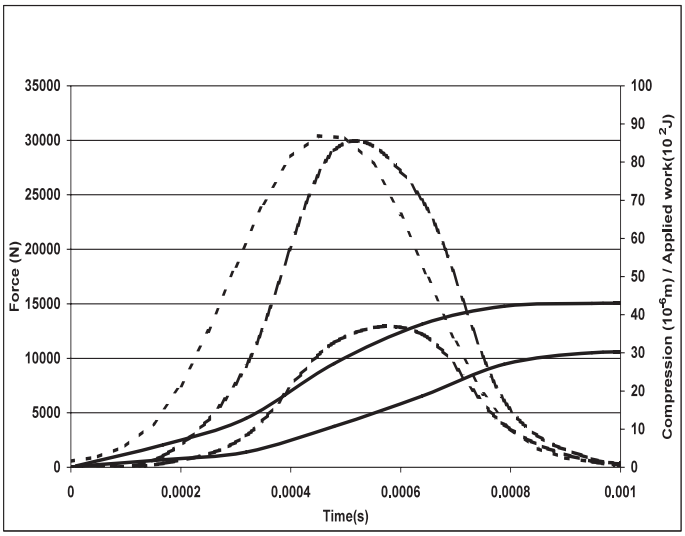

Figure 2.19: The product of paper deformation and load, work, as a function of the dwell time for soft nip.

of the loading cells and the LVDT instrumentation is less than 1% respectively. The errors in the initial and recovered thickness are due to the resolution of the micrometer that is 1 micron.

The precision limit, i.e. the interval about a nominal result was measured with the apparatus in normal running condition, and the compression measurements gave a deviation of 7%. The deviation in the initial and recovered thickness measurements was 3%. The deviation in the pressure/force measurements are lower than 0.5%.

It is found that the 95% confidence uncertainty level of the paper compression curve is in the order of 7%. The error caused by the technique is not considered in this confidence level. I.e., the contribution is mainly from the systematic error of the compression measurements. The high uncertainty of the compression measurements is due to the difficulties of measuring a small dynamic thickness reduction within a millisecond at magnitudes of 25-50kN, and the vibration disturbances of the gage head during the impact.

Conclusion

An existing pendulum apparatus has been modified in which single paper specimen may be effectively subjected to a constant kinetic impulse for periods of time down to a millisecond, during and after the application of which the thickness of the compressed specimen may be measured.

The general reliability of the dynamic compressibility tester has been shown to give results accurate to within 7%.

Thickness change is a function of pressure and of duration of pressure. The depen-

dence of thickness under load on the time of load application is much less than that of recovered thickness. Hard nip gave a smaller recovered and thickness under load than soft nip at same kinetic impulse.

Repeated pressure cycles of equal magnitudes altered the paper thickness under load, and reduced the recovered thickness.

The power analysis has shown that almost $500 Jm^{-2}$ is efficiently utilized in the in-nip compression of the paper specimen.

2.2.3 Dwell time

Roller calender

A principle sketch of a roller calender is shown in Fig. 2.20. The rollers are driven with a peripheral speed of $u(ms^{-1})$ and a line load $L(Nm^{-1})$. The nip width $a(m)$ is depending on the line load and the mechanical properties of the material of the rollers. The dwell time of the paper in the nip is then $t = a/u(s)$. It is proportionate to the nip width and is inverse to the paper speed, also a running condition. For example with a paper speed of $1500 m(min)^{-1}$ and a nip width 8mm, gives a dwell time less than 1 ms. The paper undergoes in the nip a compressive force in a sequence of rising to a maximum and then falling back to zero in a nearly symmetric function of time. The force distribution over the nip is very difficult to determine by rotating rollers, reliable experimental results are available only for stationary rollers. In the temperature gradient calendering, one of the roller is heated to a given temperature. The fibres of the paper in contact with the roller is then heated, softening the fibres, that improves the surface gloss and smoothness.

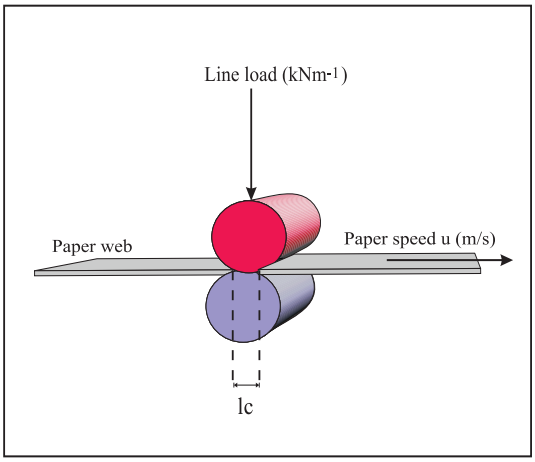

Figure 2.20: An illustration of the paper passing through a roller nip. The properties of the paper can be altered by controlling the line load and the residence time in the nip (l_c), i.e. the speed of the rollers.

By soft rollers the nip width, and thereby the dwell time of the paper, increases with increasing line load, nearly independent of the impulse that the paper experiences, i.e. of the paper speed. The literature is scanty on investigations of the dwell time by roller calenders, but the mechanics that takes place in the contact zone of two colliding bodies was first studied by Hertz (1881) who described the deformation at the contact area of two spherical bodies. Extended to cylindrical bodies, the nip width of the contact area can be described by

$$l_c = \sqrt{(4LR^*/\pi G^*)} \tag{2.19}$$

where L is line load(Nm^{-1}), R^* is equivalent radius of the rollers r_1 resp. r_2,

$$R^* = 1/r_1 + 1/r_2 \tag{2.20}$$

and G^* is equivalent modulus of elasticity, given by

$$1/G^* = (1-\nu_1^2)/G_1 + (1-\nu_2^2)/G_2 \tag{2.21}$$

where ν_1, ν_2, G_1, and G_2 being resp. the Poisson's number and modulus of elasticity for the respective rollers.

The nip width is from this expression proportionate with the square root of the line load and inverse proportional to the square root of the equivalent modulus of elasticity and so should the dwell time for paper be in the nip for a given paper speed. However, it has been shown that a paper specimen in the nip has a substantial influence upon the load distribution over the nip,(Keller (1992), van Haag (1997)). From van Haag's numerical simulation of the load distribution, can the nip width be evaluated for stationary as well as for rotating rollers. For stationary rollers the width can be expressed by the power law

$$l_c = 3.56L^{0.25} \quad (mm) \tag{2.22}$$

and, for rotating rollers at a speed of $915m(min)^{-1}$

$$l_c = 2.79L^{0.26} \quad (mm) \tag{2.23}$$

where the line load is in kNm^{-1}.

We see that the dependency of the line load is weaker than the Hertz theory indicates. The dwell time can then be calculated as

$$t_d = l_c/u \sim L^{0.27}/u \tag{2.24}$$

where u is the paper speed in $(mm)s^{-1}$.

Pietikäinen and Høydahl (1999) calendered newsprint on a 2-nips soft calender from which nominal values for the dwell time could be derived. From the results they, derived

the expressions

$$t_r = 0.051L^{0.50} \tag{2.25}$$

$$t_r = 0.031L^{0.49} \tag{2.26}$$

for respectively $769m(min)^{-1}$ and $1231m(min)^{-1}$, where t_r is in ms. Dwell time is calculated from Hertz formula.

Pendulum device

The design criteria of the pendulum device were to simulate the operation of high speed industrial roller calenders. A primary measure for the device was then to create a pressure impulse on the paper, of a duration of order 1 ms. The hammer/anvil apparatus that has been applied in relevant investigations in the literature, was during preliminary experiments, recognized not to be ideal for all the measurements that were planned, for example the mechanical energy of the impacting bodies before and after the impact. The final design of the apparatus is described in Paper I, (Fig. 2.4), and in the picture, Fig. 2.21. The essential operation of the pendulums is to let the hammers impact the paper specimen similar to the line load in a roller nip. The impact is assumed to give a force normal to the paper surface leading to radial strain in the paper. However, the strain will not be radial symmetric due to the anisotropy of the paper in MD resp. CD directions. This is different from the case of rollers where the line load leads also to force component different in the MD resp CD. The pendulum operation can be described by the laws of mechanics and quantities like impulse force

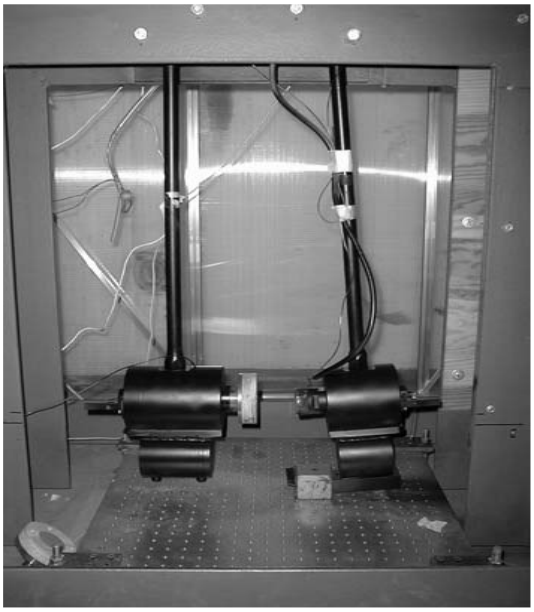

Figure 2.21: A photo of the pendulum device in operation.

versus time, impulse duration, as well as the energy transfer by the impact can be determined by simple measurements. However, the nip load at the contact zone gives differences in the impact mechanics of the roller contra the pendulum. These will be discussed in the following.

The dwell time, the duration of contact of two colliding bodies, is given as a result of several phenomena taking place in the contact zone and in the constructive parts of the bodies, in a very complex manner. When two bodies collide, in the most simple way, under the absence of sliding in the contact zone perpendicular to the direction of impact, the dwell time is depending on the masses of the bodies, their relative velocity at the collision as well as of the strength properties of the material of the bodies. An extensive literature exists on the relevant subjects. For the present, simplified considerations are assumed to be adequate, with reference to handbooks, Barkan (1964). In an elastic collision, i.e. the restitution coefficient equals 1, and the deformation is proportionate with the force, the dwell time t is, as a first approximation,

$$t \sim K^{-0.5} \tag{2.27}$$

and the maximum impact force is

$$F_{max} \sim K^{0.5} \tag{2.28}$$

where K is the stiffness of the materials involved, defined as the impulse force per unit deformation of the bodies. The pendulums are composed of several parts of different dimensions and materials. An effective stiffness can therefore to be introduced realizing the influence of the different parts. Of interest here is the relation between the nominal effective stiffness and the dwell time, expressed as the ratio

$$\eta = t/t_0 \sim (K/K_0)^{-0.5} \tag{2.29}$$

where t_0 and K_0 is a reference dwell time, resp. a reference effective stiffness. Under the present experimental condition the restitution coefficient is low, < 0.5, indicating a low effective stiffness, leading to a higher dwell time, that in the extreme tends to be independent of the impact force.

For plastic deformation the dwell time is also depending on the minimum impulse force giving plastic yielding in the material, and an effective stiffness will be a very complex property. For the present the interest is limited to the discussion of the existing experimental results of the dwell time by the pendulum impact, in view of the simple relation, Eq. 2.27.

Fig. 2.22 illustrates some measurements of the dwell time as functions of the maximum impact force and in dependency of the hammer materials, with or without inclusion of paper specimen. The upper curve in the figures is for the first impact, the

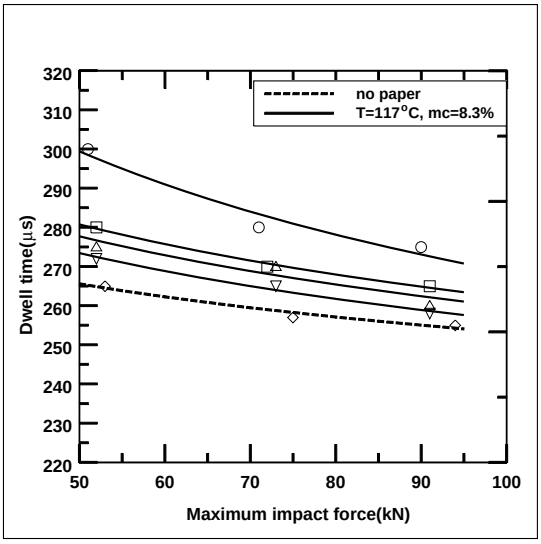

Figure 2.22: Dwell time versus impact force for newsprint impacted between to steel hammers.

following curves are for successive impacts. The results show that the dwell time decreases monotonous with increasing impact force. The curves indicate how successive impacts on the paper specimen increase the relative effective stiffness of the hammers, according to Eq. 2.29, and in this way diminishes the influence of the paper. Fig. 2.23 illustrates the experimental dwell time under the impact on a polymer covered hammer. It is substantial longer than the dwell time by the impact between the steel hammers. The measurements indicate also that the paper has a stronger influence on the dwell time, i.e. the relative stiffness of the hammers with a hard nip than a soft nip. It can be assumed that the polymer is the dominant material to reduce the stiffness.

Fig. 2.24 shows the dwell time from Figs. 2.22 and 2.23 related to the dwell time at impact force 50 kN as a reference. The curve illustrates Eq. 2.29. The experimental plots indicates less influence of the force than given by Eq. 2.27, for the elastic case.

Fig. 2.25 illustrates the fundamental difference between the roller calender and the pendulum device. As the specific impulse in the nip increases, the dwell time increases for the rollers, while it decreases for the pendulums. The plots for the dwell time for newsprint on the pendulums fit the expression

$$t = 0.0015 {i_p}^{-0.32} \quad (ms) \tag{2.30}$$

where the specific impulse i_p is in $kNsm^{-2}$. The exponent in the equation above is given for a paper moisture content of 8.3%, and a hammer temperature of 80^oC. With the same conditions, the exponent was -0.15 for SC-paper, substantially larger for newsprint. An increase of resp. moisture content and hammer temperature, decreases

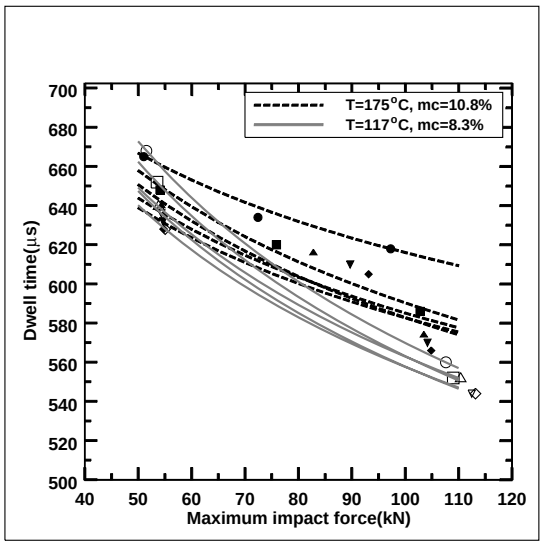

Figure 2.23: Dwell time versus impact force for newsprint impacted between one hammer of steel, the other covered with elastomer.

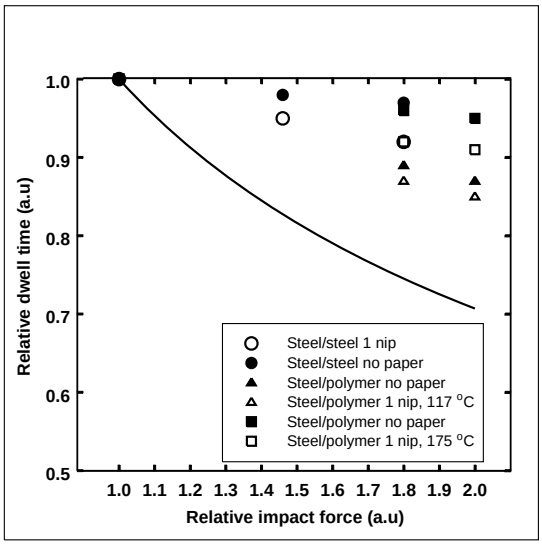

Figure 2.24: Dwell time versus impact force for newsprint related to a force of 50kN as shown in Fig. 2.22.

the exponent for both types of paper.

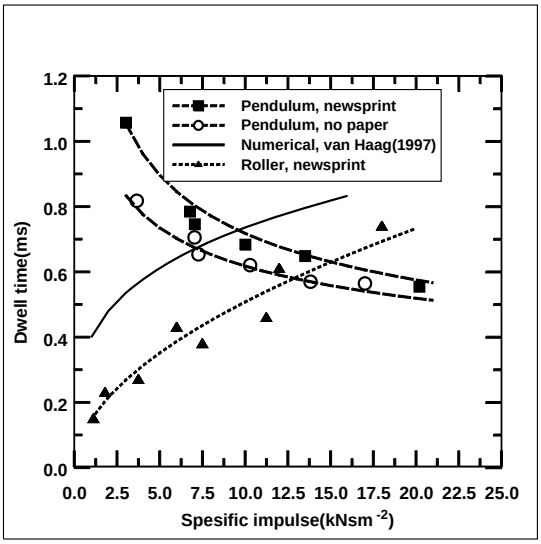

Figure 2.25: Dwell time for pendulum and roller calendering at first impact, resp. 1 nip.

The following conclusion can be given:

- the dwell time decreases with increasing impulse,
- the dwell time increases substantially as soft materials are introduced in the impacting zone like the polymer cover of the hammer
- the dwell time decreases with the number of impacts on the paper specimen. The curves indicates that after a certain number of impacts the dwell time approaches the value for the impact without specimen, i.e. the paper specimen integrates mechanically with the hammer material. Furthermore, in a supercalender will the nips act with increasing hardness from the first to the last nip. This is taken care of by the OptiLoad calender, introduced by Valmet, that allows a controlled reduction of the nip load as the paper makes the nip "harder".
- the dwell time decreases as the paper specimen turns dryer, as can be seen from the curves for a moisture content of 10.8% resp. 8.3% .

2.2.4 Paper properties

Density

Density and thickness are basic macroscopic characteristics of paper structure. Density can be used to relate several other properties of paper, including tensile strength, elastic

modulus and light scattering coefficient. These properties depend on a combination of fibre types and pigments, beating wet pressing and calendering.

It will be known from industrial calendering that the paper bulk is altered by variables as impulse, number of nips, nip temperature and moisture content. This is also demonstrated by use of the pendulum device on different paper qualities. Fig. 2.6 shows some results from our experiments with the pendulum, solid lines, together with results from the literature. The results from the work done by Keller and Waech (1992), Browne et al. (1993) support the pendulum device as a simulating means of the roller calender.

The most interesting is the comparison of our results with the results from Pietikäinen and Høydahl (1999) by calendering the same quality of newsprint on a pilot calender. The data agree qualitatively as well as quantitatively very well. The relative density versus specific impulse of newsprint for roller calendering and pendulum device is shown in Fig. 2.26. The moisture content and temperature of the trials are nearly the same. Furthermore, from the plots in the Fig. 2.27, it can be seen that the permanent bulk compression, i.e. the density, is increased as the mean moisture content is increased from 8.3% to 10.8%. This can be assumed to reflect that the fibres turn softer by

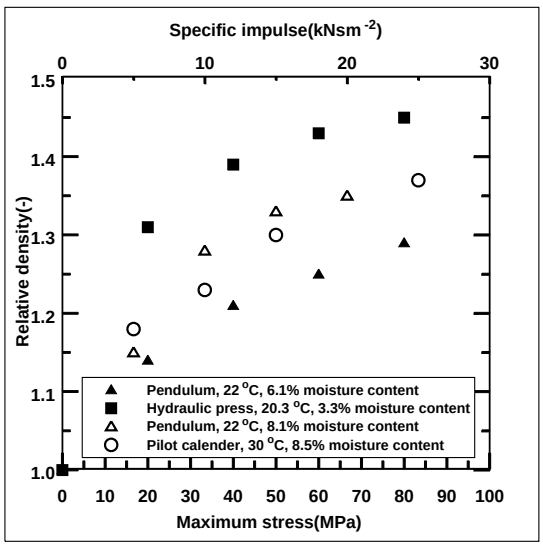

Figure 2.26: Relative density versus maximum stress for newsprint, calendered by the pendulum device, dwell time in order of 1ms, and ground wood paper calendered in a hydraulic press(Colley and Peel (1972)) with a dwell time 0.53s — shown as solid symbols. Relative density versus specific impulse for newsprint calendered by pendulum device and a 2-nips soft pilot calender(Pietikäinen and Høydahl (1999)) — shown as open symbols.

increasing moisture content.

Fig. 2.26 shows also results from investigations of Colley and Peel (1972) using the similar techniques, with hammer-anvil type apparatus. Their results gave a higher relative density versus maximum stress, due to a much longer dwell time than for the pendulum results. However, the relative change with increasing stress indicates a similar compression dynamic on the paper web.

The influence on density by surface moistening of SC-paper is shown in Fig. 2.28. As can be seen, increased moisture content gave a slightly increase of the density when the paper was sprayed before each impact. Such a small change of the density shows that the moistening of the paper is concentrated to the outer layer of the paper, i.e. a moisture gradient.

A moisture addition of one $gram(m)^{-2}$ by spraying the surface, increased tentatively the mean moisture content of the paper 1 to 2%, based on dry weight i.e. giving a mean moisture content of approximately 10%. Comparing the density values from samples with a mean moisture of 10.8% (Fig. 2.27), with the values from the case with spraying, a lesser densification could be read at the latter. After first impact, a paper density of $900kgm^{-3}$ and $875kgm^{-3}$ was achieved for even moisture content resp. from spraying. A difference of 2.7%.

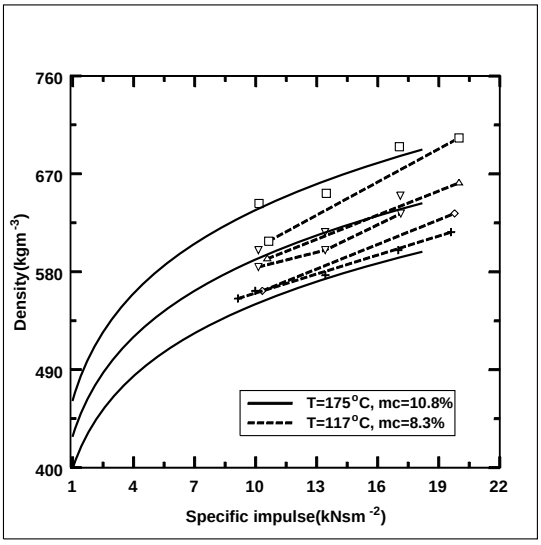

Figure 2.27: Density versus specific impulse for pendulum calendering with newsprint at different moisture content in paper and hammer temperature. Fitted data to the experimental data shown as solid and dotted lines. The standard deviation of the experimental data is $11kgm^{-3}$.
+ — first impact, ◇ — third impact, ▽ — fifth impact, △ — seventh impact, □ — tenth impact.

After the third and fifth impact, a difference of 3.5% and 4% was found, i.e the difference seems to increase with increasing number of impacts. This results shows that the paper bulk can better be preserved after calendering, if the moisture content of the paper is increased by spraying the paper surface.

The positive effect of the bulk preservation seems to be more advanced, as the number of impacts/nips are increased.

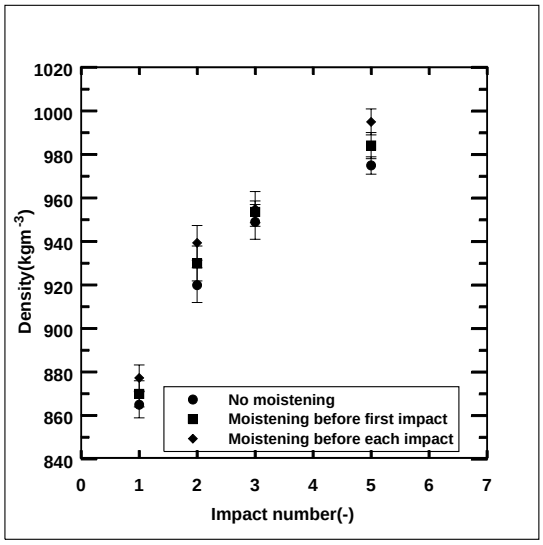

Figure 2.28: Density versus number of impacts for SC-paper calendered by pendulum. The case of no-spray, spray only before the first impact, and spray before each impact is denoted as circles, squares and diamonds respectively. Hammer temperature of 110^oC and initial paper moisture content of 8.3%. Specific impact of $10.3kNsm^{-2}$.

Surface properties

In the papermaking process, roughness and smoothness are controlled by calendering. Uncalendered paper is unsuitable for most applications. A breaker stack, machine calender, or supercalender can produce the smooth surface required. In calendering, surface roughness decreases proportionately more than thickness. In principle, strong calendering could remove all roughness but this is usually not possible because of the simultaneous loss of paper thickness. Chapter 2 (Paper I) has shown that paper gloss and PPS are strongly dependent on the impulse, number of impacts and temperature. Some results comparing a 2-nips pilot soft calender and pendulum results of newsprint with constant moisture content and variation in temperature of the roller/hammer is shown in Fig. 2.29. This figure shows a fair agreement between the two calendering

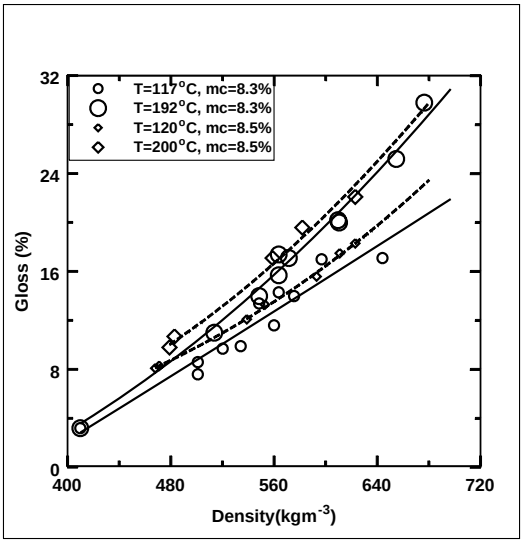

Figure 2.29: Gloss versus density for newsprint calendered by pendulum device shown as circles with fitted curve as solid lines, resp. by 2-nips pilot calendered shown as diamonds with fitted curve as shown as dotted line for different moisture content in paper and roller/hammer temperature. The standard deviation of the experimental data is 4% of the gloss value.

techniques, at similar conditions.

The effect of the moisture content of gloss versus density for SC-paper is shown in Fig. 2.30, and for newsprint with number of impacts as a parameter in Fig. 2.31. This case shows that gloss increases as the homogenous moisture content is increased, but as shown earlier, an increase of the moisture content also reduces the paper thickness. A good smoothness and roughness can be achieved without reducing the paper to a undesirable thickness, if the plastic deformation is increased near the surface.

An example of surface moistening of the paper is shown in Fig. 2.32, where gloss and PPS are measured at the same condition as shown in Fig. 2.28. Gratton (1997) made also some relevant experiments with spraying the paper surface with water, but their trial did not achieve any improvement of gloss. A reason for this difference might be that our experiments had a larger time delay after spraying before impact, allowing a better softening of the fibres. Another possibility is that the surface temperature was chilled in their experiments before the nip.

If smoothness of paper can be improved without reducing other paper qualities, a surface moistening before each nip could be an effective method in addition to high roller temperature.

Steam showers have done this on supercalenders and many references are made in the literature to what seems to have been well known by papermakers, namely that

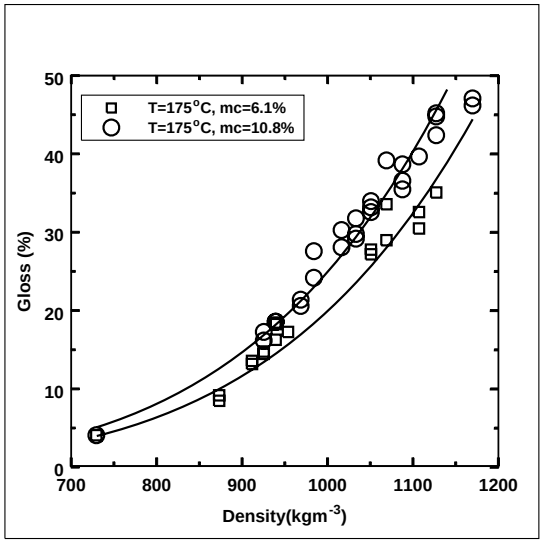

Figure 2.30: Gloss versus density for SC-paper by pendulum calendering with hammer temperature 175^oC, and two moisture contents. The standard deviation of the experimental data is 4% of the gloss value.

a moistened surface together with higher roller temperatures permit not only use of lower line loads, but also produces better bulk.

Surface roughness of roller/hammer

The influence of the hammer surface roughness of the final paper properties was not studied, but it is evident that surface is very important due to the final quality of the paper. The surface of a hard roller used in a commercial supercalender (and also the pilot calender used in this experiment) has usually a roughness (Ra number) less than $0.05\mu m$. The roughness of the steel hammer was measured by a profilometer to an average roughness almost ten times higher. This number is quite large, and might be one of the reasons of the discrepancy that has been demonstrated between the results from the pendulum device and roller calender. It might be assumed that, with a hammer surface of the same roughness as the roller surface, the measures of gloss and PPS would also be quantitatively nearer under else same conditions

In most cases the difference is difficult to explain, because the differences are so small in some cases that the effects could have been overridden by uncontrollable moisture and temperature effects.

In all the evaluations that has been done, there is also an other variable that has to be considered, namely the uncertainty there is strongest influenced by the variation of the uncalendered aggregates.

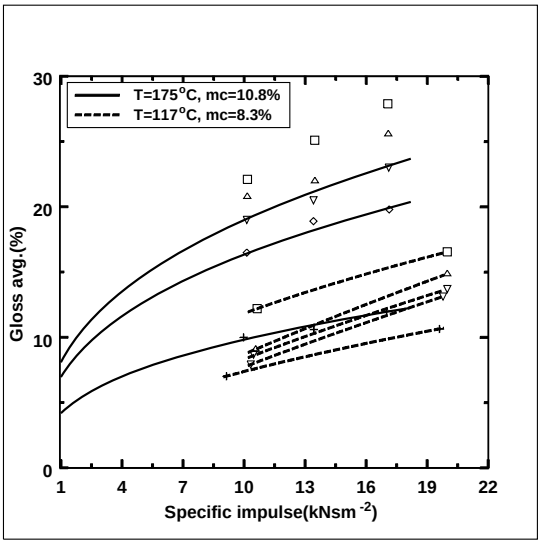

Figure 2.31: Gloss versus specific impulse for pendulum calendering with newsprint at different moisture content in paper and hammer temperature. Fitted data to the experimental data shown as solid and dotted lines. The standard deviation of the experimental data is 4% of the gloss value.
+ — first impact, ◇ — third impact, ▽ — fifth impact, △ — seventh impact, □ — tenth impact.

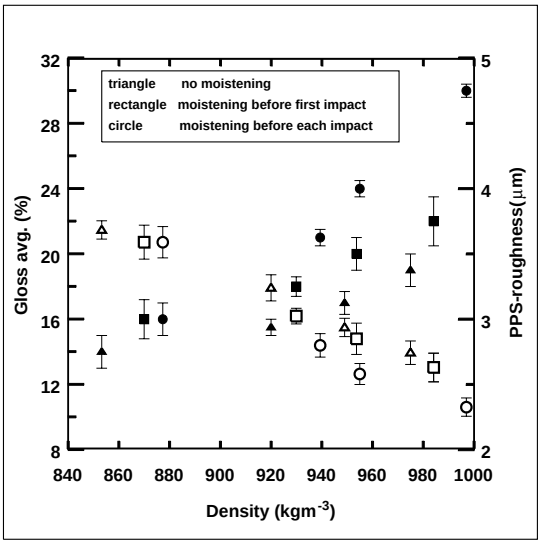

Figure 2.32: Gloss (solid symbols) and PPS(open symbols) versus density for spray moistened SC-paper calendered by pendulum.

2.2.5 Calendering equations

From the results that has been achieved using the pendulum device, and on the basis of customized roller calendering trials, some calender equations can be derived. The equations is comprehended of four variables, nip temperature, impulse, moisture content and number of nips. An example of such experiments are shown in Fig. 2.27 and Fig. 2.31, where two nip temperatures and moisture contents with three impulses and up to ten impacts could be recognized as curves fitting to calender equations. The equations can generally give us directions how to improve the calendering operations, optimize them and extrapolate them to conditions which are beyond our experience.

- The general equation for density is given as

$$\rho_n = C_0 \phi_n {i_p}^m \tag{2.31}$$

  where i_p is specific impulse of the pendulums, C_0 and ϕ_n and the exponent m, are empirical parameters, determined to fit experimental data. For ϕ_n the expression is

$$\phi_n = \mathbf{ln}[2.4 - (n^{\xi} B)^{-1}] \tag{2.32}$$

- The general equation for gloss is given as

$$gloss_n = C_0 \chi_n {i_p}^m \tag{2.33}$$

  where χ is a nonlinear function of number of impacts n given by

$$\chi_n = \mathbf{ln}[2.4 - (n^{\xi} B)^{-1}] \tag{2.34}$$

The density equation, Eq.2.31, is illustrated in Fig.2.27 for newsprint as solid curves for ten, seven and the first impact, resp. upper, middle and lower curve.

The solid curves in Fig.2.31 illustrates the Eq.2.33 for impact number five, third and the first impact, resp. upper, middle and lower curve.

The running conditions were 175^oC and 10.8% moisture content in paper. The value of the parameters C_0, m, ξ and B, used in the equations were 635 and 30, 0.15 and 0.38, 0.17 and 0.09, and finally 1.9 and 0.8 respectively for density and gloss data. A new trial with different conditions gave a new set of parameter values.

Combining the results from the density and gloss values, from Eq.2.31 an expression for impulse i_p can be solved as

$$i_p = \mathbf{exp}\left[\frac{\mathbf{log}(\frac{\rho_n}{C_0' \phi_n})}{m'}\right] \tag{2.35}$$

Replacing i_p in Eq.2.33 gives a new equation

- Calender equation

$$gloss_n = C_0 \chi_n \mathbf{exp} \left[\frac{\mathbf{log}(\frac{\rho_n}{C_0' \phi_n})}{m'} \right]^m \tag{2.36}$$

where m' and C_0' denote the exponent m and C_0 from Eq.2.31. The influence of temperature and moisture content is included in the parameters (not given here).

Chapter 3

The deformation of paper and its fibres by calendering

3.1 Calendering of wood containing paper: A laboratory study of temperature, moisture and pressure effects on fibre wall damage. Paper II

(*R.* H. Hestmo, Ø. W. Gregersen and M. Lamvik(2001).
"Calendering of wood containing paper: A laboratory study of
*t*emperature, moisture and pressure effects on fibre wall damage"
*N*ordic Pulp and Paper Research Journal, No. 4, Vol. 16.)

SUMMARY: Hard nip as well as soft nip calendering may reduce paper strength and average fibre length by cutting and damaging the fibres. In this study the fibre damage was assessed as the amount of radial cracks in the fibre wall, found in SEM images of paper cross sections. Newsprint and SC paper were calendered in a special pendulum device. The effects of mild to harsh impact energies, medium and low temperatures and normal and dry paper moisture contents were investigated. The cross sections of pendulum calendered SC-papers were compared to roller calendered SC-paper. Extensive amounts of radial cracks were found in the fibre walls calendered using dry conditions and high impact energies. In comparison with uncalendered paper samples, it was confirmed that the calender caused the observed cracks. It was also found that thick walled fibres tended to be more cracked compared with thin walled fibres. Increasing moisture content reduced the amount of cracks.

Introduction

There are rather few studies reported in the literature of the fracture of fibres caused by calendering. For TMP based newsprint, Browne et al. (1995) found a correlation between observed number of damaged fibres and machine calender line load. Page (1967) attributed damaged fibres in the uncalendered TMP sheet to shearing forces in the refiner. This effect was considered by Browne et al. (1995). The fractures caused by calendering, occured mainly on the inner fibre wall, and rarely in the outer wall. Coarse fibres tended to fracture more than thin walled fibres. The explanation of the observed fracture response was as following : The position of the fractures is a result of the tensile stresses that occur perpendicular to the load at the inner wall at top and bottom, and at the outer wall parallel to the load. Most internal fractures were observed, due to anisotropic strength properties of the fibres. The effect of temperature and humidity was not reported, but it is known that the softening of wood components is dependent of the moisture content, and that the softening temperature decreases as the moisture content is increased, Back and Salmén (1980). This softening effect has also been shown on different papers evaluated by its elastic modulus, Salmén and Back (1980).

Skowronski (1990), showed that the improvement in smoothness brought about by precalendering was lost after wetting. This, he claimed, was due to the restoration of the shape of the calendered fibres. Thick-walled fibres, giving a higher resistance to rupture of intrafibre bonds, gave a greater tendency of the sheet to recover its precalendered state. A similar work was done by Retulainen et al. (1997). They also observed fibre collapse especially at fibre crossings. Neither of the two works examined the collapsed fibres for eventually cracks caused by the calendering, which may influence the fibres ability to recover.

Back and Olsson (1983) studied experimentally the effect of pressure, temperature, and moisture content on paper properties for board grades using an apparatus developed to simulate a calender. This apparatus of a hammer and anvil type in which a polished, flat steel hammer drops on to a board sample resting on either another steel plate, supported by a rubber buffer, or on the rubber buffer on the top of the steel plate. Pressure pulses and dwell times equivalent to calender conditions were achieved. They found that the bending stiffness was independent of the temperature, except at temperatures $250 - 300^oC$, where a small decrease was found. There were no changes of the bending stiffness with increased moisture content, the reason might be that the moisture in the board was somewhat concentrated to its inner layers. The reduction of the caliper was found to increase slightly with temperature. Bending stiffness is proportional to the modulus of elasticity and to the 3rd power of the caliper. To which extent fractures of a fibre actually can affect the thickness and the bending stiffness of

calendered paper, is hard to say. Charles and Waterhouse (1988) showed that the paper strength may be reduced by calendering. Theoretically, a higher number of cracked fibres could lower the spring back effect, and thereby give a lower permanent thickness. The fibre strength and its modulus of elasticity could also be reduced due to a reduced number of intact fibres. Back and Olsson (1983) showed that a single nip gave a lower reduction in caliper and bending stiffness than a multi-nip producing the equal total impulse. This may be a result of less damaged fibres at fewer compressions. There might, however, be other effects that are influencing this result, such as fibre collapse, and drying of the paper as it is successively impacted with a heated hammer.

The printability of paper is of importance. It depends on paper qualities as smoothness, porosity and gloss. Normally, a high gloss is achieved by high calendering intensity, i.e. by high nip load, high steel roller temperature and paper moisture content. This may eventually lead to a strong paper blackening, Høydahl (2000). If the paper is compressed under conditions of high stress concentration, local blackening and irregular patches may result. Increasing the moisture content before calendering was shown by Koskinen (1998) to increase the calender blackening of SC-paper.

This study is an attempt to increase the knowledge of the fibre wall damage which is taking place by calendering of paper using industrial rollers, alternatively by using a pendulum apparatus. To achieve realistic results, the running conditions were as close as possible to each other.

Experiments

Experimental technique and measurement

For the laboratory study a pendulum device was used where a mechanical impact on the paper specimen is achieved by two hammers. The dynamics of the pendulums are simulating a roller calender where the hammers were 1) a hard steel hammer and 2) a steel hammer covered with an elastomer representing the soft roller, respectively. The dynamic impact response was recorded as a force versus time curve. The operational specifications of the pendulum apparatus covered, to a large extent, the operational domain of industrial high speed calenders. A more detailed description of the pendulum is described by Lamvik et al. (2000). In the set of experiments reported here, the fibre damage by calendering assessed as radial cracks in the fibre walls, was investigated. The effects of impact energy and paper moisture content on fibre damage were investigated and compared with uncalendered paper and with roller calendered samples.

The temperature of the paper web was set by the temperature of the polymer hammer, and was regulated by adjusting the voltage to a heating element clamped around the hammer, and the temperature was measured by use of a thermocouple

mounted just beneath the hammer surface. The temperature was measured with an accuracy of $\pm 1^oC$, and the temperature of the paper sheet was measured using an Infra Red pyrometer, type Raytek Raynger II with a accuracy of ± 1 degree.

The humidity in the air was measured by an Sauter humidity sensor, type HBC112. The moisture content of the paper was determined by weighing before and after drying at standard procedure.

Force versus time was measured and registered on a digital oscilloscope, Tektronix 420DT, by use of piezo-electric sensors, PCB Type 206A mounted in the hammers, from where peak stress was calculated.

Paper specimen and running conditions

The newsprint used is based on TMP from Norway spruce. These samples on average had an initial thickness of 105 micron, and grammage $45gm^{-2}$. The uncalendered SC-paper samples used in this study had an average grammage of $62gm^{-2}$. It was made of pulp(65%) from Norway spruce(90% TMP and 10% sulphate pulp) and kaolin(35%). These samples on average had an initial thickness of 90 micron.

The paper temperatures used (22, 60 and 80^oC) corresponded to 7.5, 3.2 and 2.2% equilibrium moisture content in the papers' fibre material respectively. The temperature of the polymer-coated hammer was some 2-4^oC higher than that of the paper for the 60 and 80^oC runs.

The paper specimens were calendered by 1, 3, 5 and 10 impacts in the pendulum device, whereby density increased.

The experimental conditions in the first set of experiments are summarized in Tab. 3.1.

Then the pendulum device was placed in a climate chamber. To allow measurements

Table 3.1: Experimental conditions for the first set of experiments. Count of radial fibre wall cracks/image. Standard deviation = 1.8 cracks/image.

Paper	Paper temperature (^{0}C)	Moisture content (%)	Peak stress (MPa)	Cracks/image
SC	22	7.5	28	3.9
SC	22	7.5	60	4.2
SC	80	2.2	28	4.9
SC	80	2.2	60	7.4
News	22	7.5	28	10.3
News	22	7.5	60	18.8
News	60	3.2	28	10.0
News	60	3.2	60	17.1

Table 3.2: Experimental conditions for the second experiment. The effect of increased moisture content on the crack count. Count of radial fibre wall cracks/image. Standard deviation = 1.8 cracks/image.

Paper	Relative Humidity (%)	Moisture content (%)	Peak Stress(MPa)	Cracks/image
SC	40	6.3	50	6.5
SC	70	10.8	50	2
News	40	6.3	50	17.5
News	70	10.8	50	2.5

at higher moisture contents a second set of experiments was made (Tab. 3.2).

The SC-paper was also calendered in a pilot softcalender to a density of approximately $1170 kgm^{-3}$ at a line load of $300 kNm^{-1}$ and a speed of $600 mmin^{-1}$. The initial temperature and moisture content were 33^oC and 9% respectively.

Characterization of paper cross sections

After calendering, the specimen was embedded in epoxy, ground, polished and cleansed as described by Williams and Drummond (1994). The specimen were carbon coated and imaged in a Hitachi S-3000 LV SEM, BEI-mode. For each calendering condition seven sheets were imaged at 250X magnification and a resolution of $0.37 \mu m/pixel$, and in some cases 200X magnification. Each image then contained 0.75 and 0.94 mm of the papers CD-direction.

Results

Effects of nip peak pressure, moisture content and paper grade on fibre damage

The first set of experiments was analyzed as a 2^3-factorial design with the variables paper grade, calendering peak pressure and paper temperature as shown in Tab. 3.1. The average count of cracks in each image is also shown in Tab. 3.1.

The data analysis showed that the higher calendering peak pressure increased the count of cracks by an average of 4.6 cracks/image for all tests. Newsprint had 9.0 cracks/image more compared with SC-paper. Changing the temperature (and then also the moisture content) did not have a significant effect compared with the standard deviation of 1.8 cracks/image. Fig. 3.1 and 3.2 show examples of the laboratory-calendered newsprint and SC-paper sheets. These sheets were calendered at 22^oC

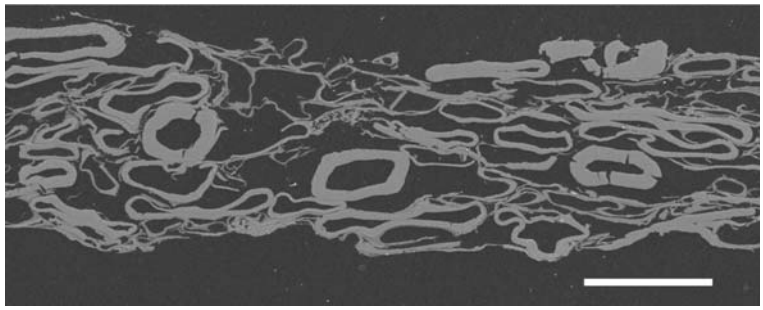

Figure 3.1: Lab calendered TMP based newsprint containing two latewood fibres with radial cracks. Bar length is $40\mu m$.

using 50 MPa peak pressure.

The properties of cracks and cracked fibres

Fig. 3.1 and 3.2 indicates that latewood fibres are more prone to cracking than earlywood fibres. To investigate this closer the fibre wall thickness was measured at each crack in the newsprint papers. The average cracked fibre wall thickness was $3.7\mu m \pm 0.15\mu m$. This is far above earlier reported values for fibre wall thickness for newsprint from Norway Spruce, e.g. $2.6 - 3.0\mu m$, Reme and Helle (2000), and $2.3 - 3.1\mu m$, Kure (1999). Thus it is likely that there is an over representation of latewood fibres among the cracked ones.

The orientation of the cracks, relative to the paper plane, was studied by making measurements on totally 305 cracks. Most of the cracks were oriented in the z-direction (Fig. 3.3). A similar crack distribution of fibres was found for TMP based newsprint, Gregersen et al. (2000). As illustrated by some examples in Fig. 3.4 it can be seen that the in-plane cracks usually starts from the outer side of the fibre whereas the cracks in z-direction starts from the lumen side. The cracks illustrate that the impact load in z-direction has created bending stresses in the fibre wall that have exceeded the tensile strength of the fibres. Assuming the fibre cross section in a xz-axis, the maximum

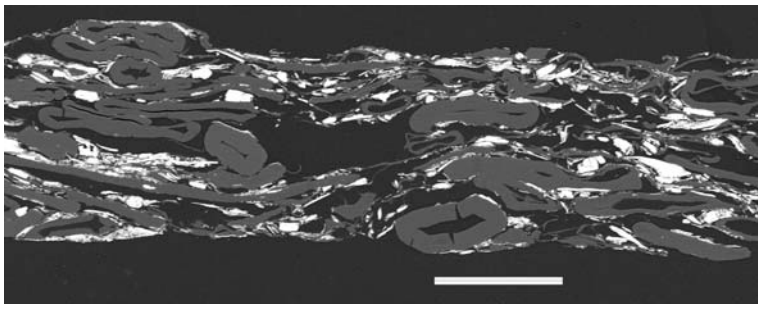

Figure 3.2: Lab calendered SC-paper containing one cracked latewood fibre.

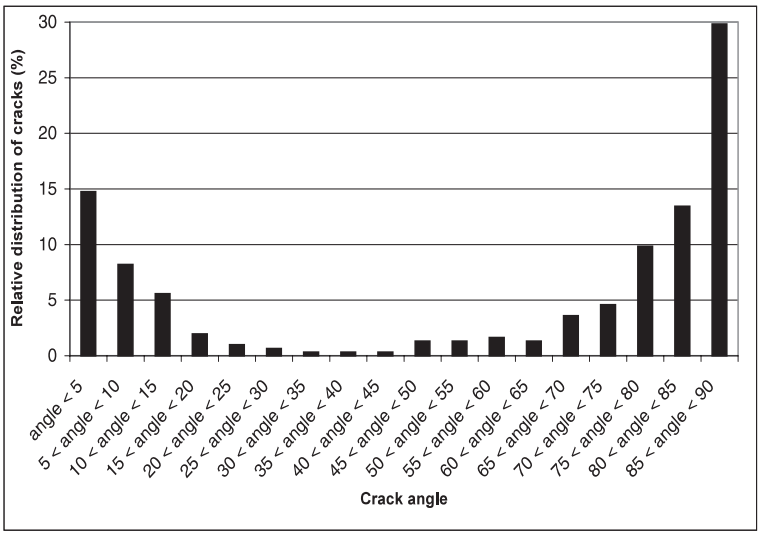

Figure 3.3: The relative distribution of cracks (%) relative to the paper plane for lab calendered SC-paper. There is a clear over representation of cracks in z-direction.

tensile stress arises theoretically at the outer side of the wall, at 0^o, and at the lumen side of wall at 90^o, counted from the inplane x-axis.

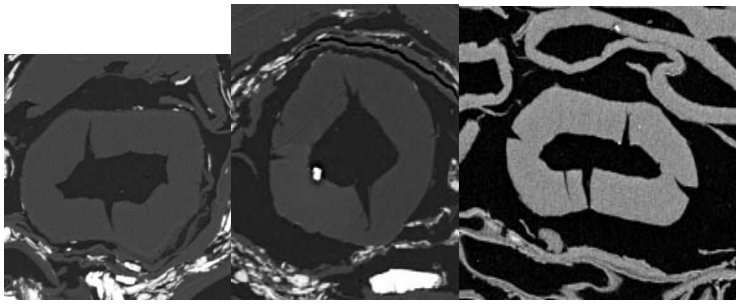

Figure 3.4: Three examples of cracked latewood fibres. Note the in-plane cracks starting from outside, and the z-directional cracks starting from lumen side relative to the paper plane.

Comparison of uncalendered and roller calendered paper

To verify that calendering caused the cracks, cross sections of uncalendered sheets were investigated in the same manner. For uncalendered newsprint no cracks were found. For the uncalendered SC paper, an average of 1.5 cracks/sheet were found for all samples. These numbers are significantly below the levels of the sheets calendered in the laboratory. Thus calendering clearly causes the cracking.

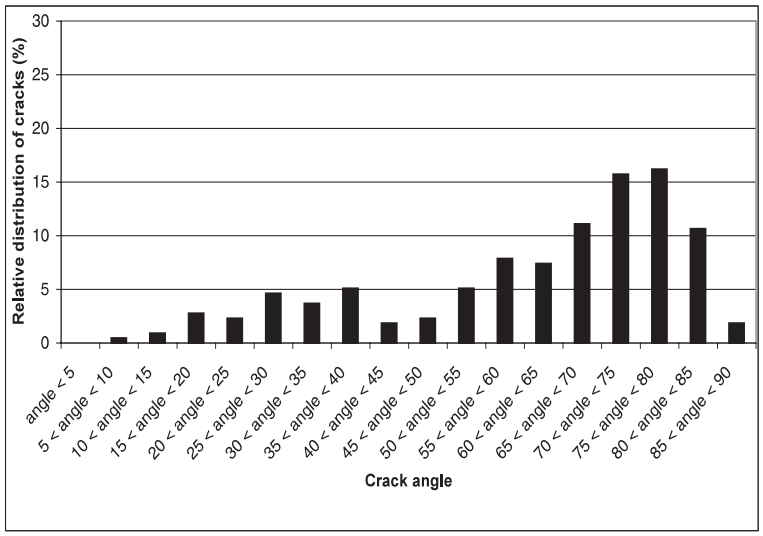

Figure 3.5: The relative distribution of cracks (%) relative to the paper plane for roller calendered SC-paper. There is a over presentation of z-direction cracks relative to the paper plane.

The fracture response of roller calendered SC-papers is shown in Fig. 3.5. A significant amount of cracks were observed distributed between angles 50^o and 80^o, and a less number in the in-plane direction. The crack levels for roller calendered SC-papers were 1.4 cracks/image. One possible explanation for this difference is that the fibres in the roller calender were more softened as the paper had a higher moisture content, 9.0% and a higher temperature, around 35^oC. Furthermore, the force components in the nip load by roller calenders may differ from the normal force by the impact of the pendulums. Our observation of the cracks in the fibres, calendered by the respective techniques, seems that the roller nip introduces forces that reduces the maximum tensile stresses in the fibre wall. The difference could also be due to different cover material and thickness of the cover for the hammer and the calender roller, giving differences in the local stress concentrations. However, the experimental knowledge of the force distribution in the nip of running rollers are, as we can see, not satisfactory known, compared to knowledge of the simpler pendulum mechanics. It is therefore still difficult to go into a meaningful discussion of details of the pressure distribution in a calender nip, of its impact on fibre damage, and finally on paper surface properties.

Results from the runs with specimens with increased moisture content, according to Tab. 3.2, are illustrated in Fig. 3.6. The results in the figure are given for three different levels of density. As expected the count of cracks were significantly reduced at higher moisture content due to the softening of the wood polymers. The results are achieved with a pressure that is rather high compared to industrially calendered paper, and local stress concentrations in fibre flocks could agitate fibre damages. The count of

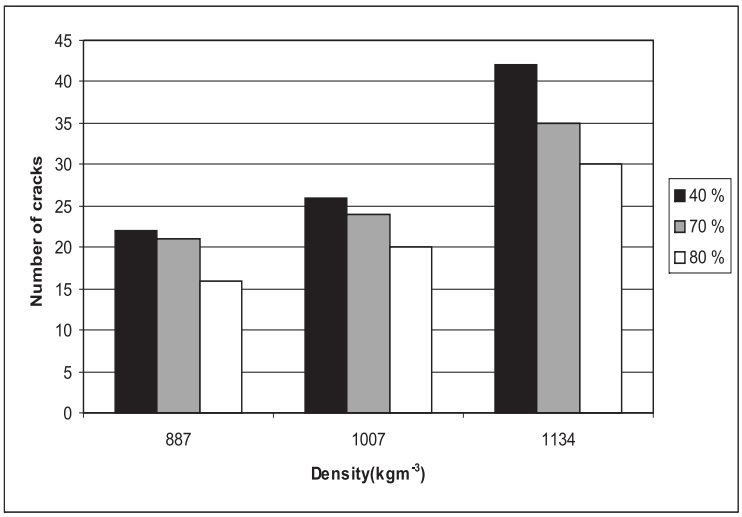

Figure 3.6: The effect of increased moisture content on the crack count per sample for SC-paper at various densities.

radial fibrewall cracks of lab calendered SC-paper with an average density of $1057 kgm^{-3}$ is shown in Tab. 3.3. The density was obtained with different number of impacts and peak stresses. Here the peak stress was 79, 61 and 44 MPa, at 3, 5 respectively 10 number of impacts, also relatively high compared to industrially calendered paper. The moisture content was 13.5%, temperature of the steel and the polymer coated hammer was 22^oC. The number of impacts at low peak stress was increased to obtain the same density as for higher peak stress, and more cracks were found.

Table 3.3: Count of radial fibre wall cracks/sample at paper density $1057 kgm^{-3}$ for three different runs.

Number of nips	Peak Stress(MPa)	Cracks/sample
3	**79**	**17**
5	**61**	**20**
10	**44**	**26**

Discussion

The radial fibre cracks in the fibre walls develop when the local strain in the inner or outer fibre wall exceeds the local fracture strain. The local strain will on average be higher for higher calendering peak pressure. This explains why a significantly higher amount of cracked fibres was found at the higher peak pressure level.

For a given deformation of a fibre the strain will also be higher for a thick-walled fibre compared with a thin walled one. This is due to the longer distance between the fibre wall center line and the outer and inner fibre surface for thick-walled fibres. This explains why the late wood fibres are more cracked compared to early wood fibres. This result agrees with earlier findings done by Browne et al. (1995).

Browne et al. (1995) also found higher degree of cracks in the z-direction of the fibres and argued that this was caused by a higher degree of orientation of fibrils on the inner fibre wall compared with the outer fibre wall. This seems to be a likely explanation provided that the primary wall and S1 of the fibres has not been removed during refining.

In the first set of experiments a significantly higher amount of cracks was found for newsprint compared to SC paper. This is explained by the fact that the SC-paper contains only some 50% TMP, i.e. approx. $31gm^{-2}$ pure TMP compared with $45gm^{-2}$ for the newsprint. This is a difference of 31% and explains half of the 64% difference between the count of cracks in SC paper compared with newsprint. The remaining difference may be explained by the fact that TMP for SC paper is more refined giving fibres with thin walls and thus less prone to be further damaged in the calender.

As the fibres get crushed during calendering, considerable damage to the fibre network is expected to occur, leading to decreased values of the physical properties. Rodal (1989) called this part of the stress-strain curve the third region, in which the tangent modulus increases rapidly with strain. Comparing the moistened paper subjected with the hammer apparatus and roller calendered SC paper, there are indications that softening of fibres will reduce the amount of cracks. This was expected as softening increases the fracture strain of the fibre material, which reduces the tangential modulus according to Rodal.

The lignin and hemicellulose of Norway Spruce fibres have different softening temperatures, which also depend on the moisture content of the fibres. Our results indicate that paper with a moisture content of 10.8 and 13.5% has fewer cracks than was found for a moisture content of 6.3%, due to the softening of the wood polymers.

To decrease the number of fibre cracks at a given sheet density, it seems advantage to increase the peak pressure and decrease the number of impacts. This is according to the findings by Back and Olsson (1983) on the caliper and bending stiffness of the paper by calendering with different number of nips and pressures.

The relation between calender blackening and fibre collapse(fibre cracks) was not investigated in this study. For a future study it would be worthy to analyze the fibres in blackened spots for comparisons to fibres from areas with no blackening, at different calendering pressure, paper temperature and paper moisture content. Furthermore, different strength tests should be done on calendered paper to verify the effect of fibre cracks.

Conclusion

Calendering of paper may cause radial cracks in fibre walls. The crack frequency increases with increasing thickness of the fibre walls, increasing calendering peak pressure, and is decreasing for increasing moisture content of the paper.

To avoid fibre cracks, and thereby loss of paper strength, the number of nips should be decreased as the peak pressure is increased.

3.2 Supplements to Paper II

Fibre cracks, a problem arisen from calendering

A crack in the fiber wall appears when the stress against the structure, exceeds a certain value. The limitation stress, before a crack starts, is dependent of the moisture content of the paper. It is not directly shown that the extent of strain of the fibres is related by the moisture content, but it is obvious to belive from our results reported earlier in this section. However, Back and Olsson (1983) has shown that the glass transition temperature of paper is lowered at increasing moisture content.

Generally, a flexible fibre withstands a relatively high pressure, and a number of successive impacts before a crack arises in the wall. If the paper strength is dependent of the number of fractured fibres, as already indicated, increased moisture content of the paper can lead to an increase in the strength. However, this will also reduce the bulk of the paper, which again can reduce the paper strength. Another problem is calender blackening.

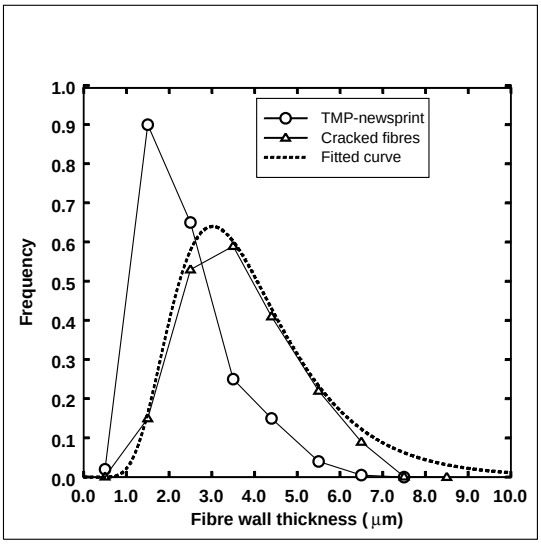

Figure 3.7: The frequency of cracked fibres, and number of fibres versus fibre wall thickness of calendered newsprint.

A way to reduce these problems, is to make paper of mostly flexible fibers, i.e thin walled.

As an example, Fig. 3.7 shows the frequency of cracked fibres versus fibre wall thickness for newsprint. The figure show clearly that the late wood fibres with a thick fibre wall, were most prone to cracks.

The crack frequency versus fibre wall thickness can be adapted to a (normal) dis-

tribution, plotted as a dotted line in Fig. 3.7.

$$Frequency = c_1 \; exp[-0.5(ln(z_{wall}/c_2))^2] \tag{3.1}$$

where z_{wall} is the fibre wall thickness. This example was given for a peak pressure of 50MPa, and a paper moisture content of 8.3%, giving $c_1 = 0.64$ and $c_2 = 0.34$. A decrease or increase of will change c_1 and c_2 in Eq. 3.1. In this way, making several experiments, a statistic equation can be governed to estimate the probability of fractured fibres in a paper web at different calendering conditions.

3.2.1 Relative crack distribution using two calendering techniques

Previous chapters has demonstrated how the qualities of a paper surface are changed after the calendering, and that this change is due to the mechanical and thermal impact in the nip.

Calendering is described to be a replication process (Crotogino and Gratton (1987)). The aim is to replicate the smooth surface of the calender roller on the surface of the paper by pressing the paper against the smooth surface with a force sufficient to cause the paper surface to deform plastically. The replication process can be enhanced by applying more pressure or by applying shear forces. It can also be enhanced by making the fibres more pliable by heating or moistening them.

The question if there is shear forces or not in a nip has been discussed for a long time and also to which extent this effect has any role on the smoothness improvement, especially for soft nip calendering, where shear deformation may arise between the soft roller and hard roller. This question is left open, and instead focus is made at different microscopic changes of the paper structure that takes place by roller and pendulum technique. Most of the fibres will be intact after calendering, but as shown in the previous section, cracks occur, and the crack response seems to be somewhat different between the pendulum and roller technique.

From SEM photographs of several calendered papers operated under different conditions, several hundred cracks were measured, and it seems that the roller nip introduces forces that reduces the maximum tensile stresses in the fibre wall. The results also demonstrate that the angular crack distribution between the two techniques was different. Fig. 3.8 shows an illustration of the crack distribution that was found, limited by looking at a quadrant of the fibres. The left figure is for roller calendered paper, and as the illustration shows, the distribution of the location of the cracks are mostly concentrated less than ten degrees angles from the in-plane and thickness direction of the fibre. The results from pendulum calendered paper show that the cracks are located in the in-plane and thickness direction of the fiber, indicating that the paper compression by the pendulum is from forces with a perpendicular direction to the paper.

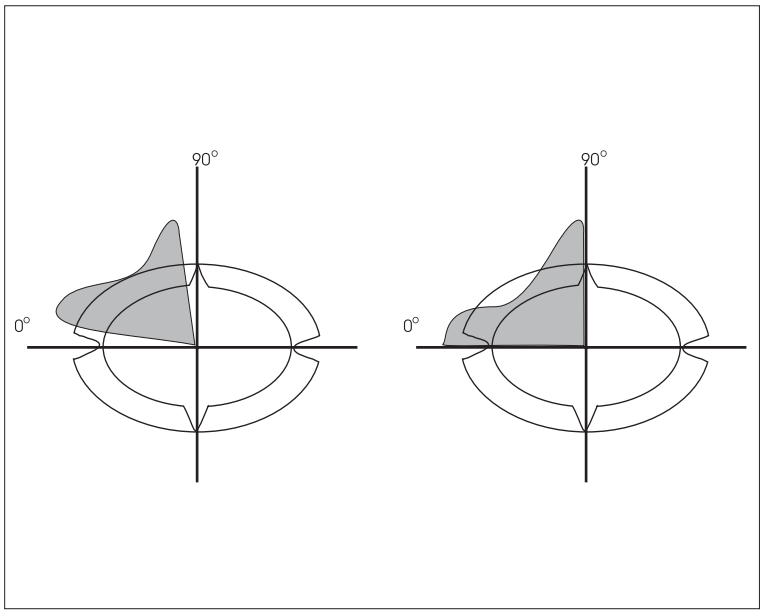

Figure 3.8: Illustration of the relative crack distribution of roller calendered and pendulum calendered paper in the first quadrant of the fibre structure, resp. left and right figure.

Paper is an inhomogeneous material, and substantial local differences in the deformation behaviour may exist, as shown in Fig. 3.1 and 3.2. In addition to the thickness variation, there is also a local variation in density of the paper due to fibre distribution.

The final density of a certain paper is set by the line load, roller temperature, temperature and moisture of the paper, and the kind of rollers and its properties. In this study, we have mainly divided between steel/steel, and steel/soft hammers.

In the picture of the cross sections of the paper, a larger number of cracks were found for steel/steel hammers compared to soft/steel hammers at same conditions. The largest number of cracks were found at areas with a high density of fibres, and especially in areas with thick walled fibres. The increased number of cracks at areas with a large number of fibres might explain the findings of Moffat et al. (1973). He clearly showed that the weak spots in newsprint changed from areas of low grammage in uncalendered newsprint to those of high grammage in machine calendered paper, concluding that fibre or bond damage at the more highly compressed zones was the cause of the 25% or so reduction in measured tensile strength.

Later Moffat (1975) reported comparisons between uncalendered and hard and soft nip calendered newsprint which showed how strength was preserved with a soft nip. However, the advantage of soft calendering has often been attributed to a more gentle compression where the stresses are concentrated at the denser parts of the paper structure. The strength properties are therefore better preserved, Rodal (1989).

3.2.2 Calender blackening

Calender blackening is a negative effect that sometimes occurs when the calendering intensity is too strong. These effects appears as black or grayish spots on the paper surface, Høydahl (2000). They appear mostly at the thickest parts of the paper, which are heavily pressed in the calender nip.

Compared to a hard nip, the more even distributed compression in soft nip calender causes a more porous paper web, and the tendency for calender blackening is therefore reduced, Stevens et al. (1989).

Koskinen (1998) showed that this unwanted optical appearance increased with increased moisture content of the paper. Whether a homogenous or a moisture gradient profile gives more or less blackening was not studied.

Any correlation between black spots and fibre cracks seems worthy to be investigated.

3.2.3 Fibre cracks versus dwell time

Roller calendering

Thickness reduction by calendering has been studied by several authors,Wickström et al. (1997b), Rättö and Rigdahl (1998a). They correlated the thickness reduction to pressure and dwell time and they demonstrated that applied pressure has a stronger influence than dwell time in the nip.

From SEM-photographs of ten samples of soft-nip calendered newsprint, a different number of cracks were observed. The samples were calendered at a constant peak pressure of respectively 19.8 and 24.2MPa (calculated from Hertz equation), with two different speeds of the calender. Giving a dwell time of 0.38 resp. 0.61ms, and 0.46 resp. 0.74ms for respective pressures.

Fig. 3.9 indicates that the number of cracks decreases with increasing dwell time (calculated from Hertz equation), for both line loads. The calendered paper samples had a thickness difference of 2% between the two pressures measured after nip.

The results in Fig. 3.9 can be explained due to a smaller rise and fall of for the pressure versus dwell time curve, at the shortest dwell time, giving a "tougher" mechanical impact of the fibres, compared to a larger dwell time, giving a "smoother" impact.

The crack response, due to the impact, is implicitly dependent of the moisture content. This again influences the fiber flexibility, and therefore an increasing moisture content may reduce the impact of fibre cracks in the nip.

The results shown, are at very small dwell times, and it might have been worthy to investigate the use of a extended nip, where a dwell time of several seconds are possible. Then the role of the dwell time could be better clarified.

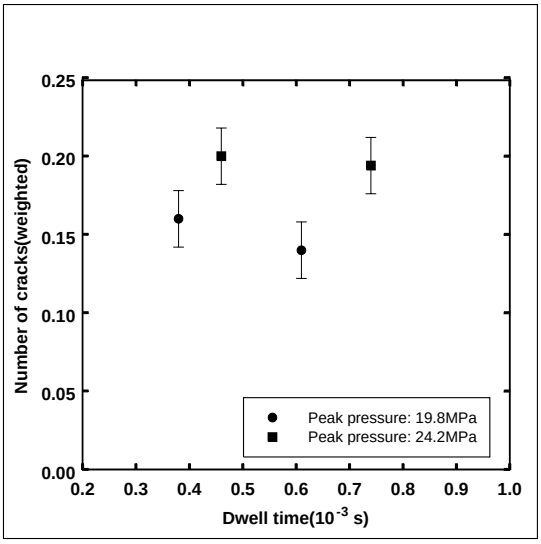

Figure 3.9: Number of cracks versus dwell time for newsprint with a constant pressure in a pilot soft-nip calender(Pietikäinen and Høydahl (1999)). Paper moisture content 8%, paper temperature 25^oC. Nip temperature 120^oC. Weighted number of cracks is the number of cracks divided by the total number of counted fibres.

Pendulum calendering

In chapter 2.2.3 a relation between dwell time, maximum impact force and the material stiffness of the hammers was given. The strength of the fibres can be assumed to be a part of that stiffness. Therefore it seems plausible to relate the number of cracks in the paper specimen with the stiffness. A characteristic quantity for the stiffness is then derived, from Eq. 2.27 and 2.28. The evaluation of peak stress and impact duration depends upon the value of the force produced at the surface of the impacting hammers. If we assume a linear elastic collision,we can set the peak stress, P_{max}

$$P_{max} \sim \sqrt{K} \tag{3.2}$$

where K is the stiffness, and further, the dwell time t_d

$$t_d \sim \left(\sqrt{K}\right)^{-1} \tag{3.3}$$

Combining Eq. 3.2 and 3.3 gives a new relation between

$$t_d/P_{max} \sim K^{-1} \tag{3.4}$$

where t_d and K are measured quantities.

The stiffness-crack characteristics are illustrated in Fig. 3.10.

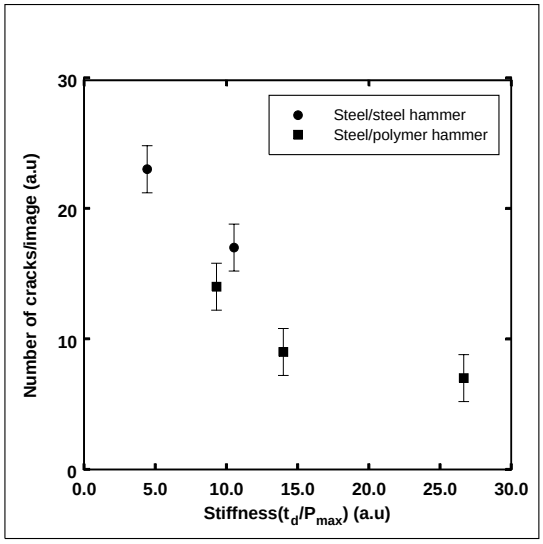

Figure 3.10: Number of cracks versus stiffness (K^{-1}) for pendulum calendered newsprint. Temperature of hot hammer was set to room temperature. Paper temperature and moisture content for steel/steel hammer test were resp. 22^oC resp. 7.5%, and 60^oC resp. 5.3% for steel/polymer hammer test.

The Fig. 3.9 showed a tendency of decreasing number of cracks with increasing dwell time, and a modest assumption can be drawn out of Fig. 3.10. If these results are representative, one would assume that the effect of a long dwell time will not reduce the paper strength noticeably due to fibre cracks.

Chapter 4

Thermal conductivity of newsprint under compression

4.1 Determination of thermal conductivity of newsprint under compression. Paper III

(*R.* H. Hestmo, M. Lamvik(2001).
"Determination of thermal conductivity of newsprint under compression".
*P*resented at the 26th International Thermal Conductivity Conference
6-8 August 2001, Cambridge, Massachusetts USA.)

SUMMARY: Thermal conductivity of newsprint is determined experimentally using an equipment where the paper specimen can be compressed, giving a density in the range of $410 - 535 kgm^{-3}$. Measurements were made by a moisture content 8% and a mean temperature 40^oC, of the specimen. The temperatures were measured by thermocouples, the heat flow through the specimen was measured by two heat flux sensors, for the evaluation of the thermal conductivity. Typical data for the apparent thermal conductivity was $0.065 W(m\ ^oC)^{-1}$ at a paper density of $500 kgm^{-3}$. A simple physical model of the paper structure was applied, to which our data and data from the literature were compared. Increasing compression leads to increasing apparent thermal conductivity, presumably due to increased contact between the fibres across the paper thickness. An empirical expression is derived for the thermal conductivity as a function of density.

Introduction

Thermal conductivity of paper is an important parameter in analyzing thermo-mechanical processes on paper, of which the calendering is one of the most interesting, seen from an engineering standpoint. By calendering the paper is conveyed through the contact line between two cylindrical rollers, of which one may have an elevated temperature, up to $\sim 250^oC$. There the paper surface in contact with the roller is heated during a short time, a millisecond or so. However, since the paper has a relatively low thermal conductivity, a relatively small amount of heat is transferred to the paper bulk. For the same reason, however, the fibres in contact with the roller can be assumed to adapt approximately the temperature of the roller. This is the general feature of the socalled temperature gradient calendering: the fibres in the surface layer are softened due to an elevated temperature, while the bulk, with its properties, is unaffected by the heat transfer from the roller.

By passing the contact line between the rollers, the paper undergoes a sequence of rise and fall of compressive force. A similar sequence will prevail for the paper density and other properties depending on the density, as thermal conductivity. The determination of thermal conductivity should therefore permit measurements on paper specimen under a controlled compression.

The thermal conductivity differs from one quality to another, depending on fibre constituent and orientation, filling materials, as well as on temperature and moisture content. The paper is generally an open fibrous structure where heat can be transferred by convection as well as by radiation. In this way is the thermal conductivity of paper not a physical property, but an apparent property for the transport of heat. It will be depending on the conditions under which it is determined, and it is, strictly speaking, valid for use only under the same conditions. When table in handbooks give a general value for thermal conductivity of $0.12W(m\,^oC)^{-1}$, it is to be recognized as a number of order. In the present study, newsprint is chosen for investigation, while it is relatively well defined, consisting mainly of fibres from thermo-mechanical refinement, ensuring a certain consistency with data from the literature. Furthermore, data for the thermal conductivity of the fibre wall in paper is scarce. On the other hand, data for wood fibres are available, and to the extent these fibres are similar in consistency with newsprint fibres, the data for the wood fibres can be used as an first approximation. Newsprint is produced in large quantities, and its calendering is one of the big challenges in the production line.

The literature refers rather few investigations on the thermal conductivity of newsprint. Kerekes (1980), resp. Burnside and Burnside and Crotogino (1984) determined the thermal conductivity on precalendered newsprint, and under conditions where the compression of the specimens were not quite clarified. Kartovaara et al. (1985) derived

thermal conductivity from measured thermal diffusivity.

In the following the investigation of thermal conductivity of newsprint is reported, using an experimental equipment where measurements can be made on specimen under compression. A simple model for the fibre structure of the paper is presented, and the experimental data, together with data from the literature, are correlated with the model.

Theoretical model

The thermal conductivity k is defined by the Fourier equation, expressing the heat flux $q = Q/A = k\delta T/\delta z$, Wm^{-2}, where Q is the heat flow through the heat transfer area A, with thermal conductivity k, $W(m\ ^oC)^{-1}$, temperature T and distance in the direction of heat flow z, respectively. Its experimental determination involves four quantities to be measured, the stationary heat flow Q, the surface area A of the specimen, the thickness of the specimen, Δx, and the temperatures T of the specimen surfaces.

The surface of paper is not well defined, and its temperature must be defined as a mean temperature of the interface with the body in direct contact with the surface. The structure of the paper itself is anisotropic, consisting of fibres, air and eventually filling materials, with the fibres orientated according to their formation on the paper machine, predominated with their length axis in the machine running direction, MD. The heat conduction in the direction perpendicular to the sheet, ZD, is of interest in the present discussion.

The classical model for the thermal conductivity in a heterogeneous material is based on two cases, where the components are coupled in parallel resp. serial with the direction of the heat flow. The model leads to two extremes for the effective thermal conductivity:
by parallel coupling :

$$k_{\parallel} = \varphi k_a + (1-\varphi)k_f \tag{4.1}$$

resp. by serial coupling of the fibres:

$$k_{\perp} = [(1-\varphi)/k_f + \varphi/k_a]^{-1} \tag{4.2}$$

where φ is the porosity, and indices f and a denotes the fibres resp. the air. The model is further extended to incorporate the serial coupling of the extremes,

$$k_{eff} = [(1-a)/k_{\parallel} + a/k_{\perp}]^{-1} \tag{4.3}$$

where a is the volumetric fraction of serial coupled fibres, i.e. with $k_{\perp}$. The value of a is to be assigned from experimental results.

Heat transfer is connected to a temperature difference over the specimen. Then heat transport through the specimen may be influenced by free convection and radiation.

The thermal conductivity determined experimentally has therefore to be considered as an apparent conductivity, incorporating the different modes of heat transfer, according to the Standard Terminology of ASTM Designation: ASTM-C-168 (1990). And the data are, strictly speaking, supposed to be valid only for application under the same conditions as given by the experiments.

The mathematical expressions require knowledge of the thermal conductivity of the solid, i.e. of the fibre wall, k_f. Data for its value is uncertain, in the literature it can be given within a wide range, from 0.16 to $1.5 W(m\ ^oC)^{-1}$. Assuming the fibres to be similar to wood fibers, however, Kollmann and Malmquist (1956) give data for the conductivity of wood fibres in the direction parallel as well as perpendicular to the fibre axis, $k_{f\parallel} \approx 0.71 W(m\ ^oC)^{-1}$, resp. $k_{f\perp} \approx 0.41 W(m\ ^oC)^{-1}$, by density $\rho_f = 1450 kgm^{-3}$. Siau (1984) recommends the values $k_{f\parallel} \approx 0.88 W(m\ ^oC)^{-1}$ resp. $k_{f\perp} \approx 0.44 W(m\ ^oC)^{-1}$, by a density of $\rho_f = 1450 kgm^{-3}$. Fig. 4.1 illustrates, in a socalled Miller-diagram, the effective thermal conductivity k_{eff} from Eq. 4.3, as a function of paper density, ρ_p, and with data of the fibre $k_f \approx k_{f\perp} = 0.43 W(m\ ^oC)^{-1}$, resp. air $k_a = 0.03 W(m\ ^oC)^{-1}$, and with a as the structure parameter.

The theoretical curves in the figure indicate how the effective thermal conductivity of paper depends on the density and on the nominal parameter a, describing the structure of the fibres. The bulk density of newsprint by passing the calender nip, can be estimated to vary from an initial value of about $500 kgm^{-3}$ to about $1000 kgm^{-3}$ in the midst of the nip. The effective thermal conductivity may then have a variation within about 60%.

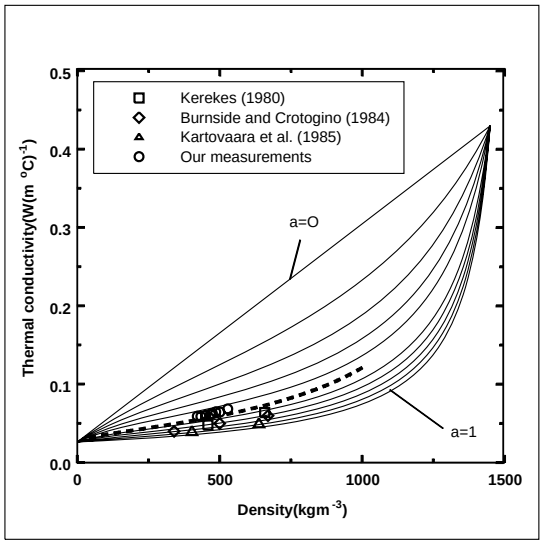

Figure 4.1: Effective thermal conductivity of newsprint versus density. Plots from measurements, see text(Miller diagram).

The value of the fraction a introduced above, needs some attention. A low value, at a given density, promotes a relatively high conductivity, leading to the assumption of a shortcut between the fibres across the sheet. The same effect can also a filling material have, noting that the thermal conductivity of clays may be an order of magnitude higher than the conductivity of fibres. A high volumetric fraction a, indicates a layered structure across the sheet, with weak contact between the fibres of the nearby layers. According to the fibre orientation of the paper web, a is expected to have a relatively high value. When the paper is compressed, its density as well as the effective thermal conductivity will increase, with the given structure parameter a.

Experimental

General

The classical equipment for the measurement of thermal conductivity of materials with low conductivity, is the guarded hot plate, where the specimen is clamped between two parallel metallic plates of high thermal conductivity, one with a high temperature that transfer the heat through the specimen to the other plate of lower temperature. Its design and operation for insulation materials are described in details in the Standard ASTM-C-168 (1990). There the thermal conductivity is referred to the difference of the temperature of the metallic plates, it is named apparent thermal conductivity since it may inhere influences of convective and radiative heat transfer as well. The temperature of the interface between the plates and the specimen is crucial for the evaluation of the thermal conductivity of the specimen. The following comment seems to be proper. When two bodies, "1" resp. "2", having different temperature, are brought to surface contact, heat will flow from the warmer to the colder body. The interface will then attain a temperature that is depending on the thermophysical properties of the bodies, i.e. of the ratio of the temperature penetration number $b1/b2 = [(k\rho C)_2/(k\rho C)_1]^{1/2}$, Gröber et al. (1955). It can be shown that for the present case, with a metallic plate, say of copper, in contact with paper, the temperature of the interface will be equal to the temperature of the plate within approximately 3% of the temperature difference of the plates. That is, presumably, within the uncertainty of any temperature measurement of the surface, especially in view of the difficulty with the definition of the paper surface itself. It is therefore reasonable to assume that the fibres in contact with the plate as well as the adjacent air attain the temperature of the plate, and the temperature of the plates represents boundary conditions of the first order for the temperature field in the paper specimen.

In investigations of the thermal conductivity, referred in the literature, a heat transfer coefficient h, related to the total paper surface, is frequently introduced. It seems,

however, from the estimate above, to be a redundant quantity. It is coupled with the thermal conductivity of the specimen with the pressure as a parameter. The thermal conductivity of the specimen and the heat transfer coefficient will increase by increasing pressure, the latter due to the increased number of fibres coming into contact with the plate.

Experimental equipment and measurements

The apparatus used for the measurements is illustrated in Fig. 4.2. It is mainly made up of a frame A, where the piston B of a pneumatic cylinder can move a heated upper plate C downwards to a cooled lower plate D to clamp the paper specimen between. The plates were made of copper, having channels for water circulation from thermostatic baths, for individually being kept at stationary constant temperatures. The paper specimen P, is further mounted between two thin copper plates E1, resp. E2 and two heat flux meter F1, resp. F2, as illustrated in Fig. 4.3.

By the experiments the following measurements were made: The pressure force between the plates was measured by a load cell, H, Maywood, Type U2000, with the Digital indicator L, Type D2000, reading in units of kilogram. The distance between the plates was measured by an Optical Displacement meter, K, using the mirror M, and made by DSE ApS, Type ODS-30-1kHz. The meter had a measuring range of 4 mm, a resolution of $1\mu m$, and it reproduced the measurements within $3\mu m$. The signal was registered on an oscilloscope, Type Tektronic TDS 420A. The measured distance gave the basis for the evaluation of the thickness, and thereby of the density of the

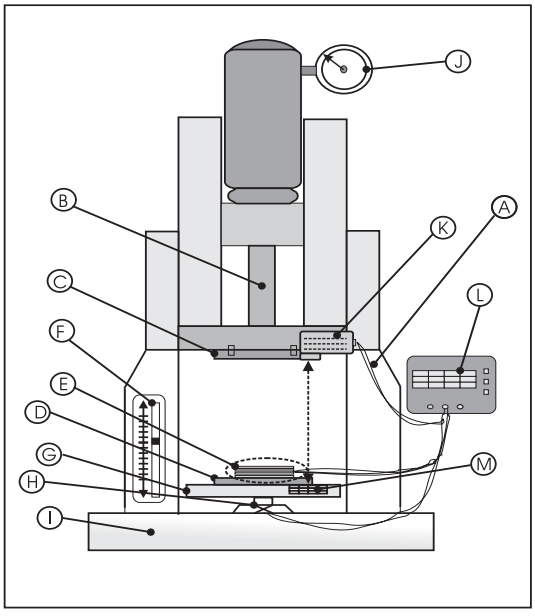

Figure 4.2: Experimental equipment. For explanation, see text.

paper specimen.

The heat flux across the specimen was measured by two heat flux meters, by TNO, Institute of Applied Physics, Type PU22T, mounted one of each side of the specimen, F1 resp. F2. They were shaped as disks, diameter 50 mm, thickness 1.5 mm, with a metering concentric zone of diameter 27 mm. The signal from the meters was calibrated from the factory, to be read as heat flux in $Wm^{-2}(mV)^{-1}$. Its uncertainty was given to 5%. The temperature of the upper and lower plates, C, was measured by thermocouples. The copper plates between the fluxmeters and the paper specimen, diameter 50 mm, thickness 0.5 mm, E1 resp. E2, constituted together with thin wires of Chromel, resp. Alumel soldered diametrically to the respective plates, the thermoelements for the measurement of the temperature of the respective sides of the paper specimen. The signal from the thermocouples was measured by a voltmeter Solatron Type 7071 Computing Voltmeter. The thermoelements were calibrated, clamped together, in a water bath of controlled temperature with a calibrated Hg thermometer as reference. Their readings differed within $\pm 0.002mV$.

Experimental procedure

The experiment started with mounting the specimen between the heat flux meters on the lower plate C2. Then the upper plate was lowered until a load pressure of 0.1 MPa was reached, and the thickness of the uncompressed specimen could be determined, since this is the condition at which thickness measurements on paper usually are made. The temperature of the upper and the lower plates was normally set to 50^oC resp. 20^oC. The pressure was then raised to a given value, and after stationary conditions were reached, measurements were made of the distance between the plates, i.e. the thickness of the specimen, the heat fluxes and the temperatures.

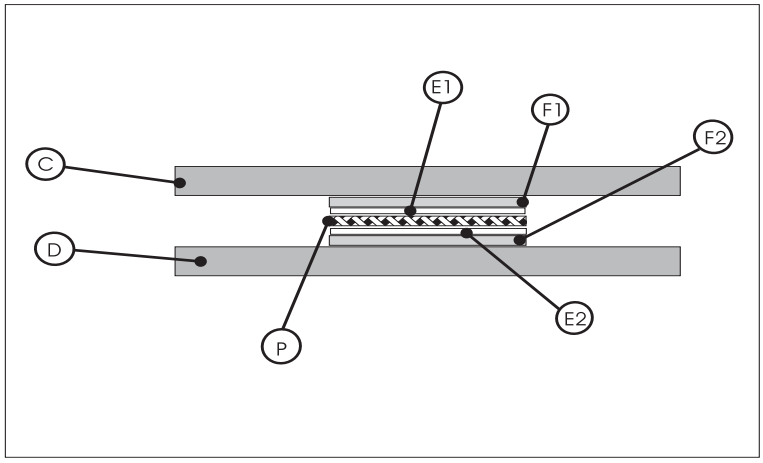

Figure 4.3: Specimen arrangement during measurements. For explanation, see text

Data analysis

Paper density

The paper density was derived from the measured relative displacement of the plate C toward the plate D. The distance between them is proportionate to the voltage reading V from the Optical Displacement meter, given as

$$\vartheta = 0.5V \quad (\mu m) \tag{4.4}$$

where V is in millivolt.

The force from the pneumatic piston cause a relative displacement ϑ_s of the components of the structure, that is dependent on the pressure, was found to be

$$\vartheta_s = 33.0 - 382.6ln(P) \quad (\mu m) \tag{4.5}$$

where P is the pressure in Pa. The thickness of the paper is then evaluated from

$$s = s_0 - (\vartheta + \vartheta_s) \quad (\mu m) \tag{4.6}$$

and the density from

$$\rho = \rho_0 \; s_0/s \quad (kgm^{-3}) \tag{4.7}$$

where s_0 is the paper thickness and ρ_0 is the density before compression.

Thermal conductivity

The apparent thermal conductivity of the specimen, k, is evaluated from the expression

$$k = q \; s/(T_1 - T_2) \quad (W(m \; ^oC)^{-1}) \tag{4.8}$$

where q is measured heat flux, k is the apparent thermal conductivity of the specimen, T_1 and T_2 are measured temperature of the copper plates on the warm resp. the cold side of the specimen, and s is the thickness of the specimen.

The evaluated data for the thermal conductivity is estimated to be uncertain within $\pm$ 10%, where the measurement of the thickness represents the strongest influence.

Results and discussion

Fig. 4.4 shows the thickness reduction of the specimen, referred to one sheet, as function of the pressure by compression of one, two and three sheets, respectively. The plots are within 95%, grouping to the linear line expressed by

$$\vartheta = 10^{-5}P - 1.05 \quad (\mu m) \tag{4.9}$$

where P is the pressure in Pa. The result indicate that the multiple of paper sheets act as one sheet, and that the interface between the respective sheets can be recognized as an integrated part of the paper structure.

Tab. 4.1 gives some data from the measurements on three paper sheets. The exper-

Table 4.1: Experimental and calculated data.

Pressure (MPa)	Heat flux (Wm^{-2})	Temp. T1 (^oC)	Temp. T2 (^oC)	Thickness (μm)	Therm. Cond. ($W(m^oC)^{-1}$)
0.10	1221	43.5	36.8	291	0.053
0.20	1247	43.5	37.0	287	0.056
0.49	1293	43.4	37.2	283	0.059
0.75	1311	43.3	37.5	270	0.061
1.00	1301	43.1	37.6	258	0.061
1.26	1311	43.2	37.9	251	0.062
1.51	1315	43.1	38.0	244	0.063
1.64	1314	43.2	38.3	242	0.064

imental results from measurements of the apparent thermal conductivity of newsprint, are plotted in Fig. 4.1 as circles. The plots follow the curve for the parameter value $a \approx 0.5$, i.e. tentatively 50 % of the fibres can be supposed being in good contact with the neighboring fibres across the sheet. A second order function is fitted to the plots. It is extrapolated by assigning a value of $0.125W(m^oC)^{-1}$ at a density of $1000kgm^{-3}$. Its mathematical expression is given by

$$k = 0.0565 - 0.2916 \cdot 10^{-5}\rho + 9.765 \cdot 10^{-8}\rho^2, (W(m\ ^oC)^{-1}) \tag{4.10}$$

where ρ is density in kgm^{-3}. To enlighten the results further, some supplementary estimates of the heat transfer between the copper plates is done, by separation of the modes: conduction through the fibres, conduction through the air and radiation through the air. As a first approximation the assumption is made that the area for the heat transfer is expressed by the porosity, i.e. heat conduction in the air as well as the radiation, is proportional to the porosity, φ, and the conduction through the fibres is proportional to $(1 - \varphi)$. Then the radiative heat transfer can be estimated to be less than 2% of the apparent conductivity. The conduction through the air can be estimated to decrease from 16 % to 12 % as the density increases from $400kgm^{-3}$ to $550kgm^{-3}$. As can be seen from the data in Tab. 4.1, the apparent thermal conductivity increases about 20 % by the same increase of the density. This indicates tentatively that the increased conduction, is dominantly due to better contact between neighboring fibres across the sheet.

By roller calendering, the paper may, under its dwell time in the nip, be compressed to a density of order $1000kgm^{-3}$, Browne et al. (1995). The surface fibres are heated to

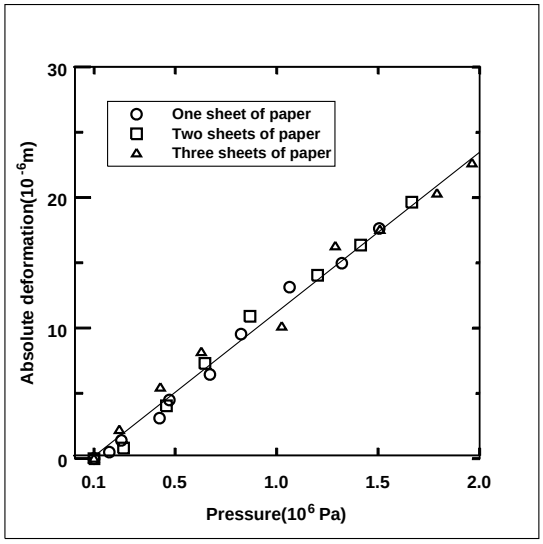

Figure 4.4: Thickness reduction of specimen, referred to one sheet, versus compressive pressure

a temperature approximately equal the temperature of the hot roller, and will thereby undergo thermal processes that alter thermal conductivity of the surface layer of the paper. It can, however be shown, in the next chapter, that the temperature of the bulk of the paper do not increase significantly, by high speed calendering, where the dwell time is very short, of order 1 ms. The present data of the thermal conductivity seems therefore to be generally adequate for the newsprint in the calendering process.

Fig. 4.1 shows additionally plots from the investigations by Burnside and Crotogino (1984), respective Kerekes (1980). They refer to the apparent thermal conductivity of newsprint that had been calendered before the measurements, thus being not under a similar pressure during measurements. The plots follow curves of higher values of $a \approx 0.7$. A weaker contact between the fibres across the sheet might therefore have been present, compared to our case. Similar tendency is indicated in the results by Kartovaara et al. (1985), where the conductivity was derived from measured thermal diffusivity of mechanical pulp without compression. Of their results shown in Fig. 4.1, the plot for the highest density is for calendered paper, the plot for the lowest density, is for uncalendered. Their study revealed also a strong dependency of the thermal conductivities upon the moisture content.

Conclusion

The apparent thermal conductivity of newsprint is determined using an apparatus that in principle simulates the Standard hot plate apparatus. The conductivity increases by increasing compression, i.e. by increasing density, and can be referred to a better contact between neighboring fibres across the sheet. Measurements of the thermal conductivity of paper with a Standard hot plate type apparatus is assumed to give results that is adequate for the heat conduction in the paper web by calendering. For a theoretical consideration of the thermal conductivity of paper there is a need for reliable data for the thermophysical data for, in dependency of temperature, moisture content, special attention should be made on the properties of the fibre wall.

Chapter 5

Heat transfer during calendering

5.1 Heat transfer during calendering of paper. Paper IV

(*A*ccepted for publishing in Journal of Pulp and Paper Science April 2002 issue.)

SUMMARY: Temperature gradient calendering is studied, and experiments are done by using a pendulum device that simulates the roller calender. A discussion is provided of the heat transfer between the pendulum hammer and the paper, with special emphasis on the paper surface as a heat transfer area. Different modes of heat transfer are analyzed. It is shown that the heat transfer is mainly governed by conduction through the fibres in contact with the hammer surface. An expression of the heat transfer coefficient is derived as a function of impact pressure. The temperature field in a paper specimen is determined experimentally and by numerical calculation, showing a temperature rise of only a few degrees C.

Introduction

Calendering is one of the final processes in a paper production line. It takes place by conveying the paper through the contact line, the nip, between two rotating parallel cylindrical rollers. Due to the line load in the nip, the paper undergoes a deformation that smooths the surface of the paper and reduces its thickness. The technological challenge of calendering is to achieve the required surface smoothness and other surface properties, together with the proper bulk density of the paper. From experience the surface smoothness is improved by increasing the line load. On the other hand, increasing the line load may also lead to increasing bulk density, to fibre collapse and to damage of the fibre bond, with a resultant reduction in the mechanical strength of the paper. The so called temperature gradient calendering tends to meet this dilemma. By

adding heat and moisture only to the outer layer of the paper, the modulus of elasticity of the layer is reduced, and the fibres are given plastic deformation by a moderate line load. A concise description of temperature gradient calendering is given by Crotogino (1982), Gratton et al. (1997).

In temperature gradient calendering the heat is normally added to the paper by keeping one of the rollers at an elevated temperature, occasionally up to 250^oC, while the other roller, possibly a soft roller, is at a lower temperature. The amount of transferred heat to the paper is to a large extent controlled by the dwell time of the, paper in the nip. The running speed of modern calenders can be up to $30ms^{-1}$, and with a nip width of, say $5mm$, the dwell time can be a millisecond or less. The characteristic time for the heat to penetrate the paper will, on the other hand, be of the order of $100ms$, assuming a paper thickness of $100\mu m$ and a thermal diffusivity of the paper equal to $10^{-7}m^2s^{-1}$. From this estimate the heat transfer to the paper can be assumed to feature pulse heating, during which the paper behaves like a semi-infinite body.

The heat transfer between the roller and the paper takes place by a transient of a series of mechanisms in the contact area. The fibres are subjected to a sequence of rising and falling pressure, during which the number of fibres in contact with the hot roller will vary like the conditions for heat transfer.

In the investigations of the stationary heat transfer between two bodies, it has been a tradition to introduce a contact heat transfer coefficient, as a phenomenological coefficient, to inhere the mechanisms taking place at the interface between the bodies, acting as temperature reservoirs.

The literature refers many investigations of heat transfer by contact between two bodies. A majority of them are dealing with solid bodies. Here Fletcher (1997) gives, as an example, a comprehensive survey with a formal treatment of the problems. Others have studied the change of the topography of interfaces and their dependency on the contact pressure, Hendriks and Visscher (1995), Dumont et al. (1999), Lee and Ren (1996), and Snaith et al. (1986)).

Fewer investigators have studied the contact heat transfer where porous materials are involved. Chapman (1947), made some interesting, and relevant, experiments to determine the effective contact area between paper fibres and a plane glass plate under pressure. Lyne (1977), measured the distribution of a surface void of paper, from which he could also derive the fraction of contact area. These investigations aimed at a correlation between printability and topography of paper, and to some extent the experimental conditions were different from the calendering conditions.

The heat transfer coefficient of the interface has been studied by several investigators. Burnside and Crotogino (1984), used an experimental technique developed by Kerekes (1980), and determined a contact heat transfer coefficient as well as the thermal conductivity of newsprint. Mohr et al. (1997) experimentally determined a heat

transfer coefficient between paper and different solid materials as function of the pressure. Sanders and Forsyth (1983), Parihar and Wright (1999), and Lor and Chu (2000), studied the contact heat transfer coefficient using different methods. Seyed-Yagoobi et al. (1992) determined the heat transfer coefficient between cast iron and bone-dry paper for pressures up to 300 kPa. None of them seems to incorporate a detailed analysis of the effective heat transfer area according to the respective investigations of Chapman and Lyne.

Thermal conductivity and thermal diffusivity of paper have been investigated by several authors, for example Kartovaara et al. (1985), Rättö and Rigdahl (1998b), and Niskanen and Simula (1999). The conductivity data show some variation, according to paper quality, density, fibre structure and filling. Tables in data books may generally give a value of $0.12 W(m\ ^oC)^{-1}$, for "paper" at room temperature. Other sources give that value for the fibre wall, which must be quite different from the bulk, having void with air. This inconsistency can only be handled by a theoretical analysis of the heat transport mechanism in the fibre structure together with experimental investigations of the same paper quality.

In the following the heat transfer by temperature gradient calendering of newsprint is investigated by theory and by experiment, using newsprint, and with a numerical simulation of the experimental procedure. The heat transfer through the interface as well as the thermal conductivity of paper are discussed. The experiments are made using a calender simulator, (Lamvik et al. (2000)). The investigation is an attempt to consolidate the understanding of heat transfer using temperature gradient calendering, in order to get a better assessment of the proper running conditions of the calendering process.

Contact heat transfer

General remarks

In the following the notation pendulum hammer is used synonymously with calender roller. The analysis of the heat transfer in the interface between the hammer and the paper, can go along several lines. For a preliminary estimate of the temperature field in the paper, a dimensional analysis may suffice, making use of a heat transfer coefficient at the interface. Further analysis has to take into account the different mechanisms for heat transport, that are involved at the interface. One has to deal with the definition of the heat transfer area, with several modes of heat transfer, and with the data from the physical properties. In all cases, however, the basis is the solution of the equation for non-stationary heat conduction. In this context, the simplified second Fourier equation

for one-dimension, will be employed, namely

$$\frac{\partial\theta}{\partial t} = \kappa\frac{\partial^2\theta}{\partial z^2} \tag{5.1}$$

where the relative temperature $\theta = (T(z,t) - T_p)/(T_r - T_p)$, $T(z,t)$ is temperature of the paper, T_p and T_r are the initial temperatures of the paper and the hammer respectively, t is time, z is the depth coordinate in the paper, $\kappa = k/\rho C$ is the thermal diffusivity, k the thermal conductivity, ρ is density, and C is the specific heat capacity of the paper. The initial and boundary conditions are

$$\begin{aligned} \theta &= 0 && for\ t = 0\ and\ z \geq 0 \\ j_r &= -k\partial T/\partial z = h_r(T - T_r) && for\ z = 0\ and\ 0 < t \leq \Delta t \\ j_a &= -k\partial T/\partial z = h_a(T - T_a) && for\ z = 0\ and\ t > \Delta t \end{aligned} \tag{5.2}$$

where j is heat flux to or from paper, h_r and h_a are the respective heat transfer coefficients between the paper, the hammer, respective the ambient air, T_a is the temperature of ambient air, and Δt is the dwell time of the paper under pressure. Solutions of Eq. 5.1, with several different boundary conditions, are given in textbooks, for example Schneider (1974).

For the calendering process it is the temperature of the fibres in the outer layer of the paper that counts, and the main question is to which extent the fibres adapt the temperature of the hammer. The temperature of the fibres that have contact joints with the hammer, depends on the thermophysical properties off the respective materials. A characteristic quantity in this connection is the so called temperature penetration number, (in German "Wärmeeindringszahl"), Gröber et al. (1955), Krischer (1963), the product $\sqrt{k\rho C}$. The relative temperature of the interface θ_{int}, can be expressed by the ratio

$$\theta_{int} = \frac{(T_r - T_{int})}{(T_{int} - T_p)} = \sqrt{\frac{(k\rho C)_p}{(k\rho C)_r}} \tag{5.3}$$

With nominal data for the hammer material, $k = 50W(m\ ^oC)^{-1}$, $\rho = 7800kgm^{-3}$ and $C = 470J(kg\ ^oC)^{-1}$, and the paper, $k = 0.12W(m\ ^oC)^{-1}$, $\rho = 1000kgm^{-3}$ and $C = 1200J(kg\ ^oC)^{-1}$, the ratio is evaluated to be $\theta_{int} = 0.03$. This indicates that the interface temperature T_{int}, and thereby the fibres, adapt the hammer temperature within 3% of the temperature difference between the hammer and paper. A heat transfer coefficient between the roller and the individual fibres in the surface, should therefore be very large, tending towards infinity.

However, the contact area of the fibres may constitute only a fraction of the total area, depending on the line load in the nip, as demonstrated by the experiments by Chapman and Peel (1969) and Lyne (1977). It may be relevant to recall two classical notations: the boundary conditions of the first order, when the temperature of the

boundary is given by the temperature of the paper surface in the nip, and the second order conditions, when a finite heat transfer coefficient is given between the surfaces. In the present case, the condition is of the first order concerning the fibres, but of the second order concerning the heat transfer to the bulk, referred to the total area. That has to be taken into account when dealing with the amount of heat transferred from the hammer (or the roller), to the bulk of the paper. The purpose of the process is preferentially the transfer of temperature to the surface fibres, and not the transfer of heat to the bulk.

In the following the heat transfer in the interface is studied under three different scenarios, by

- dimensional analysis,
- topographical considerations of the heat transfer area, and by
- analytical considerations of the heat transfer.

Dimensional analysis

The dimensional analysis of the heat transfer to the bulk, is described in standard textbooks on heat transfer, Schneider (1974). The temperature field in the paper is derived as a function of the Fourier number $F_o = \kappa \Delta t / z^2$ and the Biot number $Bi = hz/k$, where Δt is the dwell time of the paper in contact with the hammer, and h is the contact heat transfer coefficient between the hammer and the paper. For the present case, with pertinent data for the physical properties of the paper, it can be shown that the paper surface temperature approximates the hammer temperature only by a very large nominal heat transfer coefficient, say $> 10^5 W(m^2\ ^oC)^{-1}$, $(Bi > 20)$. The question is to what extent this high value can be achieved in practice. This will be enlightened upon in the following.

Topographical analysis

The heat transfer to the paper surface, is connected to the topography of the surfaces in contact. The contact surface of the pendulum hammer, is as a first assumption, assumed to be even and continuous, although, the experience is that the topography of the rollers has influence on the gloss of the paper after calendering. The paper features a more or less random set of orientated fibres, surrounded by air. A heat transfer surface is therefore difficult to define. Generally, heat is transferred from the hammer surface to the paper by conduction through the contact points, by conduction through the air in the void, and by radiation to the internal surfaces in the void. The void and the fibre contact points, as the fraction of the total area, are therefore relevant

quantities. In the following, an attempt is made to clarify the influence that these quantities have on the heat transfer mechanisms, mainly based on some findings in the literature. Chapman (1947) measured the contact area of fibres, as a fraction of the total area, by pressing a glass plate against a stack of sheets of newsprint. The data from Chapman's Fig. 10, approximately fits the equation

$$f_a = 0.0372 + 0.082ln(P) \tag{5.4}$$

where the fraction f_a increases from zero to 0.18, when the pressure P increases from 0 to 5.5 MPa. The data are illustrated in Fig. 5.1 by triangular plots. Industrial calenders may run with higher pressure, at nip loads up to $500kNm^{-1}$, giving pressures up to 80 MPa. The problem is then to estimate the fraction of the contact area in the nip, over the whole pressure range. Two sources in the literature are of interest, namely Chapman and Peel (1969), and by Browne et al. (1995).

In this context, the following relations for a relative density, are relevant:

$$\rho_{rel} = \rho/\rho_f = (1 - \varphi) = \upsilon_f/\upsilon = f_v \tag{5.5}$$

Here, φ is the porosity, ρ is the measured density, ρ_f is the density of the fibres, υ and υ_f are the respective specific volumes of paper bulk and the fibres, and f_v is the volume fraction of the fibres. From the fibre volume fraction a nominal area can be estimated, noting that the volume of a fibre is proportionate with a characteristic dimension raised to the 3^{rd} power. The projected area of fibres, perpendicular to the paper surface, can then, as a first approximation be estimated from

$$f_a \sim (1 - \varphi)^{2/3} \tag{5.6}$$

Chapman and Peel (1969) made experiments by compressing newsprint, at 20^oC, using a piston/anvil type of apparatus, and they measured the thickness reduction in the nip, depending on pressure. From data of their Table I, a nominal projected area of fibres can be derived as a function of pressure. The results are shown in Fig. 5.1 by circular plots. A simple logarithmic function fits the plots as

$$f_a = 0.486 + 0.05796ln(P) \tag{5.7}$$

Browne et al. (1995), made unique experiments by determining the porosity φ of newsprint in a roller calender nip. From their results, the volume fraction of fibres can also be derived, as a function of the pressure, (assuming a nip width 5 mm). The data are shown in Fig. 5.1 as square plots. They fit Eq. 5.7 within 15%. These experiments seem to render the most realistic results to be used in the present study. Eq. 5.7 is therefore assumed as the basis for the evaluation of the heat transfer surface of the paper. It may, however, be of interest to pay attention to the results from the following investigations:

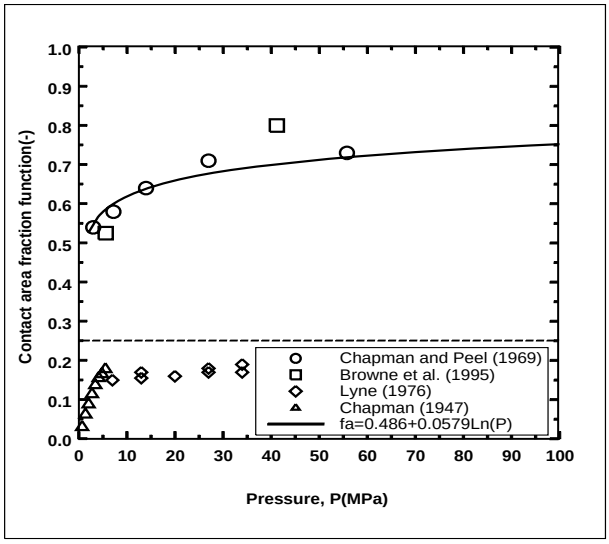

Figure 5.1: Function of fibre contact area fraction versus impact pressure.

Lyne (1977) measured the void fraction of the surface of newsprint after calendering. It may be assumed that the surface topography has been altered from nip. Fig. 5.1 show plots, as diamonds, from his results. The plots tend to be below Chapman (1947)'s results, this may be due to the expansion of the paper after leaving the nip. Lyne's and Chapman's results differ from the results of Chapman and Peel, and Browne et al., presumably because the experimental conditions are inadequate for the calendering process.

Another approach to estimate the contact area at the paper surface, can be based on the basis weight of the fibre, β_f, i.e. on the coverage of "one layer" of fibre in the paper. From Browne et al. (1995), the basis weight is in the range $5 - 10gm^{-2}$. Choosing values for $\beta_f = 7.5gm^{-2}$, for fibre density $\rho_f = 1000kgm^{-3}$, (inclusive the lumen), and for the fibre width $w_f = 30mm$, a coverage fraction f_c can be evaluated from

$$f_c = \beta_f/(\rho w)_f = 0.25 \tag{5.8}$$

For the fibres in the outer layer, this gives a maximum exposed area of the order 25 % of the total area. By increasing pressure on the paper, the fibres beyond are expected to come in contact with the hammer.

Finally, the results from the investigation of calendering with newsprint, by Burnside and Crotogino (1984) resp. Lyne (1977), provide the possibility to correlate the overall heat transfer coefficient and the contact area fraction of fibres. Burnside and Crotogino experimentally determined the heat transfer coefficient versus bulk, on newsprint, presumably by a moderate pressure on the paper, while Lyne determined

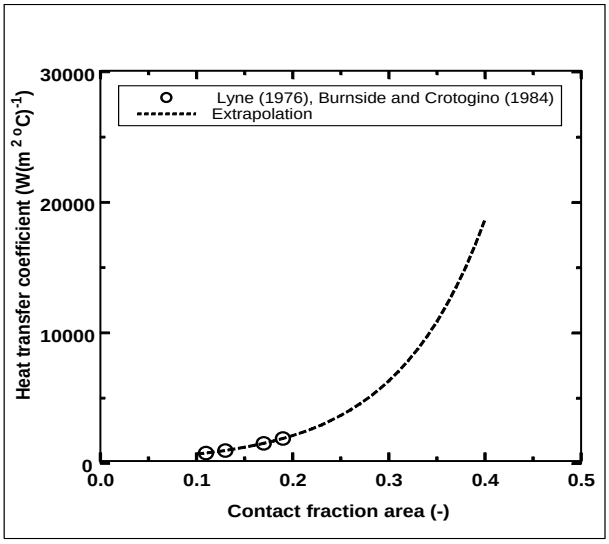

Figure 5.2: Heat transfer coefficient versus fibre contact area fraction, newsprint.

the contact fraction area versus bulk on calendered newsprint. Fig. 5.2 illustrates the results. The plots indicate a monotonous increase in the heat transfer coefficient with increasing contact area fraction. In other words, the fibre contact areas seem to be a basis for the overall heat transfer. An exponential function is fitted to the plots.

$$h = 246.64exp(10.82f_a) \tag{5.9}$$

For an increase of the area fraction, by an extrapolation of the curve function, the overall heat transfer coefficient will reach a value 100 000$(W(m^2\ ^oC)^{-1})$, by an area fraction of about 0.5. As will be shown later in this paper, an overall heat transfer coefficient of the order of 10 000$(W(m^2\ ^oC)^{-1})$, is more realistic, corresponding to an area fraction between 0.3 and 0.4. These results are only indicative, due to the scanty data. However, they point out areas of interest for further studies.

Analytical considerations of heat transfer

A theoretical consideration of the heat transfer from the hammer to the paper can be based upon the simplified one-dimensional model. The linear dimension of the contact area in the present case is 50 mm and the thickness of the paper is of the order of 0.1 mm. Furthermore, the dwell time of the contact is of the order of 1 ms. The Fourier number for the heat transfer can be evaluated to be $< 10^{-6}$. Nothing that the Fourier number is expressing the quotient between conducted heat to stored heat, in a given time interval, this low value indicates that the heat transferred to the paper is, at the end of the dwell time, found mainly as stored heat at the surface, i.e. the criterion for

a pulse heat transfer. This gives a boundary condition for a mathematical evaluation of the development of the succeeding temperature field in the paper. However, in the present case the heat transfer to the paper surface is the topic, for which an other boundary condition is given, namely the approximate surface temperature.

The heat transferred to the paper, during the dwell time Δt, can thus be derived, Gröber et al. (1955) p. 76, as

$$q_{tot} = 2\sqrt{(k\rho C\Delta t/\pi)}(T_r - T_p) \quad (Jm^{-2}) \tag{5.10}$$

This amount of heat can be written as a sum of three modes, namely,
conduction through fibres:

$$q_{cf} = f_a 2\sqrt{(k\rho C\Delta t/\pi)|_f}(T_r - T_p) \quad (Jm^{-2}) \tag{5.11}$$

conduction through air:

$$q_{ca} = (1 - f_a)2\sqrt{(k\rho C\Delta t/\pi)|_a}(T_r - T_p) \quad (Jm^{-2}) \tag{5.12}$$

radiation through air:

$$q_{rad} = (1 - f_a)\varepsilon\sigma_b(T_r^4 - T_p^4)\Delta t \quad (Jm^{-2}) \tag{5.13}$$

giving the total amount of heat

$$q_{tot} = q_{cf} + q_{ca} + q_{rad} \quad (Jm^{-2}) \tag{5.14}$$

Here the emissivity ε is set $\varepsilon \approx 1$, and the blackbody radiation constant $\sigma_b = 5.67 \cdot 10^{-8}\ Wm^{-2}\ K^{-4}$. It can be shown, by using pertinent data for the properties in the Eq. 5.12 and 5.13, that the respective values of q_{ca} and q_{rad} are relatively small, and can be omitted in estimating q_{tot}.

A nominal transfer coefficient for the heat entering the paper, can be derived from the heat flux

$$j_{tot} = q_{tot}/\Delta t = h_{tot}(T_r - T_p) \quad (Wm^{-2}) \tag{5.15}$$

as

$$h_{tot} \approx f_a 2\sqrt{(k\rho C/\Delta t\pi)} \quad (W(m^2\ ^oC)^{-1}) \tag{5.16}$$

Using the following data: $k = 0.12W(m\ ^oC)^{-1}$, $\rho = 1000kgm^{-3}$, $C = 1200J(kg\ ^oC)^{-1}$, $\Delta t = 1ms$, and a contact area fraction function, f_a from Eq. 5.7, the overall heat transfer coefficient can be estimated as a function of pressure as

$$h_{tot} = j_{tot}/(T_r - T_p) = 6582 + 785ln(P) \quad (W(m^2\ ^oC)^{-1}) \tag{5.17}$$

where P is in MPa. The equation is illustrated by the curve in Fig. 5.3. It gives values for the heat transfer coefficient that is only about 10 % of the value needed for the fibres to approximate the roller temperature, as derived from the dimensional analysis.

It is hard to find experimental results in the literature that are relevant for comparison with the theoretical estimation over the whole practical pressure range. In Fig. 5.3 some results are plotted. The black dots are from our own measurements on newsprint, Hestmo et al. (2001), and the circular plots are from Mohr et al. (1997), on "paper" in contact with aluminium. The plots show hardly any realistic functionality to the theoretical curve, due to the low pressures applied. The star plots, from Burnside and Crotogino (1984), also on newsprint, are all an order of magnitude lower than the theoretical curve.

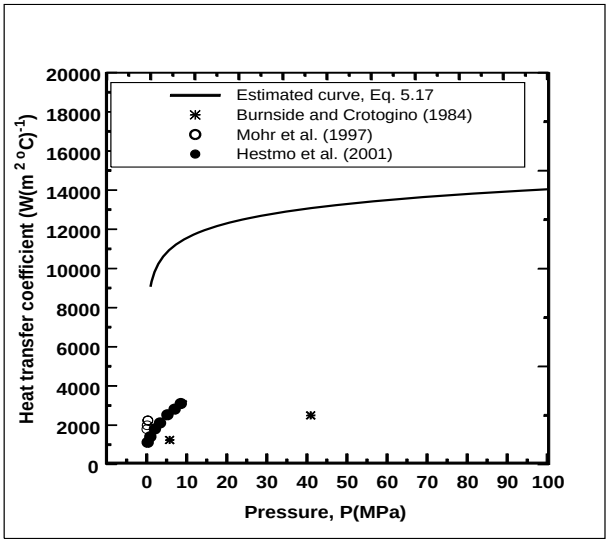

Figure 5.3: Contact heat transfer coefficient in the nip/pendulum impact area.

In the sections below, an attempt is made to measure the heat transferred to a paper specimen, using the pendulum device, and to simulate the temperature field in the specimen by numerical analysis, using realistic data for the physical properties. However, first a note about the thermal conductivity of paper under compression, based on the findings in Hestmo et al. (2001).

Thermal conductivity

Paper consists of fibres, air and possible filling materials in the open structure. The structure features a certain anisotropy in that the fibres are orientated according to their formation in the paper machine, predominated by their length axis in the sheet plane. Each component takes part in the conduction of heat, where the conduction in the direction perpendicular to the sheet is of interest in the present discussion. A classical model for the thermal conductivity in a heterogeneous material is to recognize

two cases where the components are coupled in parallel and in series with the direction of the heat flow. The model leads to two extremes for effective thermal conductivity. By parallel coupling :

$$k_{\parallel} = \varphi k_a + (1 - \varphi) k_f \tag{5.18}$$

and by serial coupling of the fibres:

$$k_{\perp} = [(1 - \varphi)/k_f + \varphi/k_a]^{-1} \tag{5.19}$$

where φ is the porosity, and indices f and a denote the fibre and the air. The model is further developed to express effective thermal conductivity composed as a serial coupling of fractions of the respective extremes, namely

$$k_{eff} = [(1 - a)/k_{\parallel} + a/k_{\perp}]^{-1} \tag{5.20}$$

where a is the volumetric fraction with serial coupling of fibres, i.e. with $k_{\perp}$. The value of a is to be assigned from the experimental results.

The mathematical expressions require knowledge of the thermal conductivity of the solid, i.e. the fibre wall k_f. Data for its value is uncertain. In the literature it is given within a wide range, from 0.16 to $1.5 W(m\ ^oC)^{-1}$. Assuming the fibres of TMP newsprint being similar to wood fibres, the data of wood can be used as a first approximation. Kollmann and Malmquist (1956) give data for the conductivity of wood fibres in the direction parallel as well as perpendicular to the fiber axis, $k_{f\parallel} \approx 0.71 W(m\ ^oC)^{-1}$, and $k_{f\perp} \approx 0.41 W(m\ ^oC)^{-1}$, with a density of $1450 kgm^{-3}$. Siau (1984) recommends the values $k_{f\parallel} \approx 0.88 W(m\ ^oC)^{-1}$ and $k_{f\perp} \approx 0.44 W(m\ ^oC)^{-1}$, with a density $1450 kgm^{-3}$. Assuming the paper to be structured with layers of fibres with their length axis oriented in the sheet parallel to the surfaces, the thermal conductivity $k_{f\perp}$ will be relevant for the effective conductivity of the paper across the sheet. By compressing the paper, the number of fibres coming into contact with the neighbouring fibres will increase. By this bridge the contact points will have the solid structure and an increase of the thermal conductivity will be expected. In a stochastic orientation of the fibres, the thermal conductivity k_{eff} will also have to be taken in account. Fig. 5.4 illustrates the effective thermal conductivity k_{eff} from Eq. 5.20, of newsprint as a function of density, ρ_p, and with the values $k_f = k_{f\perp} = 0.43 W(m\ ^oC)^{-1}$, and $k_a = 0.03 W(m\ ^oC)^{-1}$, and with a as the structure parameter.

The theoretical curves in the figure indicate how the effective thermal conductivity of paper depends on the density and the nominal parameter a, describing the structure of the fibres. The bulk density of newsprint by passing the calender nip, can be estimated to vary from initial value of about $500 kgm^{-3}$ to about $1000 kgm^{-3}$ in the midst of the nip. The effective thermal conductivity may then have a variation within about 60%.

The value of the fraction a introduced above, may need some attention. A low value, at a given density, indicates relatively high conductivity, leading to an assumption of a shortcut between the fibres across the sheet. A filling material will also give the same effect noting that the thermal conductivity of clays may be an order of magnitude higher than the conductivity of fibres. A high volumetric fraction a, indicates a layered structure across the sheet, with weak contact between the fibres in the nearby layers. According to the fibre orientation of the paper web, a is expected to have a relatively high value.

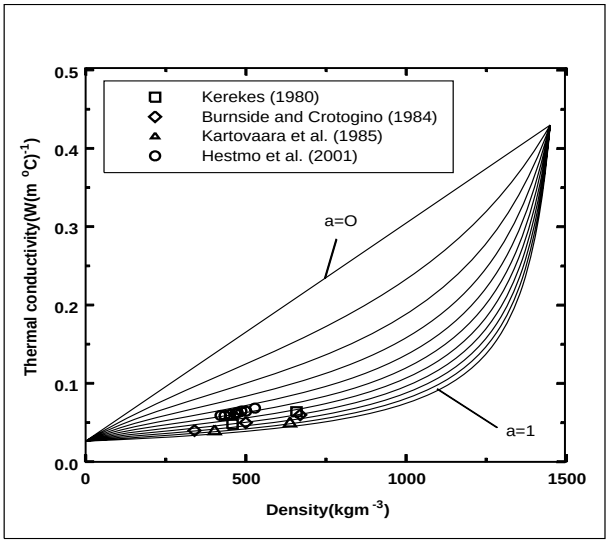

Figure 5.4: Effective thermal conductivity of paper versus density.

In Fig. 5.4 some experimental results from measurements of thermal conductivity of newsprint, are plotted. Our results, Hestmo et al. (2001), using a plate apparatus for stationary measurements, reflect a structure model for the paper with a value of $a \sim 0.5$, i.e. 50% of the web would reflect good contact between individual fibres.

Burnside and Crotogino (1984), and Kerekes and Pye (1974), determined the thermal conductivity of newsprint that had been calendered before the measurements, and thus were not under a similar pressure during measurements. A weaker contact between the fibres across the sheet might therefore have been present, compared with our case. The plots of their results, accordingly seems to follow a curve with a higher value, $a \sim 0.7$. Kartovaara et al. (1985), derived the thermal conductivity from measured thermal diffusivity on mechanical pulp without compression. The plot in Fig. 5.4 for the highest density is for calendered paper, the plot for the lowest density, is for uncalendered paper. Their study also revealed a strong dependency of the thermal conductivities upon the moisture content.

In conclusion to this section, the data of effective thermal conductivity of paper are given with considerably uncertainty. In order to estimate the conductivity, there is a need for reliable data for the fibres, and eventually the filling materials. For predicting the heat transfer into the paper by the calendering process, the thermal conductivity should be given with a dependency of the pressure in the nip.

Experimental heat transfer

Apparatus and experimental techniques

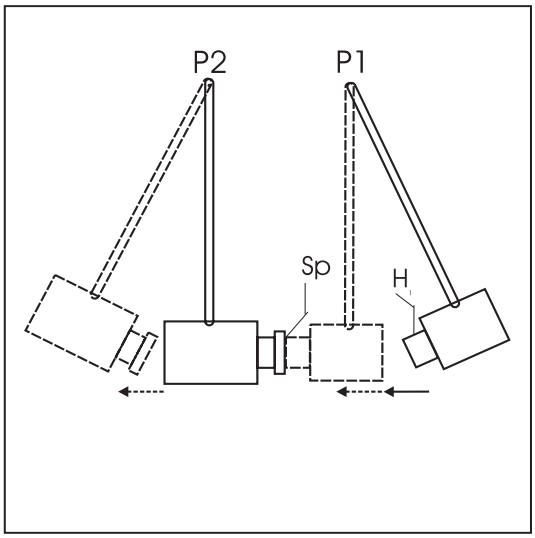

Figure 5.5: Principle sketch of the apparatus. P1, P2, pendulums, H1 heated hammer, Sp paper specimen.

In the experimental study a pendulum device was applied that simulates the mechanical impact of calender rollers to the paper. Fig. 5.5 sketches the principles of the apparatus, described further in Lamvik et al. (2000). It consists of two pendulums P1 and P2, made of steel, with individual pivots mounted in a frame, and allowed to oscillate in the same vertical plane. The weights at the lower end of the arms are facing each other as hammers with a circular area, the impact area, diameter 50 mm. By operation, P1, the active pendulum, is swung out and held at a given position, while P2, the passive pendulum, is resting at its lower position. When P1 is released, it swings back and its hammer H1 collides with the impact area of P2, on which the paper specimen is fixed. P2 has a cover of an elastomer, 24 mm thick, to simulate a soft roller. The hammers were furnished with an electric heating element, to give a controlled temperature, and with a piezoelectric pressure sensor, for force measurement.

Paper specimen

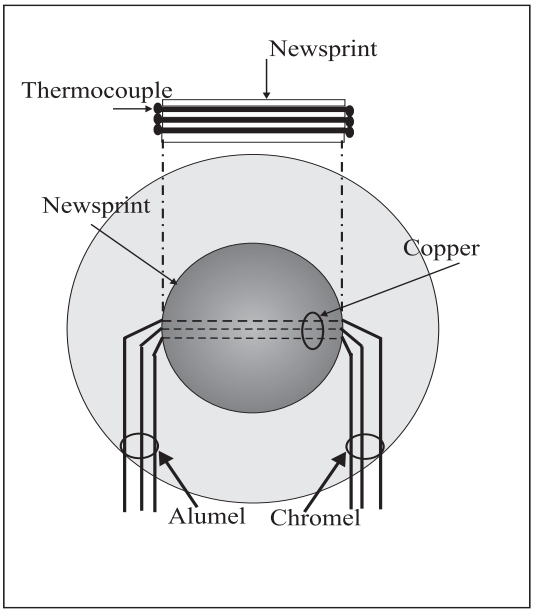

Figure 5.6: Principle sketch of paper specimen.

A paper specimen was made specially for the heat transfer study. A sketch of it is shown in Fig. 5.6. From a sheet of uncalendered TMP newsprint, $45gm^{-2}$, thickness $100\mu m$, three disks were cut, diameter 50 mm. They were sandwiched upon a thicker paper, thickness $180\mu m$, making a base for the stack of the newsprint specimen. Between each sheet a copper strip, $30\mu m$ thick, was mounted along a diameter of the disk, their positions were fixed by having the sheet glued together spotwise. The respective strips were displaced about 2 mm relative to the strip above, so as to be seen from the outside as three parallel strips. At the end of the strips, at the rim of the sheets, thin wires, diameter 0.075 mm, of Chromel and Alumel were soldered to form thermocouples. After a number of impacts by the pendulums, the thickness of the different sheets of the specimen was measured as the distance from the surface to the respective copper strips. The distance was determined by lowering a needle into the paper until contact was made with the strip, indicated electrically. The location of the thermcouples was then the measured distance plus the half of the thickness of the copper strip. In this way the middle of the thermocouples was estimated at the distances 95, 175 and 240 μm, within $\pm 5\mu m$, counted from the outer surface. They are denoted as the outer, the middle and the inner couple, respectively. It can be shown that the Fourier number for a copper strip is several orders of magnitude larger than for the surrounding paper specimen. The EMF of the thermocouples, is therefore assumed to be representative for the temperature of the paper, having the reference thermocouples in melting ice. In the experiments the paper specimen was taped to the

hammer of the passive pendulum, with the circular part fitting the impact area.

Measurements

The impact force was measured by piezoelectric cells from PCB, Type 206A, calibrated from the supplier, having a rise time $10\mu s$ and a sensitivity $0.015mVN^{-1}$. The signal from the cells was recorded versus time on a digital storage oscilloscope, type Textronix 420TDS, with 4 channels. The records gave force versus time, integrated impulse, the maximum force and the contact dwell time of the impact. The temperature of the hot hammer was measured by a thermocouple imbedded $< 1mm$ underneath the surface of the hammer, and read by a digital instrument. Its reading could flimmer 10 to $30\mu V$ during the impact, indicating a temperature disturbance $< 1^oC$. The disturbance is assumed to be insignificant for the driving temperature difference of the heat transfer during the impact. The thermopower from the elements in the test specimens was amplified, using Signal Conditioner from Dewetron, Module $DAQP-\mu V$, with gain 1000 and bandwidth 10 kHz, and recorded by the same oscilloscope mentioned above, with a pertinent time scale. The thermocouples were calibrated to a reference temperature, giving a conversion ratio of $39\mu V(^oC)^{-1}$. The uncertainty of the temperature rise in the elements, is estimated to be within $\pm 0.3^oC$. The experiments were made in a room with temperature 22 ± 1^oC and a relative humidity 45%, giving the moisture content of the paper specimen of about 6%. The paper specimen and the passive pendulum were kept at room temperature before impact. The impulse and the temperature of the active pendulum were the free variables in the experiments.

Numerical

The temperature in the bulk of the paper specimen during impact was simulated numerically by solving Eq. 5.1, with initial and boundary conditions according to the experimental conditions. A general purpose program with a finite difference scheme, developed by Patankar (1980), was used. The calculating domain was divided in 52x10 control volumes, giving an integration that was insignificantly dependent on the grid size. The time step used for the integration was tested until it was invariant for the resulting temperature field. A time step of $10\mu s$ was the starting value, slightly increasing as the integration proceeded. The heat transfer from the pendulum hammer was evaluated from Eq. 5.17 and introduced to the paper as a source term at the surface. The pressure P used in the equation is a fitted mathematical function of the recorded force versus time t during impact, given as

$$P = 0.0255 + 21.466exp\left(-0.5(\frac{t - 0.000362}{0.0001699})^2\right) \quad (MPa) \tag{5.21}$$

The data for the physical properties used in the integration were chosen as the most relevant to be found in the literature, and given in the legends of the respective figures.

Results

Fig. 5.7 illustrates the results from two runs, with temperature of the hot hammer being 190^oC, in A, and 130^oC, in B, and with a maximum impact pressure of 20.8 MPa. The input data for the numerical calculations are given in the legends. The numerical results are qualitatively in fair agreement with the experimental results, indicating a certain consistency in the earlier discussion. A certain play with the input data for the computation, can get a better fit to the experimental plots, it is, however, of less meaning at present, remembering the uncertainty of the data, for the physical properties as well as for the location of the thermocouples in the specimen. Fig. 5.8 illustrates the calculated temperature of the paper surface and the impact pressure versus time. The pressure curve was attained by separate measurement, under the same conditions as by the heat transfer measurements. The pressure curve could

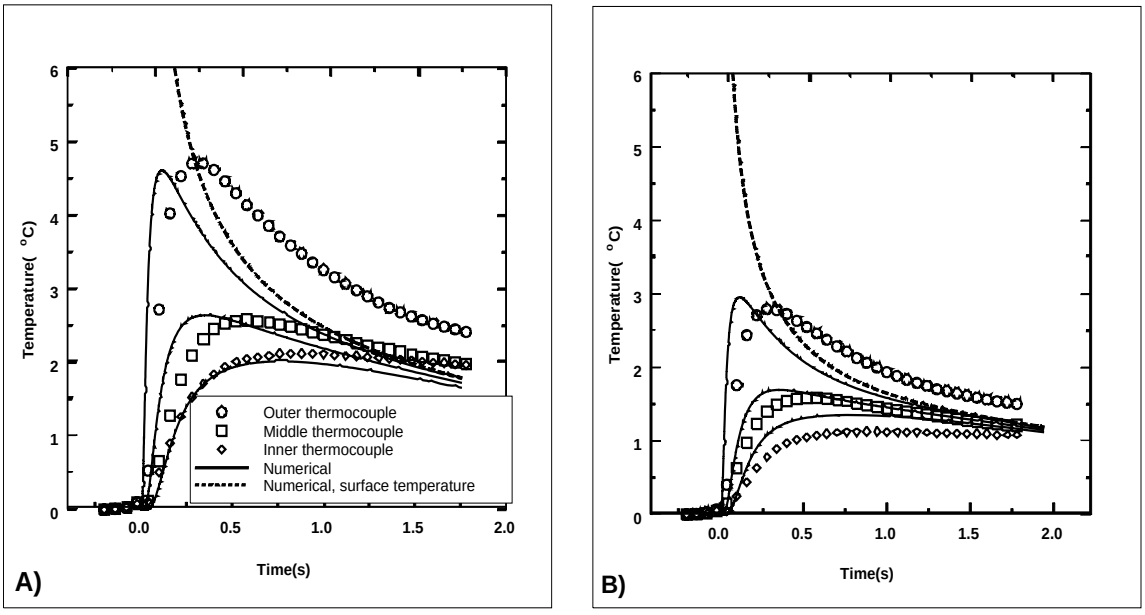

Figure 5.7: Temperature rise in paper specimen versus time. Plots from measurements in the specimen, curves from numerical simulations. A) runs with temperature of the hot hammer 190^oC, B) temperature of 130^oC. $\Delta t = 1ms$. $k_{pap} = 0.12W(m\ ^oC)^{-1}$ in contact, $k_{pap} = 0.05W(m\ ^oC)^{-1}$ after contact. $\rho = 1000kgm^{-3}$, in contact, $\rho = 600kgm^{-3}$ after contact, $C = 1500J(kg\ ^oC)^{-1}$, in contact, $C = 1200J(kg\ ^oC)^{-1}$ after contact.

be repeated within few percents. From the numerical calculation, the bulk layer of the paper surface, nominally about $10\mu m$, is seen to attain a temperature that is considerably lower than the temperature of the pendulum, $\sim 100^oC$ instead of 190^oC, reflecting the limited amount of heat transferred. Furthermore, it can be concluded that the heat transfer to the paper bulk had no significant drying effect on the moisture content of the paper. However, the discrete fibres in contact with the pendulum may still be assumed to attain the temperature of the pendulum. It can be shown by a dimensional analysis that the calculated surface temperatures corresponds to a Biot number $Bi \sim 0.9$. The corresponding heat transfer coefficient h, can be evaluated to $h = 9128W(m^2\ ^oC)^{-1}$. An estimation of the heat transfer coefficient by the theoretical expression, Eq. 5.16, gives, with the input data for the physical properties, a value $h_{the} = 2\sqrt{(0.12 * 1000 * 1200/0.001/3.14)} = 13544\ (W(m^2\ ^oC)^{-1})$. Tentatively, the value of the heat transfer coefficient, gives values of the contact fraction of the fibres in the interface area between 0.3 and 0.4, as seen from Fig. 5.8. The correlation should, however, be looked upon with considerable reservation, due to the meagre basis of the data.

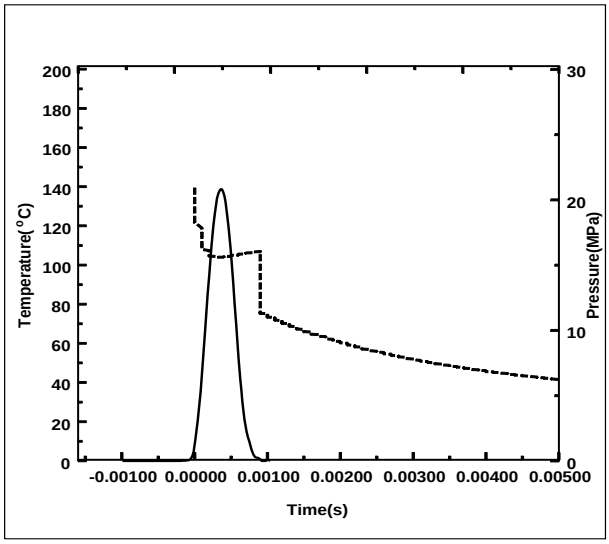

Figure 5.8: Temperature rise of the paper surface and impact pressure versus time. Dotted line - surface temperature, from numerical simulation with temperature of the hot hammer 190^oC. Solid line - pressure.

A rough calorific check of the experimental data shows the following:

From the curves in Fig. 5.7, a mean temperature rise of the specimen can be estimated to about 1.7^oC, and 1.2^oC, for the runs with a hammer temperature of 190^oC, and 130^oC, respectively.

For a temperature rise ΔT_{rise} the heat capacity of the specimen, with diameter 0.05 m, thickness $\sim 410\mu m$, density $500kgm^{-3}$, and specific heat capacity $1200J(kg\ ^oC)^{-1}$, can be estimated roughly to $0.00196 * 0.00041 * 500 * 1200\Delta T_{rise} = 0.48\Delta T_{rise}, J$. For the respective runs, a nominal heat amount of $0.48 * 1.7 = 0.8J$, and $0.48 * 1.2 = 0.6J$ is absorbed by the specimen. These values are to be compared with the amount of heat transferred from the hammer to the specimen, that can be estimated from $Ah\Delta T_{mean}$, using the mean temperature difference. Choosing the mean value of the heat transfer coefficients, $h = 11336W(m^2\ ^oC)^{-1}$, the heat transferred during the dwell time Δt, is evaluated as $0.00196 * 11336 * 0.001\Delta T_{mean}$, to 2.2 J, and 1.6 J, for the respective runs, i.e.: the absorbed amount of heat in the paper is confirmed to be of the same order of magnitude as was transferred to it, that in the end can be estimated to the order of magnitude $1000Wm^{-2}$.

In the numerical calculation, a heat transfer coefficient from the specimen to the ambient air after the impact, is set to $5W(m^2\ ^oC)^{-1}$, giving a heat loss. A rough estimate of the mean temperature difference between the specimen and ambient air, ΔT_{amb}, from the curves in Fig. 5.7, within, say 2 seconds after impact, reveals a value of ΔT_{amb} of say 2.5^oC for the runs. The heat loss can then be estimated to $0.00196 * 5 * 2.5 = 0.025, J$, i.e. of order 3% of the heat transferred during the impact.

In addition to the discussion above on the experimental temperature curves, Fig. 5.7, it is noteworthy that the data from the curves can be used to evaluate the thermal diffusivity of the paper, since they are reflecting a pulse heating of the surface.

Conclusion

The heat transfer to the newsprint a calender nip has been analysed. For high-speed calenders, giving a dwell time of the paper in the nip of order 1 ms, the heat is transferred mainly by conduction to the fibres in contact with the roller/pendulum surface. The fraction of fibres in contact is relatively small and a rather limited amount of heat is transferred to the bulk. The intention of temperature gradient calendering is thereby achieved: the fibres in the surface of the paper are heated, nearly to the temperature of the roller/pendulum, while the paper bulk beneath is little affected by the heating. The overall heat transfer coefficient, referred to the total surface area, is found to be of an order of magnitude $10000W(m^2\ ^oC)^{-1}$. An empirical expression for the heat transfer coefficient is derived in dependency with line load and the physical properties of the paper.

For further experiments by calendering of paper, it may be advice to look for improvement of the paper surface properties by increasing the roller/pendulum temperature to the highest practical level. Further investigations should also be made on the effective fibre contact area in the nip, and there is a need for reliable data of the ther-

mophysical properties of paper, in the dependency of temperature, moisture content and density. Special attention should be made to get data for thermal properties of the fibre itself.

Chapter 6

Concluding remarks

The most important findings in this work can be summarized as follows

- The pendulum device described, represents a supplement to the existing equipments for experimental studies of the calender process.
- Experiments have shown that the pendulum device simulates calendering rollers by the measures of PPS, gloss and density. Surface and bulk properties have been investigated with variation of the impulse, temperature and moisture content of paper in a large range, from which calendering equations has been developed. They can, to a certain extent, describe the results that appear by calendering, and are also suitable to predict the given paper properties with changes of the variables. The equations are therefore a useful tool to estimate results that is beyond our experimental range.
- Dynamical measurements of the compressibilty of the paper is demonstrated using the pendulum device. It is demonstrated that hard nip gives a larger peak deformation compared to soft nip.
- By studying the fracture mechanisms of the fibres in the paper, a strong relation between calendering intensity and number of fractures was found, in addition to the influence of the paper temperature and moisture content. A low intensity and an increased moisture content gave less number of cracks. Thick walled fibres were more proned to cracks. There are also indications that the pendulum technique gives a different deformation of the paper in the nip compared to the deformation between two rollers in a soft nip. This can be derived from the increased number of fractures, and the different crack response from the fibres. Use of hard nip gave a larger number of cracks compared to soft nip. Furthermore, hard nip calendering of paper indicated that fibres, at areas with higher density, were more liable to be crushed, reflecting that soft nip gives less extreme stresses. Crushed fibres at local areas may weaken the paper strength.

- Measurements of the thermal conductivity of paper with a standard hot plate type apparatus is assumed to give results that is adequate for the heat conduction in the paper web by calendering. Theoretical consideration of the thermal conductivity, turns out to suffer from a lack of reliable data of the thermophysical data for paper fibres.

- For high speed calenders, giving a dwell time of the paper in the order 1ms, most of the heat is transferred by conduction to the fibres in contact with roller/pendulum surface. The fraction of fibres in contact is relatively small and a rather limited amount of heat is transferred to the bulk. The overall heat transfer coefficient, referred to the total surface area, is found to be of an order of magnitude $10000 W(m^2\ ^oC)^{-1}$.

- An empirical expression, that describes the heat transfer coefficient as a function of the line load and the physical properties of paper, has been derived. The expression describes the heat transfer mechanisms between the roller/pendulum and the paper, from which the temperature gradient in the paper bulk can be determined.

Bibliography

ASTM-C-168 (1990). Standard Terminology Relating to Thermal Insulating Materials. pages 14–19.

Back, E. L. and Olsson, A. (1983). The effect of temperature on gloss calendering of board as evaluated in a press simulator. *Svensk Papperstidn.*, 86(3):R31.

Back, E. L. and Salmén, N. L. (1980). Glass transitions of wood components hold implications for molding and pulping processes. *Tappi*, 65(7):107–110.

Barkan, P. (1964). *Impact, in H.A. Rotbarth, ed. Mechanical Design and Systems Handbook*. McGRAW-HILL.

Baumgarten, H. L. (1975). Changes in web dimensions during calendering and supercalendering. *Symp. Calend. Supercalend. UMIST (Manchester)*.

Brecht, W. and Schadler, M. (1961). *Das papier*, (17):695–703.

Browne, T., Crotogino, R., and Douglas, W. (1993). An Experimental Calendar for In-Nip Caliper Measurements. *J. Pulp Paper Sci.*, 19(2):J92–J96.

Browne, T., Crotogino, R., and Douglas, W. (1995). The effect of paper structure on behaviour in a calender nip. *J. Pulp Paper Sci.*, 21(10):J343–347.

Buchdahl, R. and Nielsen, L. E. (1951). The Application of Nutting's Equation to the Viscoelastic Behaviour of Certain Polymeric Systems. *J. Appl. Phys.*, 22:1344–1349.

Burnside, J. and Crotogino, R. H. (1984). Some Thermal Properties of Newsprint and Their Variations with Bulk. *J. Pulp Paper Sci.*, pages J144–J150.

Burton, S. and Sprague, C. H. (1987). The Instantaneous Measurement of Density Profile Development During Web Consolidation. *J. Pulp Paper Sci.*, 13(5):145–150.

Chapman, D. and Peel, J. (1969). Calendering processes and the compressibility of paper(part1). *Paper Technology*, 10(2):116–124.

Chapman, S. (1947). The Measurement of Printing Smoothness. *Pulp Paper Mag Can*, pages 140–150.

Charles, L. and Waterhouse, J. (1988). The effect of supercalendering on the strength properties of paper. *J. Pulp Paper Sci.*, 14(3):59.

Colley, J. and Peel, J. D. (1972). Calendering processes and the compressibility of paper. Part 2 - The effects of moisture content and temperature on the compressive creep behaviour of paper. *Paper Techn*, pages 350–357.

Crotogino, R. H. (1982). Temperature-gradient calendering. *Tappi*, pages 97–101.

Crotogino, R. H. and Gratton, M. F. (1987). Hard-nip and soft-nip calendering of uncoated groundwood papers. *Pulp Paper Can.*, 88(12):T461.

De Montmorency, W. (1967). The Calendering of Newsprint: A laboratory Study of Temperature and Pressure Effects. *Pulp Paper Mag. Can.*, pages T326–T345.

Den Hartog, J. (1948). *Mechanics*, chapter XV, pages 270–293. Dover Publications Inc. New York.

Dictionary, W. (1978). *Webster's new twentieth century Dictionary.* Collins World, second edition.

Dumont, L., Moyne, C., and Degiovanni, A. (1999). Thermal Contact Resistance: Experiment Versus Theory. *International Journal of Thermophysics*, 19(6):1681–1690.

Dunfiled, L. G., McDonald, J. D., Gratton, M. F., and Crotogino, R. H. (1986). Gravure Printability of Steam-Treated Machine Calendered Newsprint. *J. Pulp Paper Sci.*, 12(2):31–38.

Fletcher, L. (1997). Recent Developments in Contact Conductance Heat Transfer. *Pulp & Paper Canada*, 98(3):62–70.

Gratton, M. F. (1997). Three-dimensjonal web deformations from calendering in a hard nip. *Tappi J.*, pages 210–218.

Gratton, M. F., Hamel, J., and McDonald, J. (1997). Temperature-gradient calendering:from the laboratory to commercial reality. *Pulp & Paper Canada*, 98(3):68–70.

Gregersen, Ø. W., Hestmo, R. H., and Kvande, K. (2000). Fibre Wall Damage Caused by Calendering. *Proceeding of the Nordic Conference in Paper Calendering. PFI, NTNU, Trondheim*, pages 107–114.

Gröber, H., Erk, S., and Grigull, U. (1955). *Die Grundgesetze der Warmeubetragnung*, page 126. 3.Aufl. Springer Verlag, Berlin.

Hendriks, C. and Visscher, M. (1995). Accurate Real Area of Contact Measurements on Polyurethane. *Journal of Tribology*, 117:607–611.

Hertz, H. (1881). *Über die Berührung fester elasticher Körper, J.f.reine u. angew. Math. 92.*

Hestmo, R. H., Lamvik, M., and Mikkelsen, E. (2001). Determination of Thermal Conductivity of Newsprint under Compression. *Proc. 26th International Thermal Conductivity Conf., Cambridge, Massachuttes, USA, 6-8 Aug.*

Howe, B. and Lambert, J. (1961). An Analysis of the Theory and Operation of High-Speed Steel Roll Calender Stacks. *Pulp and Paper Mag Can*, 60(C):T139–T160.

Høydahl, H. E. (2000). Calender blackening - The price to pay for good printability. *Proceeding of the Nordic Conference in Paper Calendering. PFI, NTNU, Trondheim*, pages 127–136.

Kartovaara, I., Rajala, R., Luukkala, M., and Sipi, K. (1985). Conduction of Heat in Paper. *in Trans. VIII Fundam. Res. Symp., "Papermaking Raw Materials"*, 1:381–412.

Keller, S. and Waech, T. (1992). The Effects of High-Temperature Soft-nip Calendering on Newsprint Properties. *J. Pulp Paper Sci.*, 18(3).

Keller, S. F. (1992). Measurements of the Pressure-Time Profile in Rolling Calender Nip. *J. Pulp Paper Sci.*, 18:J44–J48.

Kerekes, R. (1980). A simple method for determining the thermal conductivity and contact resistance of paper. *Tappi*, 63:137–140.

Kerekes, R. and Pye, I. (1974). Newsprint calendering:an experimental comparison of temperature and loading effects. *Pulp & Paper Canada*, 75(11):65–72.

Kollmann, F. and Malmquist, L. (1956). Über die wärmeleitzahl von Holz und Holzwerstoffen. *Holz als Roh-und Werkstoff*, 14.Jahrg(Heft 6):201–204.

Koskinen, T. (1998). Calender Blackening. *2nd EcoPaperTech Conference, Helsinki.*

Krischer, O. (1963). *Die Wissenschaftlichen Grundlagen der Trocknungstechnik.* Zweite Auflage. Springer -Verlag, Berlin.

Kure, K. A. (1999). *On the relationship between process input variables and fibre characteristics in thermomechanical pulping, PhD thesis, NTNU.*

Kurtz, R. and Hess, H. (1991). Soft nip calendering: the latest state-of-art for a wide range of grades. *Pulp and Paper Canada.*, 92(12):113–122.

Lamvik, M., Hestmo, R., and Mikkelsen, E. (2000). Model experiments of calendering with pendulum device. *Nordic Pulp Paper Res. J.*, 15(2):133–141.

Lee, S. C. and Ren, N. (1996). Behavior of Elastic-Plastic Rough Surface Contacts as Affected by Surface Topography, Load, and Material Hardness. *Tribology Transactions*, 39(1):67–74.

Lor, W.-B. and Chu, H.-S. (2000). Effect of interface thermal resistance on heat transfer in a composite medium using the thermal wave model. *International Journal of Heat and Mass Transfer*, 43:653–663.

Luong, C. H. and Lindem, P. E. (1995). A method to determine heat conduction in paper during calendering. *Proc. TAPPI Paper Physics Conf.*

Luong, C. H. and Lindem, P. E. (1997). Measurements of the pressure distribution in a soft calender nip. *Nordic Pulp Paper Res. J.*, 12(3):207–210.

Lyne, M. B. (1977). The effects of moisture and moisture gradients on the calendering of paper. *Proc. 6th Fundamental Res. Symp. Oxford, publ. P.I.T.A (via P.I.R.A), G.B.*

Mardon, J. (1964). *Paper Trade Journal*, (13):40–44.

Moffat, J. M. (1975). Newsprint calendering: constraints and possibilities. *Proc. UMIST Symp. Calend. Supercalend. Manchester.*

Moffat, J. M., Beath, L. R., and Mihelich, W. G. (1973). Major factors affecting newsprint strength. *Proc. 5th Fundamental Research Symp. Cambridge pub. PITA (via PIRA), GB.*

Mohr, J. W., Seyed-Yagoobi, J., and Price, D. C. (1997). Thermal Contact Conductance of a Paper/Elastomer Interface. *Journal of Heat Transfer*, 119:363–370.

Niskanen, K. and Simula, S. (1999). Thermal diffusivity of paper. *Nordic Pulp Paper Res. J.*, 14(3):236–242.

Nutting, P. (1921). page 1162. Proc. Am. Soc. Testing Materials XXI.

Osaki, S. and Yoshihiko, F. (1978). On the Z-direction Compressive Elasticity of Paper. *1978 Nonwoven Binders Seminar, Pittsburgh, Pennsylvania.*

Page, D. H. (1967). The Collapse Behaviour of Pulp Fibres. *Tappi*, 50(9):449–454.

Parihar, S. and Wright, N. (1999). Thermal Contact Resistance of Silicone Rubber to AISI 304 Contacts. *Transactions of the ASME, Journal of Heat Transfer*, 121:700–702.

Patankar, S. (1980). *Numerical Heat Transfer and Fluid Flow.* Hemisphere Publishing Corporation.

Pietikäinen, R. and Høydahl, H. E. (1999). Private communication.

Rättö, P. and Rigdahl, M. (1998a). Platen press and calendering experiments with paper - estimating the final deformation in the thickness direction. *Nordic Pulp Paper Res. J.*, 13(3):186–190.

Rättö, P. and Rigdahl, M. (1998b). Temperature distributions in a paper sheet subjected to a short pressure pulse from a heated plate. *Nordic Pulp Paper Res. J.*, 13(2):101–106.

Reme, P. A. and Helle, T. (2000). Quantitative assessment of mechanical fibre dimensions during defibration and fibre development, Annual Meeting, Technical section, CPA, Montreal.

Retulainen, E., Moss, P., and Nieminen, K. (1997). Effect of calendering and wetting on paper properties. *J. Pulp Paper Sci.*, 12(1):J34.

Rodal, J. J. A. (1989). Soft-nip calendering of paper and paperboard. *Tappi J.*, 72(5):177–186.

Rodal, R. R. (1993). Paper deformation in a calendering nip. *Tappi J.*, 76(12):63–74.

Salmén, N. L. and Back, E. L. (1980). Moisture-dependent thermal softening of paper, evaluated by its elastic modulus. *Tappi*, 63(6):117–120.

Sanders, D. J. and Forsyth, R. C. (1983). Measurements of thermal conductivity and contact resistance of paper and thin-film materials. *Rev. Sci. Instrum.*, 54(2):238–244.

Schneider, P. (1974). *Conduction Heat Transfer.* 6th printing. Addison-Wesley.

Seyed-Yagoobi, J., Ng, K. H., and Fletcher, L. S. (1992). Thermal Contact Conductance of a Bone -Dry Paper Handsheet/Metal Interface. *Journal of Heat Transfer*, 114:326–330.

Siau, J. (1984). *Transport processes in wood*, page 133. Springer Verlag, Berlin.

Skowronski, J. (1990). Surface roughening of pre-calendered basesheets during coating. *J. Pulp Paper Sci.*, 16(3):J102.

Snaith, B., Probert, S., and O'Callaghan, P. (1986). Thermal Resistance of Pressed Contacts. *Applied Energy*, 22:31–84.

Stevens, R. K., Mihelich, W. G., and Neill, M. T. (1989). On-line soft calender for uncoated groundwood grades. *Proc. TAPPI Coating Conf., TAPPI PRESS, Atlanta, USA*, page 191.

Tuomisto, M. (1992). Upgrading groundwood printing papers: what can soft calendering do. *Pulp Paper Can.*, 93(2).

van Haag, R. (1997). Physikalische Grundlagen des Glättens. *Wochenblatt für Papierfab.*, (18):872–876.

Wickström, M., Nylund, T., and Rigdahl, M. (1997a). Calendering of coated paper and board in an extended soft nip. *Nordic Pulp Paper Res. J.*, 12(4):289–298.

Wickström, M., Nylund, T., and Rigdahl, M. (1997b). Calendering of coated paper and board in an extended soft nip. *Nordic Pulp Paper Res. J.*, 12(4):289–298.

Williams, G. J. and Drummond, J. G. (1994). Preparation of Large Sections for the Microscopial Study of Paper Structure, Proc. 1994 Papermakers Conf., San Francisco, CA,USA, 24-27 Apr. *Paper Technology*, page 517.

Zotterman, C. and Wahren, D. (1978). A technique for simulating production quality of high-speed wet press runs. *Paper Trade Journal*, 15(31):p37–38.